



TAMPEREEN TEKNILLINEN YLIOPISTO
TAMPERE UNIVERSITY OF TECHNOLOGY
Julkaisu 599 • Publication 599

Eija Pirhonen

Fibres and Composites for Potential Biomaterials Applications



Tampereen teknillinen yliopisto. Julkaisu 599
Tampere University of Technology. Publication 599

Eija Pirhonen

Fibres and Composites for Potential Biomaterials Applications

Thesis for the degree of Doctor of Technology to be presented with due permission for public examination and criticism in Konetalo Building, Auditorium K1702, at Tampere University of Technology, on the 2nd of June 2006, at 12 noon.

Tampereen teknillinen yliopisto - Tampere University of Technology
Tampere 2006

ISBN 952-15-1598-8 (printed)
ISBN 952-15-1820-0 (PDF)
ISSN 1459-2045

Imagination is more important than knowledge - Einstein

TABLE OF CONTENTS

Abstract	5
Thesis Outline	6
Author's contribution	6
Abbreviations	7
Definitions.....	8
1 Introduction.....	12
2 Literature review	13
2.1 Bioactive glasses	13
2.1.1 Bioactive glass compositions	13
2.1.2 Mechanisms of Bioactive bonding.....	15
2.1.3 Reaction kinetics of bioactive glasses <i>in vitro</i>	16
2.1.4 Reaction kinetics of bioactive glasses <i>in vivo</i>	17
2.1.5 Compositional dependence to the manufacturing methods	18
2.2 Bioactive glasses with cells and tissues	18
2.2.1 Bioactive glass – cell reactions	18
2.2.2 Antibacterial property of bioactive glasses.....	19
2.2.3 Animal studies with bioactive glasses	20
2.2.4 Clinical use of bioactive glasses	21
2.3 Composites.....	22
2.3.1 Theoretical base of composites	22
2.3.2 Bioactive glass/medical resorbable polymer composites.....	23
2.3.3 Fibre reinforced composites as medical materials	25
2.4 Tissue engineering	26
2.4.1 Current trends in Tissue engineering	26
2.4.2 Fibrous tissue engineering scaffold.....	27
2.4.3 Tissue engineering scaffolds manufactured from bioactive glasses	29
3 Aims of the study	31
4 Materials and methods	32
4.1 Materials.....	32
4.2 Processing and manufacturing	32
4.2.1 Manufacturing of glass and glass Fibres.....	32
4.2.2 Manufacturing of composites.....	34
4.2.3 Porous bioactive glass fibre scaffolds.....	37
4.3 Characterization methods.....	38
4.3.1 Mechanical testing	38
4.3.2 Microscopic analysis.....	41
4.3.3 Other analysis performed.....	42
5 Results.....	44
5.1 Hydroxyapatite polyethylene composites (I),	44
5.1.1 Mechanical properties	44
5.1.2 Structural characterization	45
5.2 Bioactive glass fibres (II, III),.....	48
5.2.1 Processing of the fibres	48
5.2.2 Mechanical properties	50
5.2.3 Structural characterization	53
5.3 Polymer/bioactive glass fibre composites (IV, V)	56
5.3.1 Mechanical properties	57
5.3.2 Structural characterization	58

5.4	Sintered scaffolds (VI, VII)	60
5.4.1	Structural characterization	60
6	Discussion	64
6.1	HA/PE composites	64
6.2	Bioactive glass Fibres	64
6.3	Glass fibre composites	66
6.4	Bioactive glass fibre scaffolds	67
7	Summary and Conclusions.....	69
	Acknowledgements.....	70
	References.....	71

Abstract

The goals of this study were to investigate the effect of composite structure on the mechanical properties of various hydroxyapatite polyethylene composites; to manufacture and characterize bioactive glass fibres formed from bioactive glasses 13-93 and 9-93; and to manufacture and characterize composites from the produced bioactive glass fibres. The literature review deals with melt derived silicate based bioactive glasses and their applications, biomedical composites and tissue engineering scaffolds.

Hydroxyapatite (HA) – polyethylene (PE) composites were manufactured using various constructions. HA in composites was used as particulates, and PE as fibres and particulates. The samples were formed by hot compaction. Good adhesion was obtained between the various phases and mechanical properties were markedly better with PE fibre reinforced constructions than those without PE fibres.

The melt spinning of bioactive glasses 13-93 and 9-93 was successful and homogeneous continuous fibres were obtained. Fibres with diameters from 20 μm up to 300 μm were successfully produced. The strength of fibres correlates closely with fibre diameter; thin fibres possessing the greatest strength. The mechanical properties of the fibres are highly sensitive to abrasion of the fibre surface, and polymeric coating of the fibre surface greatly improved the properties and handling of the fibres.

When immersed in simulated body fluid (SBF), a Si-rich layer and CaP precipitates formed on the bioactive glass fibre surfaces. The degradation of fibres is highly dependent on surface area with thin fibres degrading more quickly than thick ones. In *in vitro* conditions the strength of the fibres remained at initial levels for the first weeks, after which there is drop in mechanical properties. In *in vitro* conditions the formed surface layers retarded further degradation of the fibres and the mechanical properties levelled off after 5 to 7 weeks, thus addressing the difficulty of estimating the reaction which would occur *in vivo*.

Laboratory scale composites were manufactured by piston injection moulding. The use of high strength glass fibres as reinforcement clearly improved the mechanical properties of composites when compared to the non-reinforced samples. CaP-precipitates formed on top of the composite structures when the samples were immersed in SBF, though the polymeric layer delayed the formation of the CaP layers.

Using a sintering technique, porous 3D-scaffolds were manufactured from bioactive glass fibres. The formed scaffolds have a highly interconnected porous structure, which is a crucial property for all tissue engineering scaffolds. By optimising both the dimensions of the fibre segments used and the sintering temperature, it is possible to optimise porosity, pore size, scaffold architecture and mechanical properties.

Thesis Outline

This thesis consists of a review of the literature and an experimental part, which summaries the work performed in the publications listed below.

- I. N. Ladizesky, E. Pirhonen, D. Appleyard, I. Ward and W. Bonfield: Fibre reinforcement of ceramic/polymer composites for a major load-bearing bone substitute material. *Composites Science and Technology* Vol. 58 (1998) pp. 419-434.
- II. E. Pirhonen, H. Niiranen, T. Niemelä, M Brink and P. Törmälä: Manufacturing, Mechanical Characterisation and *In Vitro* performance of Bioactive glass 13-93 fibres. *Journal of Biomedical Materials Research, Applied Biomaterials* Vol. 77B(2) (2006) pp. 227-233.
- III. E. Pirhonen, L. Moimas and M. Brink: Mechanical properties of bioactive glass 9-93 fibres. *Acta Biomaterialia* Vol. 2 (2006) pp. 103-107.
- IV. E. Pirhonen G. Grandi and P. Törmälä: Bioactive Glass Fibre/Polylactide composite. *Key Engineering Materials* Vols. 192-195 (2001) pp. 725-728.
- V. E. Pirhonen and P. Törmälä: Coating of bioactive glass 13-93 fibres with biomedical polymers. Accepted for publication in *Journal of Materials Science, Materials in Medicine*.
- VI. E. Pirhonen, L. Moimas and J. Haapanen: Porous Bioactive 3-D Glass Fibre Scaffolds For Tissue Engineering Applications Manufactured By Sintering Technique. *Key Engineering Materials* Vols. 240-242 (2003) pp. 237-240.
- VII. L. Moimas, K. Markkula, C. Schmid and E. Pirhonen: Three-dimensional Porous Bioactive Glass Fibre Scaffolds, Fluid Dynamic and Geometrical Characterization. *Materials for Tissue Engineering*. Edited by A. Ravaglioli and A. Krajewski. Published by ISTE-CNR – Faenza, Italy (2004) (9th Ceramics, Cells and Tissues Conference, Faenza, Italy, 2004). pp. 123-131.

Author's contribution

The author undertook all the work for papers II, III, IV, V and VI, including planning the experiments and testing as well as analysis of the data and writing the manuscript. For paper I, the author manufactured the materials and partly performed the testing. For paper VII, the author designed the manufacturing equipment and planned the experiments with the co-authors.

Abbreviations

3D	Three dimensional
3DF	Three dimensional fibrous scaffold
45S5	Bioglass®
AB	Autologous bone
ASTM	American Society of Testing Materials
BAG	Bioactive glass
bFGF	Fibroblast growth factor
BG	Bioactive glass
BGF	Bioactive glass fibre
BMP	Bone Morphogenic protein
CaP	Calciumphosphate
CM	Compression moulding
ECM	Extracellular matrix
E.HAPEX	Powder in which HAPEX™ and HA powder are combined
EDS	Energy dispersive spectrometer
FBGC	Foreign body giant cell
GF	Glass fibre
HA	Hydroxylapatite
HAPEX™	Tradename for HA-PE composite
HCA	Hydroxycarbonate apatite
LM	Light microscopy
ISO	International Standards Organization
MNGC	Multinuclear giant cell
M _w	Molecular weight
NIH	US National Institute of Health
PCL	Polycaprolactone
PE	Polyethylene
PGA	Polyglycolide, polyglycolic acid
PLA	Poly lactide, polylactic acid
PLGA	Co-polymer of polylactide and polyglycolide
PDLLA	Rasemic polylactide
R.HAPEX	Powder in which HAPEX™ and PE powder are combined
RT	Room temperature
S53P4	Bioactive glass type
SA/V	Surface area/volume
SBF	Simulated body fluid
SEM	Scanning electron microscopy
TRIS	Trishydroxymethylaminomethane
VEGF	Endothelial growth factor

Definitions

Definitions are from The Williams Dictionary of Biomaterials (Williams 1999).

bioabsorbable

capable of being degraded or dissolved and subsequently metabolised within an organism.

bioactive glass

1. any glass or glass ceramic that displays characteristics of bioactivity.
2. amorphous solid that is not intrinsically adhesive and that is capable of forming a cohesive bond with both hard and soft tissue when exposed to appropriate *in vivo* or *in vitro* environments, such as simulated body fluid or tris-hydroxymethylaminomethane buffer, by developing a surface layer of hydroxycarbonate apatite by release of ionic species from the bulk material.
3. any glass or glass ceramic that is used, either by itself or as a coating, to achieve a bond to mineralised tissue associated with the transfer of ion species and the formation of an apatitic layer at their interface.

biocompatibility

1. the ability of a material to perform with an appropriate host response in a specific application.
2. the quality of not having toxic or injurious effects of biological system.
3. comparison of the tissue response produced through the close association of the implanted candidate material to its implant site within the host animal to that tissue response recognised and established as suitable with control materials.

biodegradation

1. gradual breakdown of a material mediated by specific biological activity.
2. breakdown of a material mediated by a biological system.
3. alteration undergone by the biomaterial or medical device involving loss of their integrity or performance when exposed to a physiological or simulated environment.
4. series of processes by which living systems render chemicals less noxious to the environment.

biomaterial

1. non-viable material used in medical device, intended to interact with biological system.
2. material intended to interface with biological systems to evaluate, treat, augment or replace any tissue, organ or function of the body.
3. synthetic, natural or modified natural material intended to be in contact and interact with the biological system.
4. any substance (other than drug), synthetic or natural, that can be used as a system or part of a system that treats, augments, or replaces any tissue, organ, or function of the body.
5. solid materials which occur in and are made by living organisms, such as chitin, fibrin or bone.

biomedical polymer

any polymer that is used as a biomaterial.

biomimetic material

any material that is structurally or chemically analogous to a component of plant or animal tissue and which can be incorporated into any product whose use is based on the characteristics of that tissue component.

bone bonding

the establishment, by physico-chemical process, of continuity between an implant and bone matrix.

bone ingrowth

ingress of newly formed bone into the micro- or macro-porosity of a biomaterial placed in intimate contact with any part of the skeletal system.

bone morphogenic proteins BMP's

any of the non-collagenous proteins of bone matrix that may be involved in osteogenesis.

bone remodelling

absorption of bone tissue and simultaneous deposition of new bone.

coating

1. deposited layer or covering on a biomaterial or medical/dental device which is intended to protect or enhance the performance of the device or biomaterial.
2. surface layer that is relatively thin compared to the overall dimensions of the prosthetic part that has been coated.

composite material

structural material made of two or more distinctly different materials, where each component contributes positively to the final properties.

copolymer

polymer consisting of molecules characterised by the repetition of two or more different types of monomer units.

devitrification

crystallisation of an amorphous substance.

differentiation

expression of cell- or tissue-specific genes which results in the functional repertoire of a distinct cells type.

encapsulation

1. process of becoming enclosed or surrounded.
2. containment of a drug within a device such that the drug can be subsequently released under desired conditions.
3. process by which an implanted material becomes surrounded by fibrous tissue.

hydroxyapatite

1. hydrated calcium phosphate occurring widely in natural tissues such as enamel, bone, ect.
2. hydrated calcium phosphate, prepared by any one of several routes and existing in several different forms, that is used as ceramic biomaterial.

implant

1. medical device made from one or more biomaterials that is intentionally placed within the body, either totally or partially buried beneath an epithelial surface.

2. medical device that is placed into a surgically or naturally formed cavity of the human body if it is intended to remain there of a period of 30 days or more.

3. to insert any object into surgically or naturally formed site in the body, with the intention of leaving it there after the procedure is complete.

in vitro

1. literally, “in glass” or “test tube;” used to refer to processes that are carried out outside the living body, usually in the laboratory, as distinguished from *in vivo*.

2. pertaining to a situation which involves the experimental reproduction of biological processes in the more easily defined environment such as culture vessel.

in vivo

1. within the living body.

2. pertaining to a biological process occurring within the living organism or cell.

matrix

1. more or less continuous matter in which something is embedded.

2. intercellular substance of a tissue or the tissue from which a structure develops.

3. component of a composite material in which the fibres or filler materials are embedded.

osseointegration

the concept of a clinically asymptomatic attachment of a biomaterial to bone, under conditions of functional loading.

osteoconduction

process of passively allowing bone to grow and remodel over a surface.

proliferation

growth or extension by the multiplication of cells.

recombinant

describing a new cell or individual that results from genetic recombination.

resorbable

capable of being resorbed into the body.

scaffold

in tissue engineering, the porous structure, usually polymeric, which serves as a substrate and guide for tissue regeneration.

simulated body fluid

fluid that has been prepared such that it resembles, chemically, the approximate composition of a body fluid, usually the extracellular fluid that comes into chronic contact with an implanted biomaterial.

sinter

to coalesce into a single mass under the influence of heat, without actually liquefying.

stem cell

multi-potential cell from which differentiated cells derive.

tissue engineering

1. the persuasion of the body to heal itself, through the delivery to the appropriate sites of molecular signals, cells and supportive structures.

2. application of scientific principles to the design, construction, modification, growth, and maintenance of living tissues.
3. the application of the principles and methods of engineering and life sciences towards the fundamental understanding of structure/function relationships in normal and pathological mammalian tissues and the development of biological substitutes to restore, maintain and improve functions.
4. an emerging discipline that applies engineering principles to create devices for the study, restoration, modification and assembly of functional tissues from native or synthetic sources.

1 Introduction

Biomaterials science has developed rapidly in recent decades. In the past when tissues became diseased or damaged, removal of the offending part was normally the only way to cure the patient. However, human survivability in those days seldom exceeded progressive decrease in the quality of the tissues, so there was only a limited need for replacement parts. Some 30 years ago, a revolution in medical care took place with the successful replacement of tissues by transplantation, replacement with living tissues, or by implantation, replacement with synthetic biomaterials (Hench 1998). The goal of early biomaterials was to achieve a suitable combination of physical properties to match those of the replaced tissue with minimal toxic response in the host tissue, and “inertness” was the property most required of the biomaterial. These are the so-called “first generation biomaterials”. Increased understanding of the biology of cells tissues next gave rise to the “second generation biomaterials”, in which the emphasis moved away from bio-inert tissue response to producing bioactive biomaterials that could elicit a controlled action and reaction in the physiological environment (Hench and Polak 2002). There currently is enormous interest in the further development of biomaterials towards “third-generation materials” which promote specific cellular responses at the molecular level. In this development, there is also great interest in tissue engineered materials in which living cells and synthetic biomaterials are combined. One area of potential in this development is composites for creating materials with advanced properties.

In the literature review the focus is mainly on silica-based melt derived bioactive glasses; the composites made from these glasses; and the use of fibrous structures as tissue engineering scaffolds.

2 Literature review

2.1 Bioactive glasses

There are four general types of implant-tissue response; the implant-tissue reaction can be either, toxic, biologically nearly inert, bioactive or implant dissolute in tissue. In the bioactive response type, a bond forms across the interface between implant and tissue (Hench and Wilson 1993). Bioactive performance has been observed in hydroxyapatite, bioactive glasses, bioactive glass-ceramics, and β -tricalcium phosphate (Hench and Wilson 1984; Kim 2003). Kokubo et al. have also demonstrated that formation of a bone-like apatite layer is also possible on non-bioactive materials (Kokubo 1992). Bioactive glasses were first discovered by Hench and colleagues in the early 1970s (Hench and Andersson 1993). Since the discovery of the bioactive behaviour of glass, various new bioactive glass compositions has been found and studied. Bioactive glasses can be divided, according to method of manufacture, into melt derived bioactive glasses and sol-gel derived bioactive glasses (Hench and Wilson 1993). Melt derived glasses can be further divided into two major groups, namely silicate based and phosphate based bioactive glasses. This literature review deals with melt derived silicate glasses.

2.1.1 Bioactive glass compositions

The ability of a substance to form a glass does not depend upon any particular chemical or physical property. Any liquid, in principle, can be transformed into glass if cooled sufficiently quickly and brought below the crystal transformation range. A good glass-forming material is then one for which the rate of crystallization is very slow in relation to the rate of cooling. B_2O_3 , SiO_2 , GeO_2 and P_2O_5 all readily form glasses on their own and are commonly known as 'glass-formers' because they provide the backbone in other mixed-oxide glasses. (Paul 1990)

The base components in melt derived silica based bioactive glasses are SiO_2 , Na_2O , CaO , and P_2O_5 . Hench and co-workers have studied the reaction kinetics of a series of glasses in this four component system, with constant 6 wt-% content of P_2O_5 . They found four different types of glasses in this system namely, A) glasses which are bioactive and bond to bone; B) nearly-inert glasses which are encapsulated by non-adherent fibrous tissue when implanted; C) glasses which resorb within 10 to 30 days in tissue and; D) glasses which are technically difficult to manufacture. The first, and most well-studied composition, termed Bioglass®, or 45S5, contains 45% SiO_2 , 24.5% Na_2O , 24.4% CaO and 6% P_2O_5 , all in weight percent. The basis of the bone bonding property of bioactive glasses is the chemical reactivity of the glass in body fluids. The surface chemical reactions result in the formation of a hydroxycarbonate apatite (HCA) layer to which bone can bond. The rate of development of the interfacial bond between and implant and bone can be referred to as the level of bioactivity. Hench introduced an index of bioactivity as a measure of this. The index is given by $I_B = (100/t_{0.5bb})$, where $t_{0.5bb}$ is the time for more than 50% of the surface to be bonded to bone. (Hench and Andersson 1993)

In more complex bioactive glass systems it is not possible to find a simple relationship between composition and tissue bonding. Hench has proposed a compositional range for silicate based melt derived bioactive glasses which is shown in Table 1 (Ogino et al. 1985). In Table 2 the most commonly used bioactive glasses are listed.

Table 1. Compositional range of silicate based bioactive glasses as proposed by Hench (Ogino et al. 1985).

Element	Amount as mol-%
SiO ₂	35 - 60 (mol-%)
B ₂ O ₃	0 - 15
Na ₂ O	10 - 30
CaO	5 - 40
TiO ₂	0 - 2
P ₂ O ₅	0 - 15
K ₂ O	0 - 20
Li ₂ O	0 - 10
MgO	0 - 5
La ₂ O ₃ + Ta ₂ O ₅ + Y ₂ O ₃	0 - 8
F ₂	0 - 15

Table 2. Most common silicate based, melt driven bioactive glass compositions.

Name	Composition as weight-%
Bioglass®, 45S5	45% SiO ₂ , 24.5% Na ₂ O, 24.4% CaO and 6% P ₂ O ₅ ,
S53P4, 53S4	53% SiO ₂ , 23% Na ₂ O, 20% CaO and 4% P ₂ O ₅ ,
13-93	6 % Na ₂ O, 12 % K ₂ O, 5 % MgO, 20 % CaO, 4 % P ₂ O ₅ and 53 % SiO ₂

There is constant interest in developing new types of bioactive glasses and studying their reaction kinetics. Pereira et al. have studied Si-Ca-P-Mg system glasses with low SiO₂ content (25 and 29 mol-%) and high MgO contents (31 and 36 mol-%). They observed that in *in vitro* conditions (SBF) glasses induced the precipitation of Ca-P rich layer on their surfaces, although these were poorly attached to the glass substrate. (Pereira et al. 2004). Branda and co-workers studied the effect of the substitution of M₂O₃ (M=La, Y, In, Ga, Al) for CaO on the bioactivity of CaO – SiO₂ glass. They observed that the substitution of M₂O₃ for CaO in CaO-SiO₂ system progressively reduces the ability to form a calcium phosphate layer on the surfaces exposed to simulated body fluid (SBF). They concluded that the substitution of M₂O₃ for CaO affects the acidic properties of the silanolic groups (Branda et al. 2002).

Leonelli and co-workers studied Cerium-doped glasses and analysed its bioactivity. The addition of small quantities of CeO₂ up to 1.5 % into Bioglass® did not significantly alter its ability of *in vitro* apatite formation. High cerium content improves the chemical durability of glasses and the apatite formation is prevented both by glass durability and by cerium ability to interact with phosphate, giving rise to an amorphous phase (Leonelli et al. 2003). Kim et al. studied the effect of fluoride in Bioglass®. Both non-fluoride Bioglass® and fluoride containing Bioglass® (in which 40% of CaO was substituted with CaF₂) formed an amorphous calcium-phosphate layer after a 2 min exposure to the aqueous buffer solution. The addition of fluoride to the glass composition produces a distortion of the crystal structure which develops when the amorphous calcium-phosphate layer crystallizes. Fluoroapatite crystals with rod-shaped morphology are produced instead of carbonate hydroxyapatite crystals with flake morphology. (Kim, Clark and Hench 1989)

2.1.2 Mechanisms of Bioactive bonding

Hench and co-workers produced a series of publications as early as the 1970s in which direct chemical bonding between tissues and bioactive biomaterials was described for the first time (Clark, Hench and Paschall 1976; Hench et al. 1977; Hench and Paschall 1973; Hench and Paschall 1974; Hench, Splinter and Allen 1971; Piotrowski et al. 1975). The investigations of compositional and microstructural variables indicated that the critical factors controlling direct chemical bonding *in vivo* are as follows: (1) the development of an alkaline pH at the surface of the implant, (2) time required for the surface to become alkaline, and (3) surface active Ca and P sites (Hench and Paschall 1973). In other *in vivo* studies they further analysed the layers forming between the biomaterial and tissue and observed that an amorphous layer with thickness of 800-1000 Å forms between Bioglass® and Bioglass-ceramic implants and healing bone. Hench and colleagues assumed that this amorphous layer is comprised of SiO₂, CaO and P₂O₅, and that this layer may be equivalent to the substance comprising the “cement like” material in mature bone. They also found that collagen fibres produced by osteoblasts become attached to the bonding layer and mineralization within the layer occurred in an ectopic-manner yielding 600-1000 Å crystals bridging between the implant surface and mature bone (Hench and Paschall 1974). The reaction steps involved in the formation of bioactive layers have been studied later in detail by several research groups. The commonly accepted outline of the reaction process is the following two series of steps. (Ducheyene et al. 1992; Hench and Andersson 1993)

Reactions on the implant side of the interface with a bioactive glass are as follows:

- Stage 1: Leaching and formation of silanols (SiOH)
- Stage 2: Loss of soluble silica and formation of silanols
- Stage 3: Polycondensation of silanols to form a hydrated silica gel
- Stage 4: Formation of an amorphous calcium phosphate layer
- Stage 5: Crystallization of a hydroxycarbonate apatite layer

The accepted sequence of events associated with the formation of a bond with tissues is as follows:

- Stage 6: Adsorption of biological moieties in the SiO₂ – HCA layer
- Stage 7: Action of macrophages
- Stage 8: Attachment of stem cells
- Stage 9: Differentiation of stem cells
- Stage 10: Generation of matrix
- Stage 11: Mineralization of matrix

In more detail, the first five reactions in the surface of bioactive glass are the following:

Stage 1:

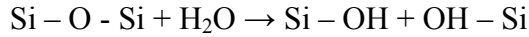
Rapid exchange of Na⁺ or K⁺ or H₃O⁺ from solution:



This stage is usually controlled by diffusion and exhibits a $t_{1/2}$ dependence.

Stage 2:

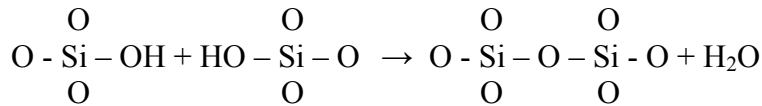
Loss of soluble silica in the form of Si(OH)₄ to the solution, resulting from breaking of Si-O-Si bonds and formation of Si-OH (silanols) at the glass solution interface:



This stage is usually controlled by interfacial reaction and exhibits a $t_{1,0}$ dependence.

Stage 3:

Condensation and repolymerization of a SiO₂-rich layer on the surface depleted in alkalis and alkaline-earth cations:



Stage 4:

Migration of Ca²⁺ and PO₄³⁻ groups to the surface through the SiO₂-layer forming a CaO-P₂O₅-rich film on top of the SiO₂-rich layer, followed by growth of the amorphous CaO-P₂O₅-rich film by incorporation of soluble calcium and phosphate from solution.

Stage 5:

Crystallization of the amorphous CaO-P₂O₅ film by incorporation of OH⁻, CO_{2,3}, or F⁻ anions from solution to form a mixed hydroxyl, carbonate, fluoroapatite layer.

2.1.3 Reaction kinetics of bioactive glasses *in vitro*

The mechanism of formation of a bioactive glass layer on the surfaces has aroused much interest and various research groups have investigated and reported the study results. There are several factors to be considered in analysing the reaction kinetics, namely substrate related aspects such as material chemistry and shape; the media used, time and temperature (Radin et al. 1997).

Initially the formations of reaction layers were detected in bioactive glasses and glass-ceramics. Kokubo and colleagues investigated the surface reaction of bioactive glass-ceramics in various solutions which simulated the real body fluid. They found that a solution which had a concentration and pH almost equal to those of human blood plasma (Na⁺ 142.0, K⁺ 5.0, Mg²⁺ 1.5, Ca²⁺ 2.5, Cl⁻ 148.8, HCO₃⁻ 4.2 and PO₄²⁻ 1.0 mM) and buffered at pH 7.25 with the trishydroxymethylaminomethane (TRIS)), most precisely reproduced the *in vivo* surface structure change (Kokubo et al. 1990). On the basis of this work, simulated body fluid (SBF) has also been widely used by other research groups to study the reaction kinetics of bioactive materials.

Filgueiras studied the reactions of Bioglass® in three different simulated body fluid concentrations. Compared to TRIS buffer, the presence of calcium and phosphate ions in SBF solutions accelerates the repolymerization of a silica-rich layer and formation of an amorphous calcium-phosphate layer and crystallization of a-CaP. Magnesium ions in SBF slow down formation of the a-CaP layer and greatly retard crystallization of HCAp (Filgueiras, La Torre and Hench 1993).

Greenspan et al. have studied the effect of surface area to volume ratio on *in vitro* surface reactions of Bioglass® particulates. They found that at high SA/V ratios, there is a rapid increase in pH and ion release from the glass which results in rapid formation of an initial calcium phosphate layer, which remains thin over time. At lower SA/V ratios, there is a less pronounced change in pH. The development of the calcium phosphate layer is more gradual and also the HCA layer is thicker

(Greenspan, Zhong and La Torre 1994). Work by Cerruti et al. (Cerruti, Greenspan and Powers 2005b) and Jones et al. (Jones, Sepulveda and Hench 2001) showed similar results. Cerruti et al also studied the effect of pH on the reactivity of small 2 μm particles of Bioglass® in TRIS buffer. Only at pH 8 total reconstruction of the glass, with the formation of both silica and a calcium phosphate rich layer, was observed. At a higher pH, calcium phosphate precipitation occurred immediately after immersion and prevented any further large ion release. In these conditions more calcium carbonate formed than HCA. At lower pH, no phosphate reprecipitation was observed and a total breakdown of glassy network occurred. They also concluded that cation leaching, silica network formation and phosphate reprecipitation occur simultaneously in small 2 μm particles during dissolution at pH 8, and cannot be considered as sequential steps of a reaction (Cerruti, Greenspan and Powers 2005a). It should be mentioned, however, that the parallel reaction was observed only with these small 2 μm particles.

2.1.4 Reaction kinetics of bioactive glasses *in vivo*

Ohura and co-workers examined the influence of the addition of 3 wt % of Na_2O_3 , B_2O_3 , Al_2O_3 , Fe_2O_3 , P_2O_5 or F^- in calcium silicate glass to bone bonding in rabbit tibia. All glasses, except glass containing Fe_2O_3 , formed a CaP-rich layer in combination with Si-rich layer on their surfaces within 8 weeks. The four other kinds of glass, except that containing Al_2O_3 , became attached to bone within 8 weeks. Glass containing Al_2O_3 became attached to bone at 25 weeks which was the other follow-up time. Fe_2O_3 containing glass did not attach to bone even at 25 weeks (Ohura, Nakamura and Yamamuro 1992).

Brink et al. made a systematic investigation of the *in vivo* behaviour of glasses in the system Na_2O - K_2O - MgO - CaO - B_2O_3 - P_2O_3 - SiO_2 . They determined the compositional limits for bioactivity, determined the relationship between various oxides and bioactivity and described the *in vivo* behaviour of glasses as a function of their composition. A total of 110 glass implants with 26 different compositions were implanted into rabbit tibia for 8 weeks and the surface layers and surrounding tissues of the implants were evaluated to determine the bioactivity of the samples. The experiment showed that bioactivity of glasses in the system occurs when the glasses contain 14-30 mol % alkali oxides, 14-30 mol % alkaline earth oxides, and <59 mol % SiO_2 . Glasses containing potassium and magnesium bond to bone in a way similar to bioactive glasses developed earlier. (Brink et al. 1997b)

Radin and Ducheyne and colleagues studied the degradation behaviour of Bioglass® granules with narrow particle size (300 – 355 μm). The aim was to use particle size that would bring about a full reaction of the particle, leading to a repaired bone defect site in which the particles would resorb, leaving the site composed only of newly formed biological matter. They observed that the internal reaction layer was removed, leaving behind an internally excavated particle primarily consisting of the *in situ*-formed calcium phosphate. Within these particles, a unique phenomenon took place: Precursor cells for the bone tissue forming osteoblasts were triggered along their pathway to express the osteoblasts function. This then led to the formation of bone tissue and a quick, extensive repair of the defect (Ducheyne 1998; Radin et al. 2000).

2.1.5 Compositional dependence to the manufacturing methods

The form of bioactive glasses in clinical use has been limited mainly to the use of glass in the form of crushed particulates. This is probably due to the property of most of the early bioactive glasses to crystallize when heated, so that further heat treatment with these bioactive glasses is very difficult.

The first report of manufacture and osteoconductivity of silicate-based bioactive glass fibre is by Pazzaglia and co-workers in 1989. The composition of the used glass was the following: 46-53% SiO₂; 4-8% P₂O₅; 9-20% CaO; 7-24% Na₂O; 2.8% K₂O; 1.11% MgO; and 0.12% Al₂O₃. The studied bioactive glass fibres showed the same bone-binding and osteoconductive properties as earlier observed in other bioactive glasses (Pazzaglia et al. 1989). Vita Finzi Zalman et al. observed that bioactive glass can be formed into fibre without devitrification when it has the following composition: 40-55% SiO₂; 5-8% P₂O₅; 20-40% CaO (MgO); 20-30% Na₂O (K₂O); 2-9% K₂O; 0.5-2.5% Al₂O₃, all by weight per cent (Vita Finzi Zalman et al. 1991).

Brink et al. studied different glasses in a system containing boron, sodium, potassium, magnesium, calcium and phosphorus oxides and silica. They carried out an extensive study of the crystallization, viscosity and biological activity of 40 different glass compositions in this system. 14 out of the studied 40 glasses had wide range working properties together with bioactive characteristics. The large working range property of these glasses enables the production of fibres from them. Bioactivity occurred when the glass contained 14-30 mol % of alkali as well as alkaline earth oxides, and <59 mol % of silica. No phosphate-free glass was considered bioactive in this study. The forming properties of bioactive glasses were improved when the content of silica in the glass was increased to 53-56 mol %. They also found that the amount of alkali oxides should be decreased and the amount of alkaline earth oxides increased compared with the bioactive glass compositions in use. (Brink 1997a; Brink 1997b)

Bioactive glass fibres have been also manufactured from phosphate-based glasses (Rinehart et al. 1999) and by using sol-gel method (Peltola et al. 2001). There are also other forms available into which large working range silicate based bioactive glasses can be manufactured. Brink et al. manufactured spherical particles from bioactive glass by flame spraying (Brink et al. 1996). Moritz and colleagues used bioactive glasses as coating on titanium substrates (Moritz et al. 2004).

2.2 Bioactive glasses with cells and tissues

2.2.1 Bioactive glass – cell reactions

The role of cell reactions related to the bioactivity of materials has been a topic of interest ever since the bioactive nature of ceramics was first discovered. But it is only now in the 21st century, as the field of cell engineering field has developed, that research groups have made extensive studies into the relationship between cells and bioactive glasses to explain the phenomena of bone bioactivity.

Ohgushi and co-workers studied the osteoblastic phenotype expression of marrow stromal stem cells on the surface of bioactive materials. From their studies they hypothesize that osteoblastic differentiation could be occurring on the surface of bioactive material. They speculate that binding of biologically active molecules to the surface activated the cell membrane receptors of stromal stem cells resulting in osteoblastic differentiation (Ohgushi et al. 1992). El-Ghannam and co-workers studied the effects on bone cell function of treated and non-treated porous hydroxyapatite and bioactive glass. The treatment to cover the glass surface with formed hydroxyapatite and serum

protein enhanced the expression of high alkaline phosphatase activity, high rates of cell proliferation, and production of mineralised extracellular matrix. The authors assumed the enhancement to be the result of the adsorption of a high quantity of fibronectin from the serum onto the reacted bioactive glass surface. In contrast, a much smaller number of cells attached to the hydroxyapatite ceramic surface which served as a control (El-Ghannam, Ducheyne and Shapiro 1997).

Matsuda and Davies investigated the response of osteoblasts to Bioglass® and compared this to quartz samples. They noticed that in quartz samples no significant production of extracellular matrix (ECM) was seen up to 4 weeks, however in Bioglass® samples, osteoblasts colonized the samples in multilayers and produced abundant ECM in the same time period (Matsuda and Davies 1987). Xynos and co-workers first made an interesting observation when they showed that Bioglass® has the ability to stimulate cell cycling and subsequently enhance osteoblast turnover of human primary osteoblasts *in vitro* (Xynos et al. 2000). Many other research groups have made further studies of this phenomenon. Most of these results have demonstrated the presence of bioactive glass as having a stimulating effect on osteoblasts (Bielby et al. 2004; Bosetti and Cannas 2005; Foppiano et al. 2004; Gough, Notingher and Hench 2004; Lossdorfer et al. 2004; Radin et al. 2005; Valerio et al. 2004; Välimäki et al. 2005), chondrocytes (Asselin et al. 2004) and fibroblasts (Day 2005; Keshaw, Forbes and Day 2005). Josset and co-workers studied the influence of the physiochemical reactions of bioactive glass A9 (50% SiO₂, 20% Na₂O, 16 %CaO, 6% P₂O₅, 5% K₂O, 2%Al₂O₃ and 1% MgO, all by weight per cent) on the behaviour and activity of human osteoblasts *in vitro*. The results did not demonstrate stimulation in DNA synthesis or modification in cell cycling with bioactive glass A9 (Josset et al. 2003). There are also other aspects of the way the bioactive glass surface or the extracts of bioactive glass affect cell behaviour (Radin et al. 2005). Bioactive glass extracts in cell culture medium have been shown to increase osteoblast cell proliferation (Bielby et al. 2004; Foppiano et al. 2004) and induce osteogenic differentiation and cell mineralization (Bosetti and Cannas 2005; Lossdorfer et al. 2004).

Gough and co-workers compared the osteoblast attachment and mineralised nodule formation on rough and smooth Bioglass® monoliths. The study demonstrated that initial cell morphology was less advantaged on the roughened surface, but the cells were able to form a greater number of mineralised nodules on the roughened surface. Hydroxyapatite formation also occurred more rapidly on the rough surface (Gough, Notingher and Hench 2004). Clupper et al. studied the bioactivity of glass Bioglass® fibres and they also evaluated the human osteoblasts attachment to these fibres. Bioglass® glass fibres formed crystalline HA layers in two to four days *in vitro* when immersed in SBF. Osteoblasts attached and spread to the Bioglass® fibre surface after 15-90 minutes and remained attached after 14 days in cell culture.

2.2.2 Antibacterial property of bioactive glasses

Within the last few years one area of interest in bioactive glass research has been the modification of the composition of glass to impart obtain antibacterial properties. Antibacterial material is material which is capable of destroying or suppressing growth or reproduction of bacteria.

Stoor and co-workers examined the antibacterial effects of a paste made from the bioactive glass S53P4 on oral micro-organisms representing periodontal pathogens, caries associated micro-organisms and benign oral microflora. They noticed that in aqueous solution the powdered bioactive glass S53P4 appeared to have a broad antimicrobial effect on micro-organisms of both supra- and subgingival plaque (Stoor et al. 1996; Stoor, Söderling and Grenman 1999; Stoor, Söderling and

Salonen 1998). The same effect has also been observed with Bioglass® particulate (Allan, Newman and Wilson 2001; Allan, Newman and Wilson 2002). Zehnder and co-workers examined the antimicrobial efficacy of bioactive glass S53P4 against *E.faecalis* in dentinal tubules *in vitro*, and observed that bioactive glass performed better than calcium hydroxide (Ca(OH)₂) suspension, which is currently the “gold standard” in endodontic medication. The group concludes, however, that the action has to be verified *in vivo*, as many factors may influence the effectiveness of bioactive glass particles in the root canal system (Zehnder et al. 2004).

2.2.3 Animal studies with bioactive glasses

The pioneering *in vivo* work with bioactive glasses and glass ceramics was performed by Hench and co-workers in the early 1970s. They first observed the strong bond between bioactive glasses of glass–ceramics and hard and soft tissues *in vivo* (Hench and Paschall 1973; Hench, Splinter and Allen 1971; Piotrowski et al. 1975). Later the *in vivo* studies with bioactive glasses have concentrated mainly on resorption, biocompatibility and bone healing (Gasser 2000; Ito et al. 1987; Lin et al. 1991; Merwin et al. 1986; Wilson et al. 1981).

On the basis of *in vivo* animal studies, several areas of potential have been proposed for bioactive glasses in clinical use. Extensive *in vivo* animal studies have been conducted with bioactive glass S54P4, developed by Andersson et al., Lindfors et al. studied the use of S53P4 glass particulates as bone graft material in spine fusion in a rabbit model (Lindfors, Tallroth and Aho 2002). Heikkilä, and co-workers examined new bone formation after filling cancellous bone defects with bioactive glass in granular form, and concluded that bioactive glass is a promising material for that particular indication (Heikkila et al. 1995). The surface reaction in dense S53P4 glass cones also indicated bone bonding (Aho et al. 1993). Comparative studies have been carried out to compare the performance of bioactive glass granules with materials which are currently in clinical use as bone substitute materials. Turunen et al. compared Bioactive glass S53P4 granules and calcium carbonate granules (Biocoral®) in the medullary space of rabbit tibia. A significantly larger bone-biomaterial area was obtained around titanium implants with bioactive glass than with calcium carbonate (Turunen et al. 1997). Peltola et al. compared three synthetic granular bioactive materials, BAG1 (S53P4), BAG2 (13-93) and hydroxyapatite (HA) in a frontal sinus and a skull bone defect obliteration. In histomorphometry, the new bone formation increased with all the investigated materials throughout the study, but the results showed higher new bone formation in the defects filled with BAG1 than corresponding BAG2 and HA (Peltola et al. 2003). Turunen and co-workers studied the performance of S53P4 glass as bone filler around dental implants using rabbit tibia model. Better bone-implant contact was obtained at the defect site with bioactive glass S53P4 than with titanium implants (Turunen et al. 1998). Significantly larger bone-biomaterial area was also obtained around dental titanium implants using bioactive glass S53P4 than with calcium carbonate granules as bone filler (Turunen et al. 1997).

Schepers et al. compared the BioGran™ (45S5) product with commercial HA bone fillers in the bone defects in jaws of five beagle dogs (Scepers et al. 1991). Elshahat compared Novabone C/M (45S5) product with commercial Norian bone filler (Elshahat et al. 2004). Both studies demonstrated that the bioactive glass performed better as bone filler material than the control material. Heikkilä et al. compared the osseointegration of dense S53P5 glass cones and HA cones in rabbit femur epiphyseal and metaphyseal region. Cones from both material groups bonded equally well to bone, and it was concluded that the osseointegration rate of bioactive glass S53P4 does not differ from that of hydroxyapatite (Heikkilä et al. 1993).

Lai and co-workers studied the pathways of resorbed Silicon of bioactive glass in rabbits. They observed that virtually all of the silicon initially implanted from the bioactive glass granules is removed from the granules in soluble form and is transported in the blood and filtered by the kidneys into urine. The lack of silicon accumulation in the organs analysed (blood, kidney, lymph nodes) further supported their hypothesis (Lai, Garino and Ducheyne 2001). Vogel and co-workers examined the development of multinuclear giant cells during the degradation of Bioglass® and less soluble bioactive glass particles in rabbits. Bioglass® particles degraded either in Si-rich remnants or in CaP-rich cells, and both multinuclear giant cells (MNGC) and foreign body giant cells (FBGC) were found on the surfaces of these particles. Osteoclast-like cells were detected on the particles which were transformed into CaP-shells; bone formation was also only observed in CaP rich surfaces. The reactions were alike in all the studied glasses, but delayed in slower degrading compositions. However the reason for the effect finally triggering the formation of FBGC or osteoclasts, or leading to the formation of bone, which all occur on surfaces of particles remains unclear (Vogel et al. 2004).

Välimäki and co-workers evaluated the enhancement of new bone formation of bioactive glass (13-93) microspheres and adjunct bone morphogenetic protein 2 (BMP-2) gene transfer in non-critical bone defects in rat tibia. The study was initiated to determine the molecular mechanism behind bioactive glass action with or without adjunct BMP-2 gene transfer. The hypothesis is that a combination of osteoinductive BMP-2 gene transfer and osteoconductive bioactive glass could have a synergetic promoting effect on new bone formation. On the basis of this study the impact of bioactive glass seems to saturate new bone formation on its surface and thereby overshadow the effect of BMP-2 gene transfer in non critical bone defects (Välimäki et al. 2005).

2.2.4 Clinical use of bioactive glasses

The clinical use of bioactive glasses has been most widely adopted in oral applications. The first devices based on bioactive glass were indicated for oral and periodontal bone defects, namely PerioGlas® (NovaBone Products, LLC, Alachua, FL, USA) and BioGran® (3i Implant innovations, INC, Palm Beach Gardens, FL, USA). Currently there are several other products commercially available. NovaBone – C/M® is indicated for cranio-maxillofacial bone defects and NovaBone®, which is indicated for orthopaedic bone defects; both are manufactured by NovaBone Products, LLC. All these devices are based on the Bioglass® - composition. The latest bioactive glass devices on the market are AbMinGranio™ granules and AbMinGranio™ plates manufactured by Vivoxid Ltd (Turku, Finland); both are manufactured from S53P4 bioactive glass. The granules are indicated for the obliteration of chronically infected frontal sinuses and frontal bone defects. Plate is indicated for the treatment of a broken orbital floor.

In early clinical studies where Bioglass® was used for the first time, it was used as middle ear prosthesis (Merwin 1986) and in oral and facial bone augmentation (Stanley et al. 1987; Wilson and Merwin 1988). Several subsequent clinical reports have been published, mainly on the use of bioactive glass particulates in periodontal defects (Low, King and Krieger 1997; Schmitt et al. 1997; Zamet et al. 1997).

Some clinical studies with S53P4 bioactive glass have been carried out in Turku (Finland) within recent decades. Peltola, Aitasalo and co-workers used S53P4 glass granules in human frontal sinus obliteration. They concluded that bioactive glass is a promising and well-tolerated bone graft suitable for osteoplastic frontal sinus operations. Total accurate obliteration of the sinus is achieved with different sizes of granules and blocks. The results of the obliteration are maintained owing to

the stability of the material (Aitasalo et al. 1997; Peltola et al. 1998). Heikkilä and co-workers have used S53P4 bioactive glass granules as bone filler in benign bone tumour surgery. Clinically, BG granules were well accepted with no adverse effects and observations indicated bone formation in bone defects. According to the authors, the results demonstrate that bioactive glass S53P4 alone can be used as filler in bone defects (Heikkilä et al. 1995). Aho and co-workers reported a 13 year follow-up of successful remodelling of the tibia after grafting a large cavity with particulate bioactive glass S53P4-hydroxyapatite (Aho et al. 2003). Turunen et al. studied the effect of bioactive glass S53P4 granules as a bone adjunctive material in maxillary sinus floor augmentation. Bioactive glass granules were mixed with autologous bone (AB) chips in a 1:1 mixture; as a control autologous bone chips alone were used. The results indicated that the combined use of bioactive glass S53P4 granules with AB chips for augmentation of the maxillary sinus floor diminishes the amount of bone needed for augmentation and results in the same quantity of bone as when AB chips alone are used (Turunen et al. 2004).

2.3 Composites

2.3.1 Theoretical base of composites

Composite materials consist of two or even more different material components or phases which are combined with the aim of improving physical, mechanical and/or biological properties. The different phases can be selected from various material classes such as metal, ceramics or polymers, but combinations of the same material types are also possible. The main reason for using composites materials has been the opportunity of optimising mechanical properties to mimic the properties of living tissues. Various different types of composite have been developed and used for medical application. There is a detailed review of polymer-composite materials used in biomedical applications within last 30 years by Ramakrishna and colleagues (Ramakrishna et al. 2001). The focus of this review is on bone tissue mimicking composites, mainly in biodegradable bioactive glass – biomedical polymer composites. The hydroxyapatite (HA)-polyethylene (PE) fibre and self-reinforced polylactide fibrous composites are also briefly reviewed.

Composites make up a very interesting class of bioactive materials mostly because it is possible to tailor their structure and properties to suit the service conditions. A great deal of research has been carried out into composite science to understand how the structure can be tailored to meet the property requirements of the composite. One of the simplest estimations of the properties of composites is the equation called ‘Rule of Mixtures’

$$E_1 = (1-f)E_m + fE_f$$

in which E_1 is the modulus of the final composite, E_m the modulus of matrix and E_f the modulus of the reinforcing element (most commonly fibre) and f the volume fraction of the reinforcing element. The ‘rule of mixtures’ indicates that composite stiffness is a simple weighted mean between the moduli of the two components, dependent only on the volume fraction of the reinforcing elements. (Hull and Clyne 1996)

One of the early ways of using composite technology as bone mimicking material was the use of hydroxyapatite (HA)-polyethylene composite by Bonfield (Bonfield et al. 1981). Here it was demonstrated that an increase in the volume fraction of particulate HA from 0 to 0.5 in HA-polyethylene composite produced an increase in the Young’s Modulus of this composite. Transition from ductile to brittle fracture occurs as the volume fraction of HA increases above 0.45. (Bonfield

1988; Bonfield 1993). It was observed that new bone formed in close contact to the HA-PE implant. They also found that where bone is seen growing directly on the implant the crystal, the growth is often epitaxial to the nearest crystalline HA in the composite (Doyle et al. 1990).

2.3.2 Bioactive glass/medical resorbable polymer composites

Despite osteoconductive potential and superior bone bonding character, the direct application of bioactive glass in load-bearing situations has been limited. Bioactive glasses are ceramic in nature and although they possess high compressive strength, they are unfortunately very brittle. In order to utilize the osteoconductive and bioactive properties of bioactive glass, many groups have started to explore the potential of combining bioactive glass and biomedical resorbable polymer. By combining biomedical resorbable polymers and bioactive glass phase, the following improvements are expected: (1) a better growth environment due to good osteoconductivity properties provided by the bioactive phase, (2) the acidic degradation by-products from polyesters may be buffered, and (3) the mechanical properties may be improved by using the traditional composite approach (inclusion of a stiffer particulate ceramic phase in the polymeric matrix) (Boccaccini and Maquet 2003).

There is a good deal of interest in finding good alternatives to metal implants from resorbable materials since they may overcome the problems associated with metal implants, such as stress protection, potential for corrosion, wear or debris formation, as well as the necessity of implant removal. Among synthetic resorbable biomedical polymers, polyhydroxyacids are the most commonly used. These are poly(L-lactide), poly(glycolide) and copolymers based on L-lactide, L/DL-lactide, DL-lactide, glycolide, trimethyl carbonate and ϵ -caprolactone (Gogolewski 2000; Törmälä, Pohjonen and Rokkanen 1998). The bioactive glass in composites has been used mainly as particulates. The mechanical properties and *in vitro* performance of bioactive glass reinforced polymers have been studied by several groups. There are attempts to manufacture porous composites for tissue engineering applications, materials for use as artificial bone graft and materials for use in orthopaedic fixation devices.

2.3.2.1 Porous composites

Roether et al. fabricated a composite material containing macroporous poly(DL-lactide) foams which were coated by Bioglass® particles. Stable and homogenous Bioglass® coatings were achieved throughout the porous network using a slurry-dipping technique in conjunction with pre-treatment of the foams in ethanol. *In vitro* studies in simulated body fluid showed HA formation in composite surfaces (Roether et al. 2002). Maquet and co-workers manufactured highly porous composite scaffolds of poly-D,L-lactide (PDLLA) and poly(lactide-co-glycolide) (PLGA) containing different amounts of Bioglass® by thermally induced solid-liquid phase separation and subsequent solvent sublimation. The addition of increasing amounts of Bioglass® into the polymer foams decreased the pore volume while increasing the mechanical properties. The polymer molecular weight was found to decrease more rapidly and more extensively in the absence of Bioglass® when compared to composites containing Bioglass®. The formation of a hydroxyapatite layer on the surface of composites containing Bioglass® was also observed (Maquet et al. 2004).

Phase separation technique has also been used to manufacture poly L-lactide/bioactive glass (PLLA/BG) composites by which large pores (> 100 μ m) are present in a network of smaller interconnected pores. The porous microstructure of the composites was not significantly influenced by the glass content. Silane pre-treatment of bioactive glass (BG), (4.6% MgO; 44.7% CaO; 34.0%

SiO₂; 16.2% P₂O₅ and 0.5% CaF₂, all in weight-%) particles in PLLA/BG composites enhanced the increase in modulus and prevented a decrease in tensile strength when the amount of bioactive glass was increased. Both of the composites formed a bone-like apatite layer both inside and on their surfaces when soaked into SBF, though the silane treatment of the glass particles delayed *in vitro* apatite formation (Zhang et al. 2004).

Lu et al. fabricated poly(lactide-co-glycolide) (PLGA)-Bioglass® composites in disc and composite microsphere forms using a solvent casting technique. A porous polymer-ceramic composite with a porosity of 43% was obtained. In cell studies the scaffold was found to support the growth, differentiation and mineralization of human osteoblast-like cells *in vitro*. The scaffold was also found to be bioactive, as it formed surface calcium phosphate deposits in the presence of cells and proteins *in vitro* (Lu, El-Amin and Laurencin 2001; Lu et al. 2003). They further studied the compositional effects on the formation of a calcium phosphate layer and the response of osteoblast-like cells on PLGA- Bioglass® composites. With increasing Bioglass® content, incubation time required for the formation of Ca-P nodules increased. The growth and differentiation of human osteoblast-like cells on the composite was a function of Bioglass® content, the composites with 10 wt% and 25wt% of Bioglass®, were more suitable for osteoblast differentiation than the 50 wt% group. The findings of this study suggest that there is a threshold Bioglass® content which is optimal for osteoblast growth, and the interactions between PLGA and Bioglass® may modulate the kinetics of Ca-P formation as well as the overall osteoblastic response (Lu et al. 2005).

Verrier and co-workers examined the effect of the content of Bioglass® (0-40 wt%) in poly(DL-lactide acid) (PDLLA) porous foams on the behaviour of MG-63 (human osteosarcoma cell line) and A549 cells (human lung carcinoma cell line). An increase in cell adhesion with an increased content of Bioglass® present in the foams was observed for both cell types. Better aptitude of the A549 cells to proliferate on PDLLA foams containing 5 wt% Bioglass® compared to the foams with 40 wt% Bioglass® was shown. Moreover, the lowest proliferation rate was obtained for cells on pure PDLLA foams (Verrier et al. 2004). Using a modified emulsion method, Yao et al. manufactured porous poly(lactide-co-glycolic acid) (PLGA)/Bioglass® microspheres, which were then poured into a mould and heated to form a porous scaffold. This PLGA-(30 wt%) Bioglass® microsphere-based porous scaffold was found to be bioactive because it formed a Ca-P layer on the composite surface *in vitro*. The scaffold demonstrated that it supported cell growth and promoted the differentiation of marrow stromal cells into osteoblast cells (Yao et al. 2005).

2.3.2.2 Injectable composites

Rich, Jaakkola, and co-workers have manufactured injectable composites of poly(ϵ -caprolactone-co-DL-lactide) and bioactive glass S53P4 by compounding and compression moulding. A homogeneous distribution of the bioactive glass granules was achieved with amounts of 40, 60 and 70 wt% of glass. The formation of a biologically active Ca-P layer was detected, the fastest rate of formation was observed in composites containing smaller-range glass (< 45 μ m) and 60wt% of glass. The presence of bioactive glass affected the rate of polymer degradation and the greater the amount and the smaller the particle size range of the bioactive glass particles, the more rapid was the deterioration in molecular weight of the samples (Jaakkola et al. 2004; Rich et al. 2002). The developed composite materials were further studied for bone and cartilage construction in cancellous and cartilaginous subchondral bone defects in rabbits. The glass granules of the composites resulted in good osteoconductivity and bone bonding that occurred initially at the interface between glass and host bone. The bone bioactivity index as well as bone coverage index,

correlated with the amount of glass in the composite. According to the study, the composites were osteoconductive and easy to handle with a short setting time. They were also biocompatible with a low foreign body cellular reaction. (Aho et al. 2004) Another study was performed with the composite in bone defects in rabbit femoral condyles and the tibia. In this study composites with 60 wt% of small bioactive glass particles, and composites with 40 wt% and 60 wt% of large particles were investigated. Copolymer without glass was used as control. The study showed that bioactive glass granules improve the bone response. However, the authors concluded that although the composite initiated new bone formation, it is not yet really an optimal bone filler material. Glass granules can only conduct bone growth efficiently provided that a direct glass-to-bone contact can be achieved. (Närhi et al. 2003)

2.3.2.3 Particulate reinforced composites

Niiranen and co-workers developed self-reinforced poly(L/DL)lactide/bioactive glass (13-93) composite rods for fracture fixation (Niemelä et al. 2005; Niiranen et al. 2004). Osteotomies of the distal femur of rats were fixed with the developed composite rods. The study showed that developed composites are suitable for fracture fixation as long as the fixation technique is correct. It was also observed that the used composite rods seem provoke an osteostimulatory response at the tissue-implant interface after implantation (Pyhältö et al. 2004).

2.3.3 Fibre reinforced composites as medical materials

There are some early reports of bioactive phosphate glass fibres being used as part of biodegradable composites. The processing and mechanical properties of bioactive or resorbable calcium phosphate glass fibre reinforced composite materials has been reported by Dunn (Dunn, Casper and Kelley 1985) by Lin (Lin 1986), and by Krebs (Krebs, Lin and King 1993). Subsequently, Andriano et al. performed experiments in which absorbable crystalline, calcium-sodium-metaphosphate microfibrils were treated with trimethoxy-based silane coupling agents. The treated fibres were further used as a reinforcing part in a composite. poly(L-lactic acid) and poly(ortho ester) were used as polymer phase. In both experiments the treatment increased the mechanical properties of the composite compared with the composites reinforced with untreated fibres (Andriano and Daniels 1992; Andriano, Daniels and Heller 1992).

Marcolongo et al. have published *in vitro* and *in vivo* studies of bioactive glass fibre reinforced polysulfones. They found that bone tissue exhibited direct contact with the glass fibres and adjacent polymer matrix, resulting in interfacial bond strengths significantly higher than with polymer controls (Marcolongo et al. 1998; Marcolongo, Ducheyne and LaCourse 1997).

Another interesting possibility is to use polymer fibres as a reinforcing phase with the isotropic/amorphous phase of the same material being a matrix. Törmälä and co-workers developed a composite material, which is self-reinforced i.e. it is formed of polymer or co-polymer matrix and is reinforced with the units which have the same chemical composition as that of the matrix (Törmälä et al. 1988). The composites were initially manufactured by compressing fibrous polymeric sutures, just below their melting temperature to obtain a solid form. The self-reinforcing (SR) technique was further developed so that the fibrillated oriented structural units were formed by solid state extrusion (i.e. pulling the polymer billet through a die, below the melting temperature of polymer) to obtain molecular orientation. The oriented structures have significantly higher mechanical properties than non-oriented forms (Törmälä, Pohjonen and Rokkanen 1998; Törmälä

et al. 1990). The improved performance of self-reinforced structures has been demonstrated in several studies (Saikku-Backstrom et al. 1999; Törmälä et al. 1991). The self-reinforcing technique has also been applied with polyethylene by Ward and co-workers (Hine et al. 1993; Maxwell, Unwin and Ward 1996; Morye et al. 1998; Olley et al. 1993).

2.4 Tissue engineering

2.4.1 Current trends in Tissue engineering

Tissue engineering presents an alternative approach to the repair and regeneration of damaged human tissue, eliminating the need for permanent implant. The underlying principle involved is the regeneration of living tissue, where loss or damage has occurred as a result of injury or disease. Tissue engineering is a new and very rapidly growing area in the medical arena and huge potential is seen in it. However, it is also agreed that many challenges remain and further development in this area will require ongoing interaction and collaboration among scientists from multiple disciplines. (Bonassar and Vacanti 1998; Chapekar 2000; Griffith and Naughton 2002; Stock and Vacanti 2001; Vats et al. 2003; Williams 2004). The huge interest in tissue engineering can be seen, for example, in the number of publications and granted patents which have been growing rapidly during the last decade. Figure 1 shows the number of publications from 1991 to 2002 and Figure 2 presents the number of US patents granted in the field of tissue engineering between 1988 and 2001.

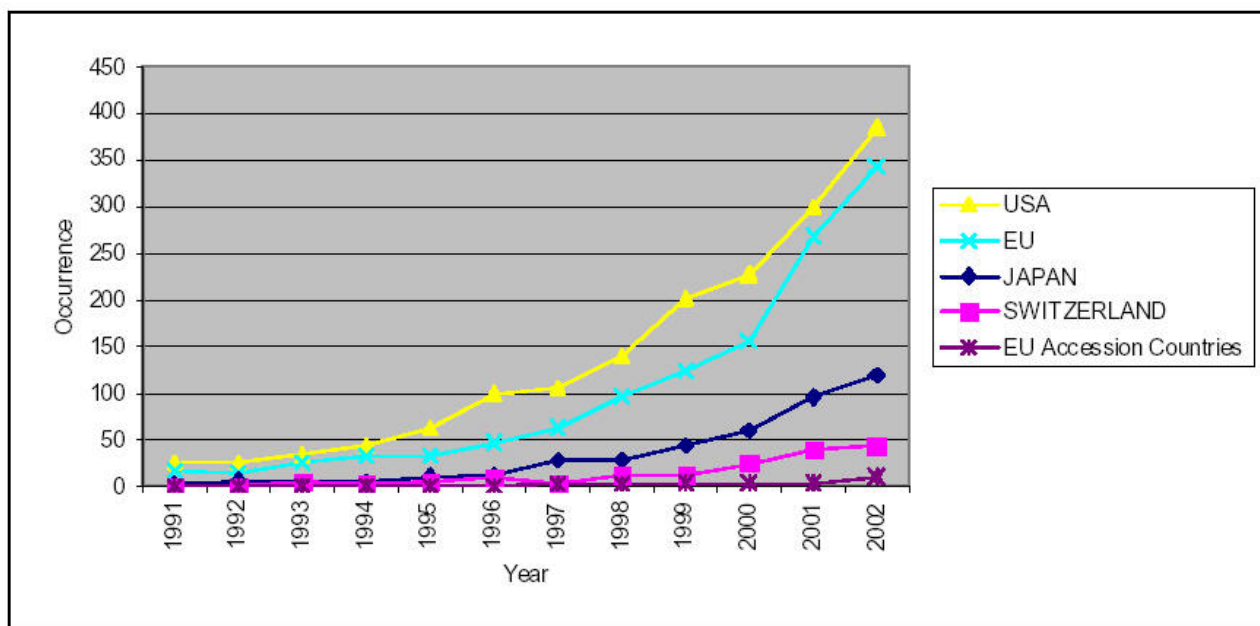


Figure 1. Tissue engineering Publications 1991-2002 (Senker and Mahdi 2003).

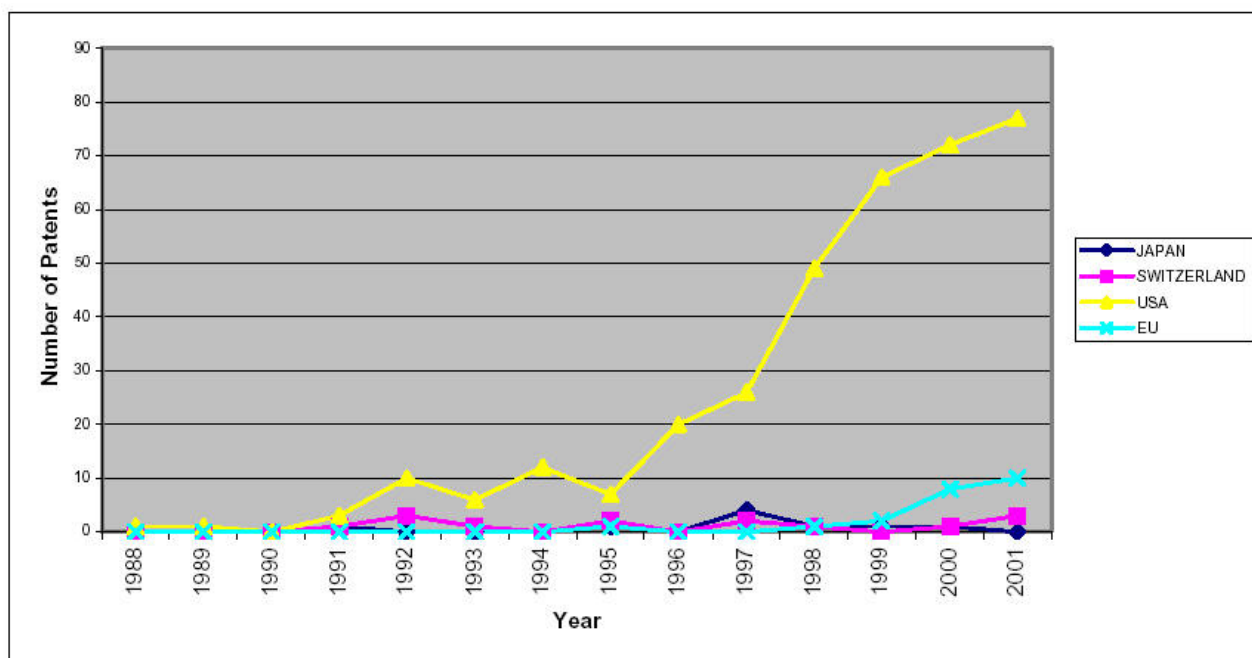


Figure 2. Tissue engineering USPTO Patents 1988 - 2001 (Senker and Mahdi 2003).

The main current research topic in tissue engineering is the creation of new tissues. This involves constructing artificial scaffolds from biomaterials to mould or guide the growth of cells, with biomolecules regulating the behaviour of both biomaterials and cells. In addition the large-scale production of tissues, cell expansion, storage, and transport are issues seen as challenges for the future (Senker and Mahdi 2003). Currently there are tissue engineering products made for skin and cartilage repair. Nonetheless, the field is clearly experiencing difficulty transitioning from a development stage industry to one with a successful product portfolio and profitable industry (Lysaght and Hazlehurst 2004).

There are several good review articles on tissue engineering scaffolds (Burg, Porter and Kellam 2000; Hutmacher 2000; Shin, Jo and Mikos 2003; Temenoff and Mikos 2000a; Temenoff and Mikos 2000b). The research interest has been mainly in porous polymeric and composite foams. In this review the main focus is on the use of fibres for scaffolds or as parts of scaffolds.

2.4.2 Fibrous tissue engineering scaffold

Despite today's large investment in tissue engineering research (Lysaght and Hazlehurst 2004), the need to further optimise biomaterial scaffolds used for tissue engineering purposes is widely recognized (Cancedda et al. 2003; Hutmacher 2000; Ma 2004). There are a number of research groups investigating the optimal characteristics for the scaffold. One important consideration in tissue engineering constructs is nutrient transport to the scaffold interior as well as the metabolic and degradation waste outflow from the scaffold. The aim here, involves the simultaneous optimisation of several factors related to scaffold architecture, including porosity, pore size, permeability, channel tortuosity, and degradation properties (Karande, Ong and Agrawal 2004). These factors must all be considered along with the choice of biomaterial and manufacturing method which will also have a bearing on important matters such as the mechanical properties and clinical manageability of the scaffolds.

2.4.2.1 Fibrous scaffolds for bone and cartilage tissue engineering

Tissue engineering poses new challenges in the area of biomaterials research. For bone and cartilage tissue engineering applications, in particular, there is a need for the development of even better scaffold materials (Bonassar and Vacanti 1998; Hutmacher 2000). In tissue engineering the scientific issues involve an understanding of cells, their mass transport requirements and biological environment as well as the development of suitable scaffold materials to achieve cell adhesion, growth and proliferation. Depending on the tissue under consideration, the scaffold must fulfil several physicochemical and biological requirements. Hutmacher has summarized the requirements for scaffolds in the field of musculoskeletal engineering (Hutmacher 2000). For use in this field, the ideal scaffold characteristics should be the following: (1) three dimensional and highly porous with an interconnected pore network for cell growth and flow transport of nutrients and metabolic waste, (2) biocompatible and bioresorbable with controllable degradation and resorption rate to match cell/tissue growth *in vitro* and/or *in vivo*, (3) suitable surface chemistry for cell attachment, proliferation, and differentiation and (4) mechanical properties to match those of the tissues at the site of implantation. For bone tissue application, osteoconductivity would also be a desirable property (Boccaccini and Maquet 2003).

Mahmood and co-workers have studied the geometric effect of matrix upon cell differentiation (Mahmood et al. 2001). They used bioactive glass (CPSA = 32.24% CaO; 9.26% P₂O₃; 41.00% SiO₂; 17.59% Al₂O₃, all in mol-%) fibres with a diameter of 8-30 µm and studied BMP-induced osteogenesis in glass fibre samples with different geometry. The CAPA fibre samples studied were either formed into balls with an open random structure or used as a fibre bundle. The measured alkaline phosphatase activity, osteocalcin content and bone formation were all significantly higher in the ball samples. The author concluded that BMP-induced bone formation is highly dependent on the porous vasculature-inducing geometry of the matrix.

In the field of tissue engineering, cartilage is seen as the potential “next tissue” to be formatted because it is not vascularized and incorporates only one cell type (Temenoff and Mikos 2000b). However, cartilage defects have only limited capability to heal, and major cartilage damage is often followed by implantation of prosthesis in the joint. Malda and co-workers compared two scaffolds manufactured with different methods, namely compression-moulding/particulate-leaching (CM) and 3D fibre deposition (3DF), which resulted in different pore architecture for tissue engineered cartilage (Malda et al. 2005). Average pore size of tortuous CM scaffolds was 182 µm, while 3DF scaffolds had an organized structure of 525 µm pore size; both structures had porosity between 75 to 80 %. *In vivo*, significantly more cartilaginous tissue was formed within the 3DF constructs compared with the CM constructs. Scaffold architecture had no effect on the formation of type II collagen. Miot and co-workers extended the study to evaluate the effect of scaffold composition (Miot et al. 2005). They found that by increasing the hydrophilic nature of the scaffold in combination with highly interconnecting and accessible pore architecture, it is possible to promote chondrocyte redifferentiation and cartilaginous matrix accumulation in 3D porous scaffolds. This study also compared the 3DF scaffold with the CM scaffold, demonstrating the improved performance of the former. In order to construct a more optimal scaffold for cartilage engineering, the author envisions a composite containing a porous template scaffold with appropriate mechanical properties which could be coated with another substrate capable of promoting chondrocyte redifferentiation and cartilaginous matrix deposition. Moroni et al. have studied various different 3DF structures to evaluate the influence of pore geometry and architecture on the dynamic mechanical properties of 3D fibre-deposited scaffolds. Their study showed that viscoelastic properties of 3DF scaffolds can be modulated to attain the mechanical requirements needed in tailored tissue engineered applications (Moroni, de Wijn and van Blitterswijk 2005).

2.4.2.2 Fibrous scaffolds by novel manufacturing methods

Method of manufacture greatly affects the scaffold's properties and there are a variety of different manufacturing methods utilizing fibres to form scaffolds for tissue engineering applications. One novel technique is electrospinning. Polymeric nanofibre matrix manufactured by electrospinning is similar to natural non-woven fibrous extracellular matrix (ECM) protein, and is thus a suitable candidate ECM-mimetic material. Functionalisation of polymeric nanofibres, which can be realized by bulk or surface modification, is likely to find wide application in biotechnology (Chua et al. 2005; Khil et al. 2005; Ma et al. 2005). However, the reaction condition of nanofibrous scaffolds should be further optimised to prevent the material being degraded too fast (Ma et al. 2005). There are several groups proposing the use of electrospinning to create scaffolds for tissue engineering (Kidoaki, Kwon and Matsuda 2005; Lee et al. 2005; Shin, Yoshimoto and Vacanti 2004; Yoshimoto et al. 2003).

Other novel ideas are fibrous hybrid structures in which different materials and/or different structures are combined. Kellomäki et al. have developed composite structures for guided bone regeneration. The developed hybrid composites combine either PLA70 plate and PLA96 mesh or P-(ϵ -CL/L-LA) film and PLA96 mesh. In *in vivo* tests, bioabsorbable mesh protected the bone graft from resorption and enhanced the osteogenic activity in the grafted maxillary alveolar cleft area when compared with control defects (Kellomäki et al. 2000). Hokugo and co-workers manufactured a hybrid scaffold from fibrin and biodegradable PGA fibre. PGA fibre incorporation enabled the fibrin sponges to significantly enhance their compression strength. In the *in vitro* cell culture studies the number of fibroblasts attached was also significantly larger in PGA reinforced sponges and this is considered to be caused by the suppressed shrinkage of these sponges (Hokugo, Takamoto and Tabata 2006). Shao and co-workers developed a hybrid composite for osteochondral defects which combines a 3DF scaffold made of polycaprolactone (PCL) for the bone compartment and fibrin glue which is used for the cartilage part. The results demonstrated that PCL scaffold is a potential matrix for osteochondral bone regeneration, while fibrin glue was shown not to inherit the physical properties to allow cartilage regeneration (Shao et al. 2005). Chen et al. developed a novel PLGA fibre/collagen composite scaffold for engineering of articular cartilage tissue. The composite scaffold has web-like collagen microsponges formed in the openings of a mechanically strong knitted mesh of poly(lactid-co-glycolic acid). The developed structure facilitated cell seeding, cell distribution, and tissue formation. The biomechanical properties, namely dynamic complex modulus and stiffness, were measured in bovine native cartilage and engineered cartilage (after 12 weeks from implantation) and the results demonstrated similar biomechanical properties in both tissues. One benefit of the developed structure is the adjustability of the size and thickness of the scaffold by simply rolling or laminating the web sheets (Chen et al. 2003). Yamane and co-workers developed fibrous chitosan-based hyaluronic acid hybrid biomaterial for cartilage tissue engineering. In cell culture studies with the scaffold, chondrocytes proliferated, and maintained their morphological phenotype. A rich extracellular synthesis was observed around the cells (Yamane et al. 2005).

2.4.3 Tissue engineering scaffolds manufactured from bioactive glasses

Bioactive glass is considered to be a good material choice for achieving repair of bone tissue because of its resorbability and its osteo-stimulating effect (Ducheyne and Qiu 1999). Currently there are two types of tissue engineering scaffolds manufactured from bioactive glass being reported. Livingston and co-workers developed a porous block from bioactive glass 45S5 particles by mixing the particles with camphor particles and then dry pressing and heating the block with decomposition of camphor additive resulting in a porous scaffold. The blocks were further conditioned in SBF to form a carbonated hydroxyapatite surface for optimum bone cell activity. *In*

vitro synthesized bone was formed to this ceramic scaffold and the tissue engineered construct was then implanted into anterolateral, femoral diaphysis of rats. The study demonstrated a more rapid return of mechanical function by initially providing early bone tissue integration, though the new bone formation over the primary group (scaffold without cells) was not enhanced by cell seeding into the scaffold (Livingston, Ducheyne and Garino 2002). Jones and co-workers have manufactured a porous sol-gel bioactive glass 58S (60% SiO₂; 36% CaO; 4% P₂O₅ all in mol-%) scaffold by foaming (Jones, Ahir and Hench 2004; Jones, Ehrenfried and Hench 2006; Jones and Hench 2004).

There is also interest in enhancing neovascularization of tissue-engineering constructs since this has been a limiting factor in the engineering of large tissue constructs. Day studied the ability of bioactive glass to stimulate the secretion of angiogenic growth factors from human stromal cells and subsequent angiogenesis *in vitro*. Results showed that surfaces coated with Bioglass® produced a significant increase in the secretion of endothelial growth factor (VEGF) and basic fibroblast growth factor (bFGF). The increased proliferation of human dermal microvascular endothelial cells and the significant increase in the formation of anastomosed networks of human endothelial cell tubules were also detected with stimulated fibroblasts (Day 2005). Keshaw and co-workers also obtained similar results with alginate beads containing Bioglass® particles (Keshaw, Forbes and Day 2005). It can be concluded that the ability of Bioglass® to stimulate the release of angiogenic growth factors and also promote angiogenesis provides a novel alternative approach for stimulating neovascularization of tissue-engineered constructs.

3 Aims of the study

The aims of the study were to investigate the following four issues;

1. The effect of the composite structure on the mechanical properties of various hydroxyapatite polyethylene composites (I)
2. The manufacture and characterisation of bioactive glass fibres (II, III).
3. The manufacture and characterisation of biomedical polymer/bioactive glass fibre composites (IV, V).
4. The manufacture and characterisation of scaffolds by sintering bioactive glass fibres (VI, VII).

4 Materials and methods

4.1 Materials

The following materials were used in this study. Roman numerals identify the publications in which they were used.

Bioceramics:

1. Synthetic hydroxyapatite [Ca₁₀(PO₄)₆(OH)₂] Grade P88, with average particle size of 4.14 μm, Biotad Ltd, UK. (I)
2. Bioactive glass 13-93, with composition of 6 % Na₂O, 12 % K₂O, 5 % MgO, 20 % CaO, 4 % P₂O₅ and 53 % SiO₂, all in weight-%. Manufactured in Institute of Biomaterials, Tampere University of Technology and in Inion Oy. (II, IV, V, VI)
3. Bioactive glass 9-93, with composition of 12 % Na₂O, 15 % K₂O, 5 % MgO, 1 % B₂O₃, 11 % CaO, 2 % P₂O₅ and 54 % SiO₂, all in weight-%. Manufactured in Inion Oy. (III, VII)

Polymers:

1. Polyethylene Rigidex HM 4560XP, BP Chemicals Ltd, UK. (I)
2. Polyethylene GUR 412, medical grade, Hoechst Ltd, UK. (I)
3. HMPE fibres, manufactured by SINS Fibres, Cesano Maderno, Italy, These continuous fibres were either woven as plain weave by James Carr and Sons Ltd, UK, or chopped (3.5 mm nominal length) by Hoechst Celanese Fibres, Charlotte, NC, USA. (I)
4. Poly(L-lactide-co-D,L-lactide)(70/30), Resomer LR 708, Boehringer Ingelheim, Germany. (IV, V)
5. Poly (L-lactide-co-trimethylene-carbonate) Boehringer Ingelheim, Germany. (V)
6. Poly (L-lactide), Purac, Holland. (V)
7. Poly (DTE Carbonate), Intrgra LifeSciences Corporation, USA. (V)
8. Poly (ε-caprolactone-co-L-lactide)(50/50), Helsinki University of Technology, Finland (Hiljanen-Vainio, Karjalainen and Seppälä 1996) (V)
9. Poly (ε-caprolactone-co-L-lactide)(80/20), Helsinki University of Technology, Finland (Hiljanen-Vainio, Karjalainen and Seppälä 1996) (V)
10. Polyactive®. H.C. Implants B.V., Holland. (V)

4.2 Processing and manufacturing

4.2.1 Manufacturing of glass and glass fibres

Manufacturing of Bioactive glass

The raw materials used for the manufactured bioactive glasses were analytical grade Na₂CO₃, K₂CO₃, MgO, CaCO₃, CaHPO₄ • 2H₂O as well as SiO₂. The raw materials were weighed and mixed in a plastic container and then melted in a platinum crucible for three hours at 1360°C. In order to achieve a homogeneous glass, the formed glass was crushed into pieces of approximately 1 cm³ and re-heated for 3 hours at 1360°C. The same manufacturing method was used to manufacture both 13-93 and 9-93 bioactive glasses.

Manufacturing of bioactive glass fibres

The glass fibre manufacturing equipment was set up to perform melt-spinning tests. The apparatus contained a furnace with an opening at the bottom, as well as a fibre spinning unit. The unit was placed approximately 1.5 m below the furnace to enable the fibres to fully cool down before being spun onto a roll. The speed of the spinning roll was controlled by adjusting the rolling speed of the motor and by changing the roll diameter. To perform the melt spinning of the fibres, the formed glass block was heated in a platinum crucible with orifices at the bottom. After a while, the glass melt started to drain slowly, forming continuous fibres from each of the nozzles. The drained glass drops/fibres were attached to a spinning roll creating continuous fibres. The achieved fibre diameter could be adjusted from approximately 20 μm up to 300 μm . The optimum fibrillation parameters were determined by varying the diameter of the orifices and melt temperature over a series of experiments. It was observed that with a nozzle diameter of from 3.7 mm to 4.1 mm, the melt spinning of bioactive glasses 13-93 and 9-93 was successful. The optimal melt temperature for glass 13-93 was 960°C and 810°C for glass 9-93.



Figure 3. Fibre manufacturing equipment.

4.2.2 Manufacturing of composites

Four main types of composites were manufactured in this study, namely 1) polyethylene (fibre or/and particle) -hydroxyapatite particle composites, 2) bioactive glass fibres with polymer coating, 3) bioactive glass fibre reinforced polymer rods, and 4) porous bioactive glass fibre scaffolds.

4.2.2.1 Polyethylene-Hydroxyapatite composites

There are three main production routes which have been followed in mixing hydroxyapatite particles (HA) and polyethylene (PE);

1. Compounding HA and PE (Rigidex) powders in a twin screw extruder. The HAPEX™ contains 40 vol.-% of HA and 60 vol.-% of PE, and R.HAPEX contains 20 vol.-% of HA and 80 vol.-% of PE. The technique was developed at the ICR in Biomedical Materials (Wang, Porter and Bonfield 1994). These materials were supplied for this project by IRC in Biomedical Materials, Mary Queen College, London.
2. “Dry” mixing of HA and PE powders in a mechanical blender. HA particles were mixed either with PE powder (GUR 412) or with HAPEX™ to obtain composite powders with 50 and 60 vol.-% HA content. This composite was prepared by first blending hydroxyapatite either with HAPEX™ or PE, after which the mix was moulded into rods at 180°C - 220°C, and then chopped and powderised in a centrifugal mill. The powder with HA and HAPEX™ is later referred to as E.HAPEX (E.HAPEX contains 60 vol.-% of HA).
3. Mixing HA or HA/PE composite particles with PE woven fibres using liquid nitrogen. HA or HA/PE powder was poured into a bowl containing liquid nitrogen (LN). Boiling of LN caused dispersion of particles in the liquid. PE fibre mats were immersed in this liquid causing the particles to adhere to the surface of fibre mats.

Figure 4 shows the samples of the used PE woven fibre mats; at the top is the reduced woven fibre mat and below the standard woven fibre mat.

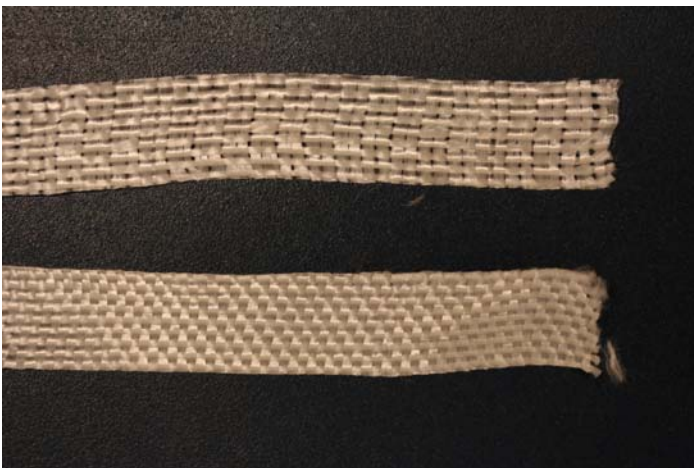


Figure 4. Woven fibre mats. Reduced woven fibre mat above and standard woven fibre below.

Composite samples were manufactured by first loading the composite powder and the woven fibre mats into a steel mould. The quantity of the powder and fibre mats was measured by weight. The powder was mostly HA/PE composite or, occasionally, 100% HA. The woven fibre mats were used

as supplied (referred to as ‘standard’ weave) or with one out of every three picks from the weft removed (referred to as ‘reduced’ weave). The picks were removed under a magnifier with hand-held tweezers. The samples were further hot-compacted in a uni-axial hydraulic hot press and specimens with thickness of approximately 2 mm, width of 10 mm and length of 150 mm were obtained. The temperature during compaction was monitored with a probe connected to an electronic thermometer, inserted with a tight fit into a hole bored into a mould. The material inside the mould was maintained at a pre-determined temperature for 20 min under low pressure to ensure good thermal contact between the mould and the two hot plates of the press. The compression load was then increased rapidly to 9 tonne (60 MPa pressure), when heating was switched off and water cooling of the hot plates then started. The mould was maintained at constant pressure until reaching 50 °C, after which it was left on a bench to cool to room temperature before removing the sample. A more detailed description of the process can be found in manuscript I.

In order to measure the fraction of HA and PE in the manufactured samples, fractions of samples (an approximate mass of 0.1 g was used in each case) were heated at ceramic crucible 500 °C for 30 minutes, so that all PE was burned, whereas HA remained in the crucible. By measuring the initial dry weight of the composite and the remaining HA (both with accuracy of 0.0001 g) the weight fractions of the components were calculated. Three parallel pieces from each sample were used for each measurement.

4.2.2.2 Bioactive glass fibres with polymer coating,

Two different methods were used to coat bioactive glass 13-93 fibres with biodegradable polymers, namely 1) dipping, and 2) pulling through. Figure 5 presents a schematic diagram of the coating methods.

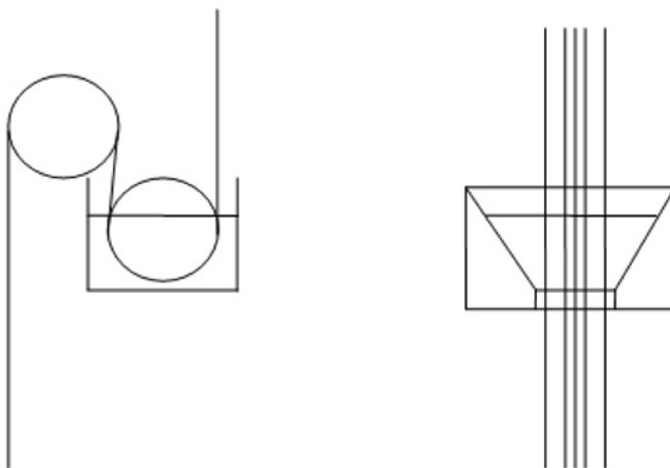


Figure 5. Schematic diagram of the coating methods. Dipping on left and pulling through on right.

Coating fibres with dipping method

Bioactive glass 13-93 block was first melted in a platinum crucible, which had 7 orifices at the bottom. Directly after the fibre formation process, the fibres were coated by immersing them into a solution of poly(L-lactide-co-D,L-lactide)(70/30), (PLA 70/30) polymer and acetone (1.5 g in 100 ml of acetone). Soon after dipping in the solution the acetone evaporated and fibres with a polymer coat were wound up with a spinning roll. In the dipping method fibres are pulled as a fibre bunch. Figure 6 shows a photograph of the dipping system.



Figure 6. Photograph of the dipping system.

Coating fibre with pulling through viscous solution

In the pulling through method the bioactive glass was formed into fibres as described above. Prior to being spun onto a roll, the fibres were pulled through a viscous solution which contained polymer with an appropriate solvent. The polymer concentrations and solvent used are shown in Table 3. The acronyms shown in Table 3 are used later in Tables and Figures.

Table 3. Acronyms and concentrations of the coating polymers used.

Polymer	Acronym	Concentration	Solvent
Poly(L-lactide-co-D,L-lactide) (70/30)	PLA 70/30	0.05 g/ml	acetone
Poly(L-lactide-co-trimethylene-carbonate)	P(LTMC)	0.175 g/ml	chloroform
Poly(L-lactide)	PLLA	0.032 g/ml	chloroform
Poly(DTE Carbonate)	P(DTEC)	0.243 g/ml	chloroform
Polyactive®	Polyactive	0.20 g/ml	acetone
Poly(ε-caprolactone-co-L-lactide) (50/50)	P(CL/L) 50/50	0.12 g/ml	acetone
Poly(ε-caprolactone-co-L-lactide) (80/20)	P(CL/L) 80/20	0.14 g/ml	acetone

4.2.2.3 Bioactive glass fibre reinforced polymer rods

Bioactive glass 13-93 fibres were manufactured and chopped manually using scissors. PLA 70/30 polymer was first solved into acetone and the chopped fibres were admixed to the viscous solution to form composite preforms. To allow the acetone to evaporate, the solution was then spread into a flat container for approximately 24 hours. The sheet-like composite performs were then cut into square billets of approximately 1 cm × 1 cm. The composite billets were next dried in a vacuum oven at room temperature for 3 days and then at 80°C for 16 hours to ensure that all the acetone evaporated. Five different compositions were produced containing 0, 10, 20, 30, and 40 volume-% of bioactive glass fibres. A piston injection moulder (SP2 Chippenham, England) with a steel mould was used to form composite rods from the billets.

4.2.3 Porous bioactive glass fibre scaffolds

Glass 13-93 fibres with mean diameter of 100 µm and glass 9-93 fibres with mean diameter of 75 µm were manufactured from the glasses by melt spinning as described earlier. In the fibre manufacturing process, the fibres were chopped into lengths of 3 mm. The fibre segments were then randomly packed into a cylindrical ceramic mould with diameter of 12 mm and height of 15 mm. The mould containing the fibre segments was then placed in a heated furnace for 45 minutes. The sintering temperature for glass 13-93 fibres was varied from 690 °C to 740 °C, and for glass 9-93 fibres from 590 °C to 620 °C, at 10 degree intervals. The moulds and the sintered blocks are shown in Figure 6.



Figure 7. Sintering moulds and sintered scaffolds.

With the sintering method, cylindrical specimens were obtained and a surgical knife was used for finishing the shape of the test specimens. Using a sintering mould with an inner diameter of 12 mm, sintered specimens of approximately 9 mm diameter were obtained. The height of the specimens was approximately 8 mm.

4.3 Characterization methods

The following table summarizes the characterisation methods performed for each sample type. A description of the tests performed and the analysis methods is given in more detail later in the text.

Table 4. Summary of tests and analyses performed.

Sample type	Tensile test	Flexural test	Microscopic analysis	Other tests
HA/PE composites	x	x	x (LM)	
Bioactive glass fibres	x	x	x (SEM+EDS)	<i>in vitro</i> reactions in SBF
Coated bioactive glass fibres		x	x (SEM)	<i>in vitro</i> reactions in SBF
BGF/PLA 70/30 composite rods		x	x (SEM)	
Bioactive glass fibre scaffolds			x (SEM)	permeability

(LM = light microscopy; SEM = Scanning electron microscopy)

4.3.1 Mechanical testing

4.3.1.1 Tensile testing

Tensile testing was performed with the HA/PE composites and manufactured bioactive glass fibres. Table 5 presents details of the tensile tests performed. With HA/PE composites the tensile strength, tensile modulus (at 0.1 % strain) and ductility were determined. For tensile test, the rectangular bars were machined into dumbbell shapes according to ISO specification. The length of the middle region with constant cross-section was 30 mm. An Instron knife extensometer of 25 mm gauge length was mounted on the sample for accurate measurement of extension. The load-extension curves were recorded with an X-Y plotter.

In tensile testing of the bioactive glass fibres, ASTM D3379-75 instructions were followed in principle. A gauge length of 50 mm and a testing speed of 1mm/min were used. The diameter of the fibre was measured from both free ends of the fibre sample with a micrometer screw gauge with an accuracy of 1 μ m. Prior to testing, care was taken to avoid touching the fibres in order to prevent contamination of the surfaces.

Table 5. Summary of details of tensile tests performed.

Sample type	Sample size (cross section)	Gauge length	Cross head speed	Test machine	Standard used	Publ. No
HA/PE samples	5 mm \times 2 mm	25 mm	0.5 mm/min	Instron	ISO 527	I
13-93 Glass fibres	\varnothing 25 μ m - \varnothing 180 μ m	50 mm	1 mm/min	Instron	ASTM D3379-75	II
9-93 Glass fibres	\varnothing 20 μ m - \varnothing 140 μ m	50 mm	1 mm/min	Zwick Z020/TH2A	ASTM D3379-75	III

4.3.1.2 Flexural testing

Flexural tests (3-point bending) were performed with HA/PE composites, bioactive glass fibres and manufactured bioactive glass fibre composite rods. Table 6 gives details of the 3-point bending tests. The flexural strength, flexural modulus (at 0.03 % maximum strain) and ductility (the maximum strain in the sample at a given deflection) of the HA/PE composites were determined.

The flexural strength of bioactive glass fibres was measured using a 3-point bending test fixture with fibres with a diameter between 230-800 μm . The support span radius of $r = 0.15 \text{ mm}$ was used in the lower jig and $r = 1 \text{ mm}$ for the upper loading nose. The span length was calculated to be $16 \times$ mean nominal diameters for all sample series. With 13-93 fibres, cross-head speed was 0.5 mm/min. With 9-93 fibre series crosshead speed was calculated as presented in ASTM C1161-02c.

The flexural modulus was calculated by using the following equation:

$$E = \frac{8 \cdot L^3 \cdot (XH - XL)}{6 \cdot \Delta L \cdot \pi \cdot d^4} \quad (1)$$

where;

L = support span,

XH = end of E-Modulus determination in kN,

XL = beginning of E-Modulus determination in kN,

ΔL = Flexure in mm between XH and XL, and

d = specimen diameter.

XH and XL were determined from the initial part of the curve where clearly only elastic deformation was present.

Table 6. Summary of details of the 3-point bending tests performed.

Sample type	Sample size (cross section)	Gauge length mm	Cross head speed mm/min	Test machine	Standard used	Publ . No
HA/PE samples	10 mm \times 2 mm	50	2.0	Instron	ASTM 790	I
13-93 Glass fibres	\varnothing 229 – \varnothing 338 μm	3.8	0.5	Instron		II
9-93 Glass fibres	\varnothing 500 – \varnothing 600 μm	8.8	0.14	Zwick Z020/TH2 A	ASTM C1161-02c	III
	\varnothing 600 – \varnothing 700 μm	10.4	0.17			
	\varnothing 700 – \varnothing 800 μm	12.0	0.19			
BGF/PLDLLA composite rods	\varnothing 3 mm	30	5.0	Instron	SFS-EN ISO 178	IV

Strength retention of 13-93 Fibres

The flexural properties of 13-93 fibres after immersion in SBF were measured using a 3-point bending test fixture on fibres with diameters from 229 μm to 338 μm . Prior to testing, care was taken to avoid any contamination of the fibre surfaces. After immersion in SBF, the samples were flushed with distilled water and kept moist until testing was carried out. The average and median strength and modulus values were calculated for fibres series immersed in SBF for various periods of time.

4.3.1.3 Statistical Weibull analysis of fibre strength

As bioactive glass fibres are brittle, they do not have well-defined strength because they sustain little or no plastic deformation and fail catastrophically. The stress at which they fail depends mainly on the presence of flaws, which may occur randomly along their length. The high strength of fibres, compared with corresponding bulk materials, is often attributable to the absence of large flaws. A population of flaws is expected along the length of fibres, so that variability in strength is to be expected. (Hull and Clyne 1996)

The Weibull plot is a graphical, statistical technique for determining data populations with variability. The scatter in bioactive glass strength data follows Weibull distribution, enabling the use of this method to statistically analyse the scatter in strength data (Hull and Clyne 1996). N strength values are ranked in descending order; the highest strength value having the rank $j=1$, the next highest $j=2$, and so on until the smallest, $j=N$. A probability of survivability, $S_j=j/(N+1)$, is then assigned to each value of strength. A minimum of 30 values of fracture strength is required for statistical validity. A Weibull diagram is obtained by plotting $\ln \ln (1/S_j)$ against $\ln (\text{strength})$. The gradient of the line of regression on $\ln \ln (1/S_j)$ upon $\ln (\text{strength})$ is the Weibull modulus, m , which enables an estimate of the probability that a material will survive a given stress. The Weibull modulus is an important parameter for characterising the strength distribution exhibited by the fibre. If the value, m , is large, the failure probability is predictable. Conversely, a low Weibull modulus introduces much more uncertainty about the strength of a fibre. The Weibull modulus for fibre strength values was evaluated as outlined above for all the fibre series when the number of parallel samples in that series was ≥ 30 .

4.3.1.4 Maximum apparent strain measurement for fibres

To compare coated and non-coated bioactive glass fibres, the ultimate apparent strains sustainable in bending were measured using a loop bending test which was modified from a knot bending test (Schoppee and Skeleton 1974). This straightforward test involves tying a semi-circular loop in the fibre, pulling it progressively tighter using a sliding gauge, and directly measuring the diameter (D) at which the failure occurs. See Figure 8.

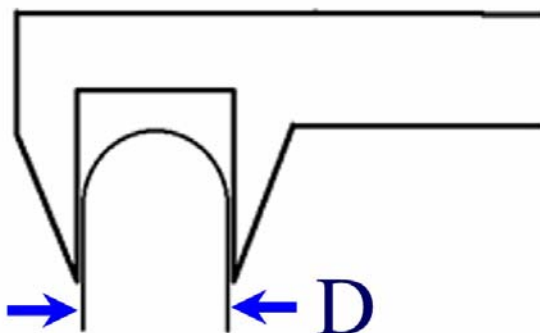


Figure 8. Schematic diagram of the loop bending test.

The maximum apparent strain ε for a fibre of diameter d is calculated from the loop diameter D using the expression:

$$\varepsilon = \frac{d}{D} \quad (2)$$

in which it is assumed that the fibre neutral axis coincides with the central axis of the fibre at all states of stress. This test was carried out for fibres which were coated by pulling through gel as single fibres and also for non-coated fibres (fibre diameter approximately 200 μm).

To estimate the effect of the abrasion in fibre surfaces, the bunch of fibres was slightly chafed between fingers for approximately 10 seconds to introduce scratches on the fibre surfaces. The apparent strain of these treated fibres was then measured as described above. With the control of “pure fibres” extra care was taken to handle them as little as possible to prevent scratching their surfaces.

To minimise the effect of variation in coating thickness on the apparent strain value, the apparent strain was also calculated so that the diameter of the underlying glass fibre was measured directly after test and used as d in the equation. The elastic modulus of glass is approximately 10 to 15 times greater than the elastic modulus of polymer so the effect of the polymer coat on the value of measured apparent strain is negligible.

4.3.2 Microscopic analysis

For microscopic analysis, the HA/PE specimens were sectioned, moulded in an epoxy resin and further ground and polished. The prepared samples were examined under a Leitz DMRX microscope (Welzlar, Germany) using incident light illumination and interference contrast set up.

For scanning electron microscopy (SEM) observations, fibre and coated fibre samples were first immersed in liquid nitrogen and then bent to break. Scanning electron microscope images were obtained using JEOL JSM T-100 (Japan) scanning electron microscope.

For SEM/EDS analysis, test specimens were first prepared using hot mounting techniques. The fibres were placed into the specimen holder perpendicular to the surface prior to mounting in order to achieve a cross-sectional view of the fibre. After casting, the specimens were ground and finally polished using No. 4000 SiC-paper. A scanning electron microscope Model XL30 (Philips, The Netherlands) equipped with an energy dispersive spectrometer (EDS) (Model DX-4, EDAX International, USA) was used for compositional analysis. The analysis was performed by scanning the formed surface layers to achieve a compositional analysis for each layer. For each sample two or three parallel runs were performed. The analysis data were transferred to Excel and, by using the initial images, the distances could be calibrated. The compositional analysis data presented in this thesis is taken from samples which have been immersed in SBF for 24 hours and for 5 weeks.

Relative porosity and pore size distribution were characterized for the glass fibre scaffolds by first casting the specimens into epoxy. From these samples sections with a two-dimensional (2-D) image were achieved by polishing. From the 2-D images the ratio of the glass and epoxy was measured to obtain the relative porosity value. Three sections were analysed from each sample. The 2-D images

were further used to estimate the pore sizes in the scaffold. All pores greater than 100 μm in networks were identified as elliptical areas and the diameters of the ellipses were measured using a microscope (Smaertscope flash, Optical Gauging Products Inc.) and image analysis software (Image tool 2.0, UTH SCSA and SigmaScanPro5, SPSS Inc.).

4.3.3 Other analysis performed

4.3.3.1 Differential scanning calorimetry (DSC)

The melting behaviour and fibre morphology of the woven fibre mats were studied using a Perkin-Elmer differential scanning calorimeter DSC7 (Perkin-Elmer Corp., Norwalk, Connecticut, USA), at a scanning rate of 10 $^{\circ}\text{C}/\text{min}$ and with 2 to 10 mg of material for each run.

4.3.3.2 Elemental analyses

Elemental analyses were performed to discover if there was a change in the glass composition during the fibre manufacturing process. The elemental analyses were carried out by Rautaruukki Steel (Raahe, Finland) with X-ray spectroscopy (Philips PW 2404 RGT). Two elemental analyses were performed, one on manufactured bioactive glass fibres and the other on the remnants of the glass in the platinum crucible.

4.3.3.3 *In vitro* analysis

Three sets of analysis were performed for samples with *in vitro* conditioning, namely 1) flexural strength retention of the fibre rods, 2) change in mass, and 3) scanning electron microscopic analysis of the sample surface after immersion in SBF.

To study the strength retention of the non-coated bioactive glass 13-93 fibres and the surface reactions of the coated and non-coated 13-93 fibres *in vitro*, fibre samples were immersed in simulated body fluid (SBF) by Kokubo (Kokubo et al. 1990). The samples were kept in closed plastic containers which were stored in a thermo closet at + 37 $^{\circ}\text{C}$. The sample surface area to SBF volume (SA/V) ratio of 0.1 cm^{-1} was used for all test samples. The pH of the solution was monitored and SBF solution was changed once every two weeks. Scanning electron microscope images were acquired from the test samples using JEOL JSM T-100 scanning electron microscope.

To analyse the changes in mass, three series of fibre samples were prepared, namely fibres with nominal fibre diameters of 38 μm , 100 μm and 210 μm . The surface area/volume (SA/V) ratio of 0.1 cm^{-1} was also used for all tested samples in this test series. The surface area of the samples was kept constant for all samples, so the average sample sizes were as follows; 27 mg for 38 μm fibres, 67 mg for 100 μm fibres and 137 mg for 210 μm fibres. The initial weight of the sample as well as the weight after immersion was measured to an accuracy of 0.01 mg. There were two parallel samples tested for each series at each time point, and the average of these two measurements is reported here.

4.3.3.4 Permeability analysis for the scaffolds

Permeability measurement is based on a method in which a fluid under a known pressure is allowed to flow through the porous specimen and the flow rate measured (Grimm and Williams 1997). The samples were placed in a permeability chamber, which consisted of a soft rubber tube connected to a fluid (water) reservoir. The pressure at the bottom surface of the specimen was zero, while the pressure at the top surface was generated by the level of the water between the reservoir and the specimen's top surface, which in this study was on average 25 cm, corresponding to a pressure of 2.5 kPa. A maximum allowable flow volume of 100 ml resulted in a 0.5 mm drop in water level and a negligible pressure variation of less than 5 Pa of the original pressure. The volumetric flow rate through the specimen was measured by determining the volume of water that had flowed through the specimen into a 250 ml graduated cylinder in a span of time measured with a digital chronometer. All measurements were carried out ten times in succession on each specimen. The first run was used to fully saturate the specimen with fluid to reduce measurement error. The values of the latter nine trials were then averaged.

The most important law in this kind of analysis is Darcy's law. According to this, the volumetric flow rate of a liquid through a specimen of porous material is proportional to the hydrostatic pressure difference across the specimen, inversely proportional to the length L of the specimen, and proportional to the cross-sectional area A of the specimen:

$$\Delta Q = \frac{k \cdot A \cdot \Delta p}{L} \quad (3)$$

where k is defined as the Darcian permeability of the material, $[k] = [L^3 T M^{-1}]$.

If the hydrostatic pressure is then expressed as pressure potential P , $[P] = [L]$ and care is taken to eliminate the dependence of k on material and fluid by introducing fluid viscosity η , $[\eta] = [MT^{-1}L^{-1}]$, then Darcy's law assumes the simplified form:

$$\Delta Q = \frac{k' \cdot A \cdot \Delta P}{\eta \cdot L} \quad (4)$$

where k' is defined as the intrinsic permeability of the material, $[k'] = [L^2]$

The data of the permeability trial were collected and correlated to specimen porosity.

5 Results

5.1 Hydroxyapatite polyethylene composites (I),

5.1.1 Mechanical properties

The tensile and flexural properties of the stack, single sandwich and multiple sandwich systems are presented in Table 7.

Table 7. Tensile and flexural properties of the stack, single sandwich and multiple sandwich systems.

Sample type Woven fibres + Powders	Total HA content vol%	PE fibre content vol%	Comp. temp. °C	Tensile modulus GPa	Tensile strength MPa	Flexural modulus GPa	Flexural strength MPa
Stack system							
100 vol% stand.	0	100	136.5	16.9	173	17.3	97
		100	138.5	14.9	152	13.6	74
		100	140.0	7.3	56	5.0	52
100 vol% red.	0	100	136.5	21.3	190	20.1	-
		100	138.5	17.8	152	15.4	83
82 vol% stand. + HA	18	82	138.0	10.5	103	-	-
69 vol% red. + HA	31	69	139.0	8.1	57	7.1	33
85 vol% red. + E.HAPEX	9	85	137.0	-	-	16.4	92
85 vol% red. + E.HAPEX	16	73	137.5	-	-	14.4	109
Single sandwich system							
5 stand. + HA+HAPEX	21	29	136.0	8.1	57	-	-
5 stand. + HAPEX	28	29	136.5	9.0	57	5.7	45
Multiple sandwich system							
5 stand. + HAPEX	28	29	136.5	8.2	63	7.6	60
10 stand. + HAPEX	18	57	137.0	12.2	123	12.7	-
5 stand. + E.HAPEX	41	30	136.5	11.2	70	11.0	66
5 stand + E.HAPEX + R.HAPEX	21	30	136.5	7.7	68	10.6	59
5 stand. + HA	34	32	136.5	8.6	65	7.4	46
5 stand. + HA+R.HAPEX	21	30	136.5	7.2	69	6.8	54
5 stand. + HAPEX	33	20	136.5	-	-	7.6	55
10 red. + HAPEX	23	43	137.5	11.4	95	9.1	-
5 red. + E.HAPEX	45	21	137.0	10.2	52	11.1	-
10 red. + E.HAPEX	33	45	137.0	12.0	101	13.9	93
15 red. + E.HAPEX	17	72	137.5	-	-	15.3	107
Control							
HAPEX™	40	-	-	4.3	21	4.7	32

In the table *stand.* refers to standard PE woven fibre mat and *red.* refers to reduced woven fibre mat. The first three sample types are samples which are composed only of woven fibre mats, and are compacted at different temperatures. The mechanical properties of HAPEX are used as control

values in order to compare the obtained values with a material which is already known and used in medical devices. Data of coefficients of variation of the mechanical measurements are presented in paper I.

Figure 9 shows the DSC-curves for woven fibre samples compacted at temperatures of 136.5, 138.0, 138.9 and 139.6 °C. The increase in the compaction temperature reduces the fibre morphology content. At compaction temperatures 136.5 °C and 138.0 °C most of the fibre structure remains. When compacted at 138.9 °C the content of melted phase and fibre phase are approximately in equal proportion in the sample. When the woven fibres are compacted at 139.6 °C, the proportion of melted phase in the structure is clearly larger.

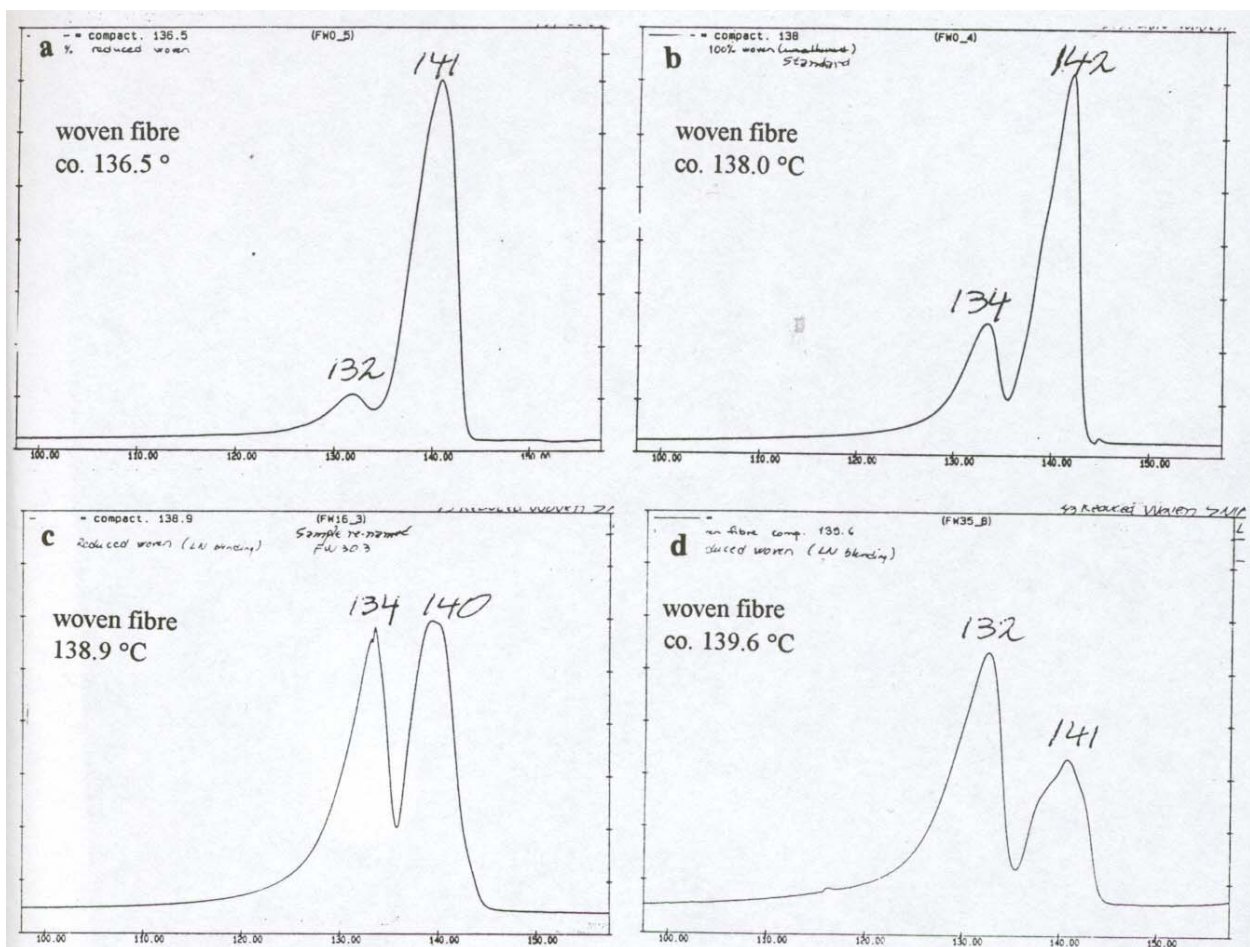


Figure 9. DSC-curves for woven fibre samples compacted at temperatures of 136.5, 138.0, 138.9 and 139.6 °C.

5.1.2 Structural characterization

Optical microscopy of polished cross-sections cut perpendicular to the long axes of the bars revealed the actual distribution of the phases (woven fibres and powder composites). It should be noted that the observed cross-sections cut the woven fibres perpendicular to the warp (the series of yarns extended lengthways in the loom and crossed by the weft). Picks of the weave can be seen emerging at right angles and lying in the plane of the cross-section.

Figure 10 shows the structure of a single sandwich system, namely, HAPEX™ reinforced with 5 standard woven layers. Figure 11, Figure 12 and Figure 13 are images of cross-sections of multiple layer configurations with 5 standard fibre mats. Woven fibres are used as reinforcing phase for HAPEX™ in Figure 10, for HA/GUR powders in Figure 11 and for composite in which R.HAPEX is used in the inner part of the composite. HA/GUR powder is used in the outer layers in the composite in Figure 13. As initially intended, the layers of woven fibres are stacked together in the middle of the thickness of the single sandwich configuration, whereas in multiple sandwich configurations they are separated by approximately equal distance.



Figure 10. Polished cross-section of single sandwich system. 5 standard woven fibre layers + HAPEX™. Cursor = 200 μm .

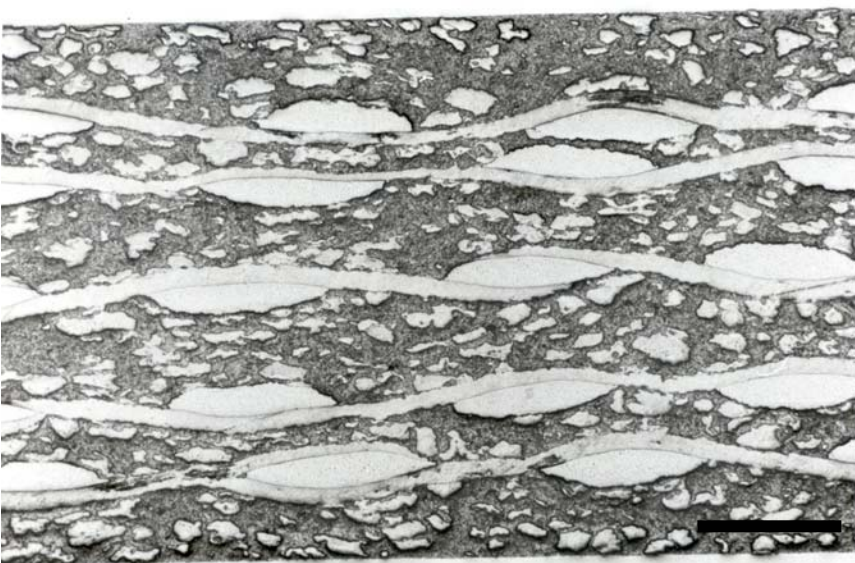


Figure 11. Polished cross-section of multiple sandwich system. 5 standard woven fibre layers + 50 vol% HA/GUR 412. Cursor = 500 μm .

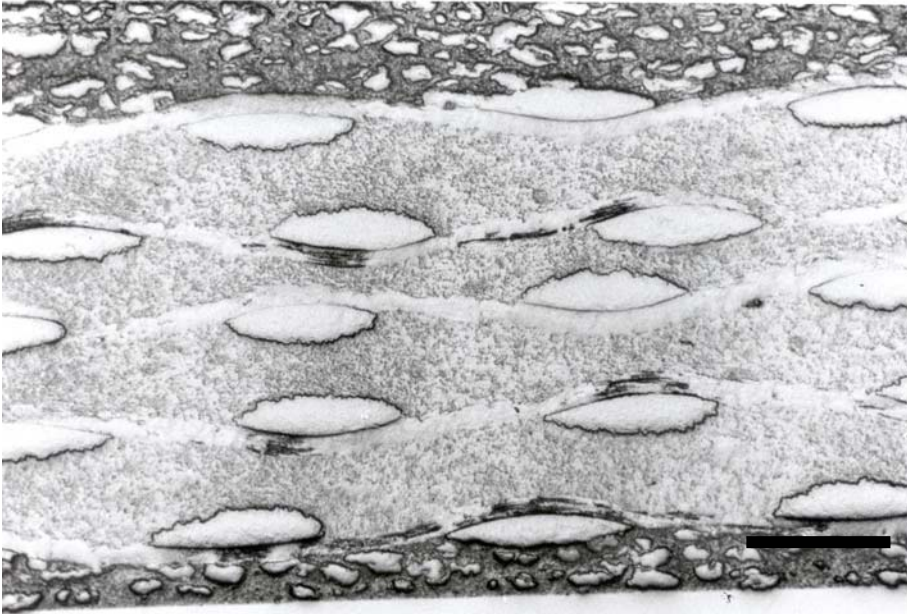


Figure 12. Polished cross-section of 'combination' multiple sandwich system. 5 standard woven fibre layers + 50 vol% HA/GUR 412 (outer layers) and R.HAPEX (inner layers). Cursor = 500 μm .

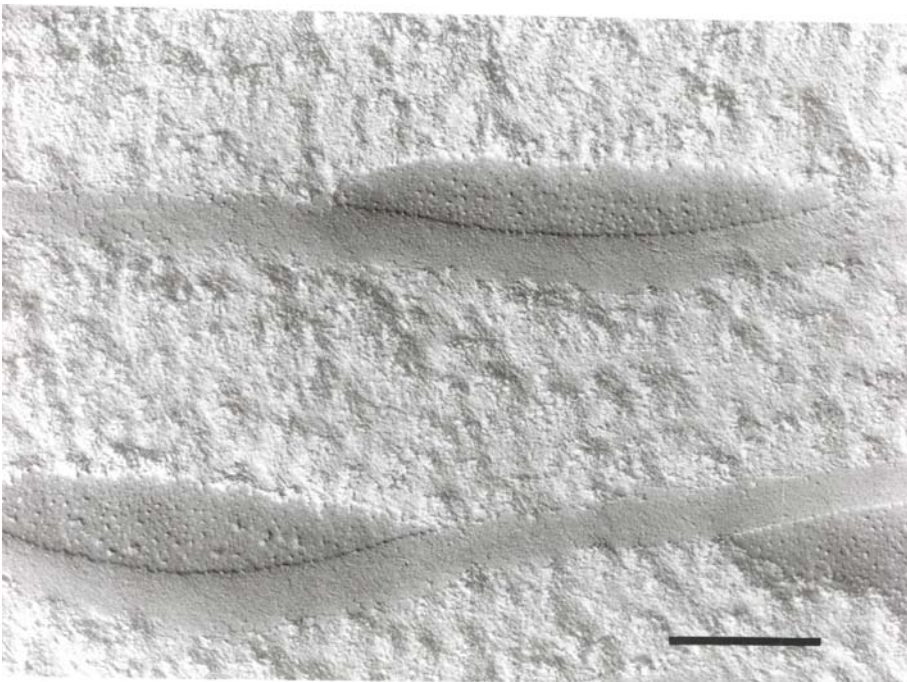


Figure 13. Polished cross-section of multiple sandwich system with 5 standard woven fibre layers and HAPEX™. Cursor = 200 μm .

Figure 14 presents a higher magnification image. The images show the excellent compatibility between the fibres and the powdered composites, with no voids observed. In addition, the woven layers coalesced in the single sandwich system, whilst for the multiple sandwich configurations, similar excellent coalescence is seen between individual fibres and between fibres in weft and warp. Each fibre also maintained its distinctness, as can be clearly seen in the emerging ends.

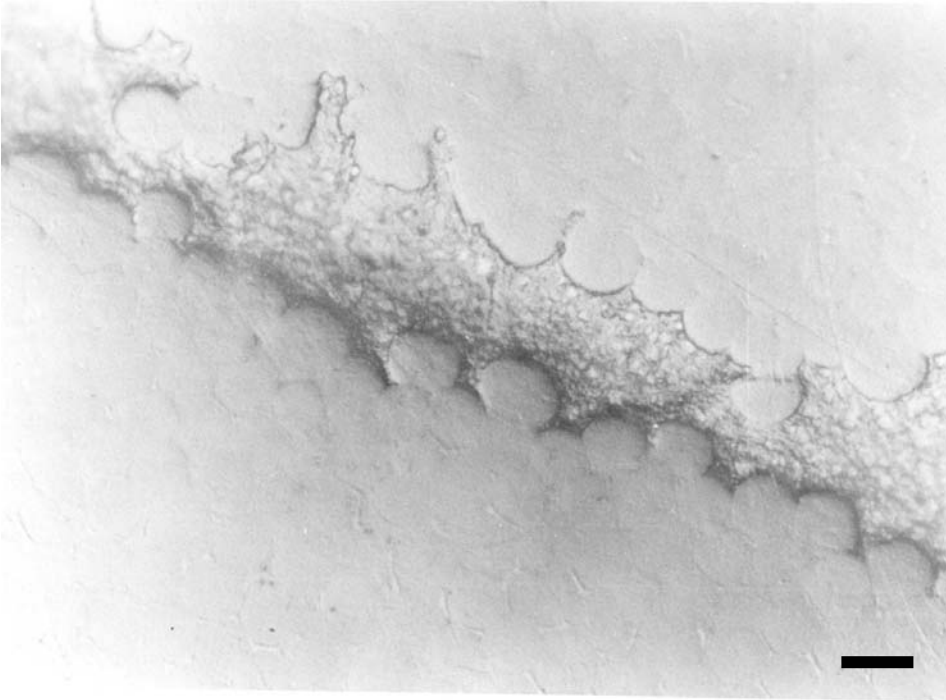


Figure 14. Polished cross-section of multiple sandwich system sample with PE fibres bunches and E.HAPEX in between. The fibre cross-sections are clearly visible (fibre diameter 13-15 mm). Cursor = 10 μm .

In HA/GUR composite phase (Figure 11) white particles of up to 100 μm can be observed. This may have been due to imperfect room temperature during blending of the hydroxyapatite and polyethylene particles. This inhomogeneity is not observed in phases related to HAPEX™ because this material was blended in a hot compounding machine, giving excellent dispersion of the hydroxyapatite particles. However, the inhomogeneity of HA/GUR did not seem to affect the mechanical properties of the corresponding systems.

5.2 Bioactive glass fibres (II, III),

5.2.1 Processing of the fibres

During melt spinning, the upper surface (the one in contact with the air) of the glass block crystallized slightly. Only a solid glass block was successfully drawn into fibres. Glass particles were used in early tests, but it was soon noticed that their surfaces started to crystallize at the melt spinning temperature. Some crystallites also transferred to the fibres. When a solid block of glass was used, homogeneous fibres were successfully manufactured and only the upper surface of the glass crystallized. Using this manufacturing method, approximately 50% of the initial weight of the initial glass block was successfully drawn into fibres in each case.



Figure 15. Photograph of bioactive glass drop, slowly falling down from the glass melt.

The results of the elemental analyses are shown in Table 8. The compositions are given in weight-%. As seen in Table 8, there are no significant compositional changes in the glass during the fibre manufacturing process. The manufactured glass fibres, as well as the remnants of the glass (partly crystallized), possessed identical compositional structures. It can also be seen that with this manufacturing method, homogeneous glass batches can be achieved with only minor variations in composition compared with the theoretically calculated values.

Table 8. Results of the elemental analyses of glass 13-93. All values are given in weight-%.

Sample	Na ₂ O	K ₂ O	MgO	CaO	P ₂ O ₅	SiO ₂
Glass fibres	5.93	11.7	4.82	20.4	4.05	53.0
Glass remnants	5.90	11.8	4.83	20.2	4.05	53.0
Theoretical value	6	12	5	20	4	53

5.2.2 Mechanical properties

5.2.2.1 Tensile testing

In tensile testing all the fibres exhibited brittle failure and a linear force-deflection response to the point of failure. As seen in the tensile test results in Figure 16 and in Table 9 and Table 10, there is a large scatter in the tensile strength results of bioactive glass 13-93 and 9-93 fibres. It also can be seen that tensile strength is highly dependent on the diameter of the fibre, and a linear correlation between fibre strength and fibre diameter can be detected. The Weibull modulus varies slightly from batch to batch and there is no clear correlation between diameter of the fibres and Weibull modulus value.

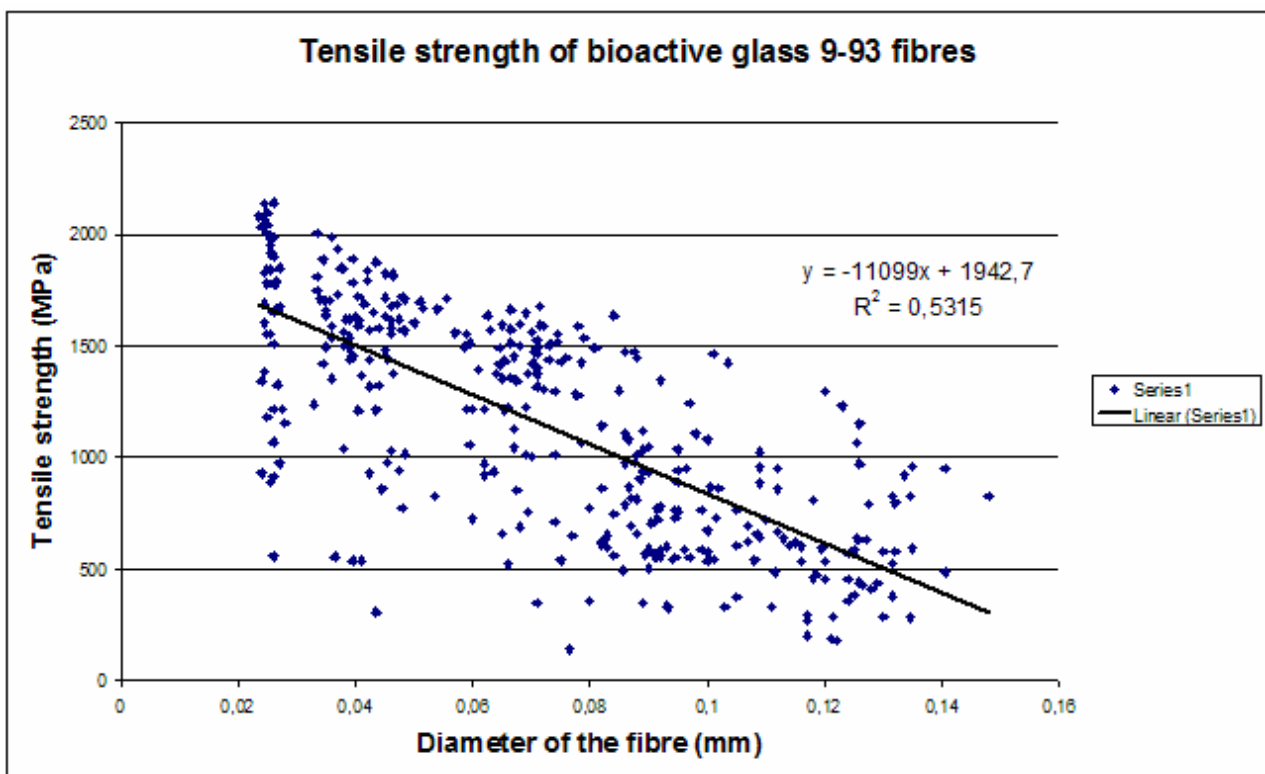


Figure 16. Tensile strength values for bioactive glass 9-93 fibres.

Table 9. Effect of the fibre diameter on the values of median tensile strength, average tensile strength and Weibull modulus of the bioactive glass 13-93 Fibres.

Fibre diameter μm	Number of samples	Median strength MPa	Lowest – highest strength MPa	Average strength MPa	Standard deviation MPa	Weibull modulus
25-33	31	910	165 – 1694	862	357	1.8
34-47	30	810	148 – 1919	796	320	2.2
48-91	31	601	211 – 1888	651	389	2.0
93-160	32	425	150 – 726	441	151	3.1

Table 10. Summary table of tensile test results for bioactive glass 9-93 fibres.

Fibre diameter µm	Number of samples	Average strength (Stdev) MPa	Weibull modulus
20-30	42	1625 (416)	3.7
30-40	37	1573 (321)	3.6
40-50	45	1443 (368)	3.0
60-70	36	1237 (319)	3.8
70-80	34	1277 (380)	1.9
80-90	37	916 (338)	2.9
90-100	34	720 (241)	3.3
100-120	40	672 (273)	2.7
120-140	35	617 (292)	2.3

5.2.2.2 Flexural testing

The flexural properties of bioactive glass 9-93 glass fibres are presented in Table 11. The measured average flexural strength value for bioactive glass 9-93 fibres with a thickness from 0.5 to 0.6 mm was approximately 1240 MPa. The flexural strength was slightly lower with thicker glass fibres. The scatter in flexural strength results is high, thus leading to low Weibull modulus values. The average flexural modulus was approximately 64 GPa for all tested series, and the standard deviation in modulus values is rather low.

Table 11. Flexural properties of bioactive glass 9-93 fibres.

Fibre diameter mm	Number of samples	Average flexural modulus (Stdev) GPa	Average flexural strength (Stdev) MPa	Weibull modulus
0.5 – 0.6	42	63.8 (2.8)	1240 (492)	2.5
0.6 – 0.7	45	63.6 (2.5)	897 (399)	2.6
0.7 – 0.8	32	64.5 (2.9)	915 (453)	2.3

Flexural strength retention of bioactive glass 13-93 fibres *in vitro*

The results of the 3-point bending tests for 13-93 fibres after various immersion times are shown in Table 12. The flexural strength of fibres first started to decrease when immersed in SBF, but the strength recovered from 2 days to 1 week of immersion in SBF. From 1 week's immersion, the flexural strength started to decrease again and after 7 weeks, the flexural strength was less than 15% of initial strength. The decrease in strength was reasonably small from 7 to 40 weeks. The flexural modulus of bioactive glass 13-93 fibres started to decrease when they were immersed in SBF. The scatter in modulus values was initially minor, but increased after 5 weeks' immersion time. Initially the Weibull modulus was approximately 2 and reached its maximum of 3.6 after two days of immersion. After 3 weeks of immersion, the Weibull modulus decreased and a large scatter in strength as well as lower strength values were detected, as Figure 17 shows.

Table 12. Flexural test results for bioactive glass 13-93 fibres.

Immersion time in SBF	No. of samples	Median strength MPa	Lowest and highest strength values MPa	Weibull moduli	Average strength MPa	Standard deviation (strength) MPa	Average modulus of elasticity GPa	Standard deviation (modulus) GPa
0	40	1354	333 – 3073	2.1	1443	697	68.1	6.8
1 day	40	937	500 – 2433	2.6	1098	501	63.5	7.6
2 days	40	970	526 – 1970	3.6	1025	327	66.9	5.1
3 days	42	1336	486 – 2727	3.2	1368	429	62.6	5.5
1 week	40	1584	664 – 2633	3.3	1523	477	63.4	5.2
2 weeks	40	1318	523 – 1948	3.1	1265	421	61.3	5.6
3 weeks	40	961	190 – 2688	1.5	1177	732	54.4	6.1
4 weeks	40	576	126 – 1548	1.7	619	370	57.4	8.0
5 weeks	41	238	116 – 959	2.5	285	162	47.7	10.4
7 weeks	40	277	100 – 1164	1.9	324	227	41.9	10.7
9 weeks	35	205	72 – 638	2.5	210	100	39.6	7.2
11 weeks	34	176	40 – 352	2.2	178	77	42.9	11.0
13 weeks	19	206	109 – 337		215	67	43.6	6.7
15 weeks	20	149	24 – 282		154	65	49.7	14.6
20 weeks	18	168	59 – 243		164	50	53.9	12.4
25 weeks	20	152	31 – 355		157	69	43.8	18.0
30 weeks	20	158	42 – 244		160	47	49.0	9.7
35 weeks	19	121	64 – 364		140	70	41.6	12.9
40 weeks	20	122	50 – 194		124	40	44.1	12.9

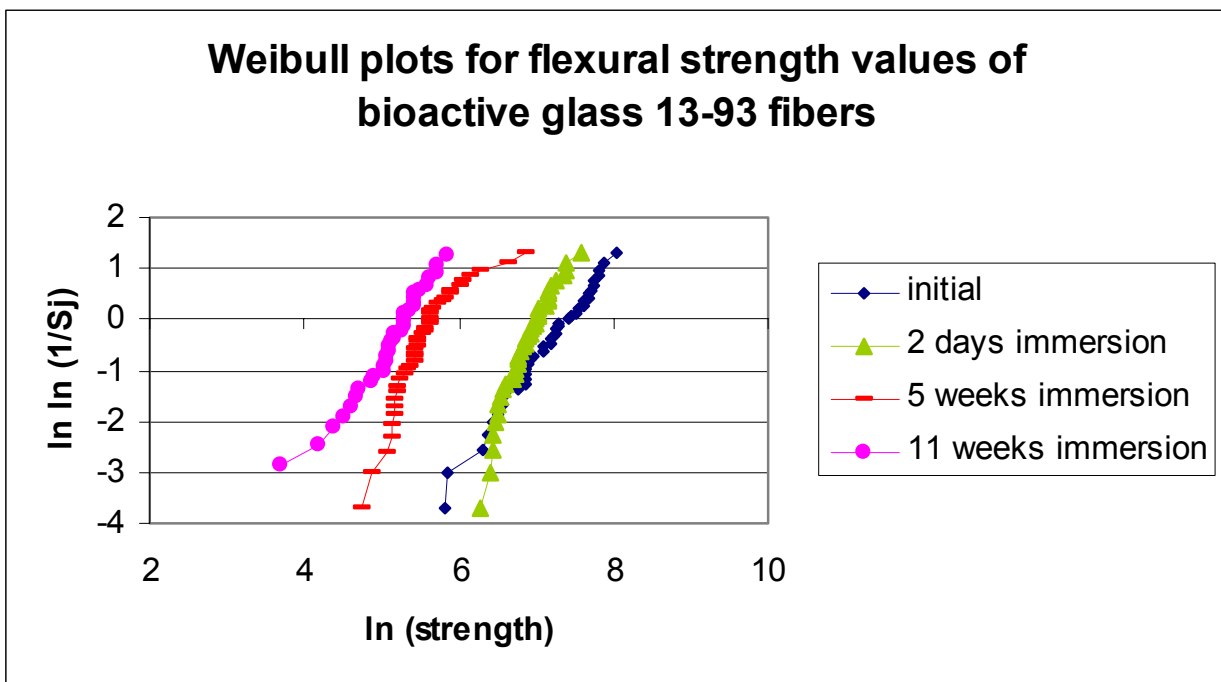


Figure 17. Weibull plots for flexural strength values of bioactive glass 13-93 fibres after immersion into SBF.

5.2.3 Structural characterization

Changes in mass

The changes in mass of the bioactive glass 13-93 fibres are presented in Figure 18 and Figure 19. In Figure 18, the changes in mass of the fibres with a diameter of approximately 38 μm are shown for the first 72 hours in SBF. Within the first 12 hours, there was a rapid decrease in mass, but already after 24 hours the mass again increased. The same behaviour was also observed for fibres with a nominal diameter of 100 μm and 210 μm .

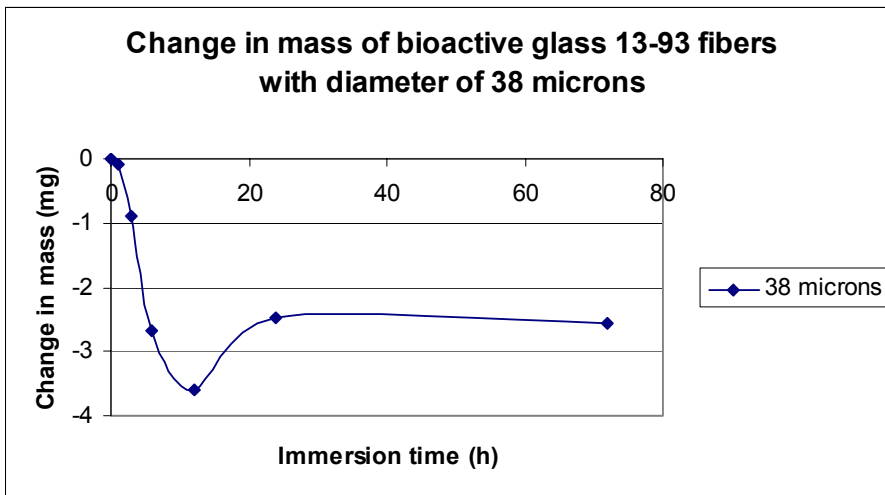


Figure 18. Change of mass of bioactive glass 13-93 fibres with diameter of 38 microns.

For all three sets of fibres with variable diameters, namely, 38 μm , 100 μm and 210 μm , there was an almost identical change in actual mass during the time period, even though the initial mass of samples did differ significantly (27 mg for 38 μm fibres, 67 mg for 100 μm fibres and 137 mg for 210 μm fibres). The mass increase with the thinnest (38 μm) fibres is slightly lower after 52 weeks of immersion compared to the thicker fibres, as shown in Figure 19.

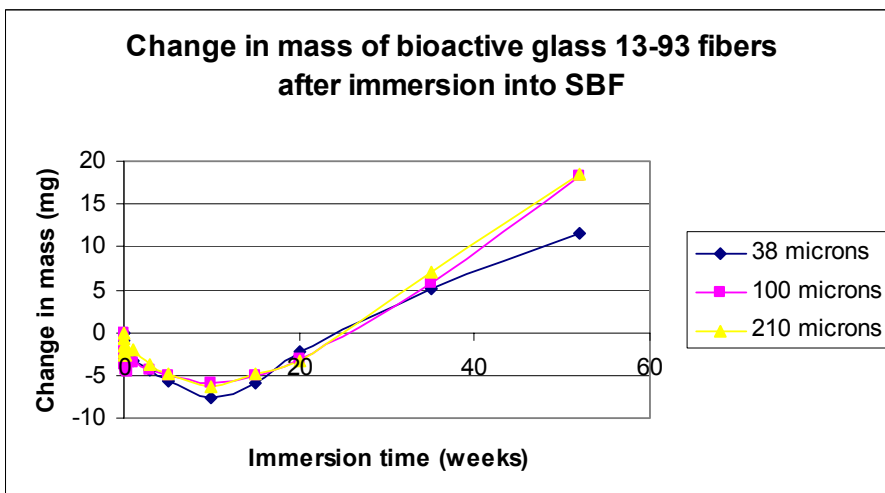


Figure 19. Change of mass of bioactive glass 13-93 fibres with nominal diameters of 38, 100 and 210 microns.

Compositional analysis

The compositional analysis performed on samples immersed 24 hours is presented in Figure 20. From the compositional analysis data it can be seen that after 24 hours the Na^+ , K^+ , and Ca^{2+} have started to diffuse out from the glass surface, and there is an increase in the amount of silicon in the glass surface. The transformed layer has a thickness varying from 2 to 3 μm after 24 hours of immersion.

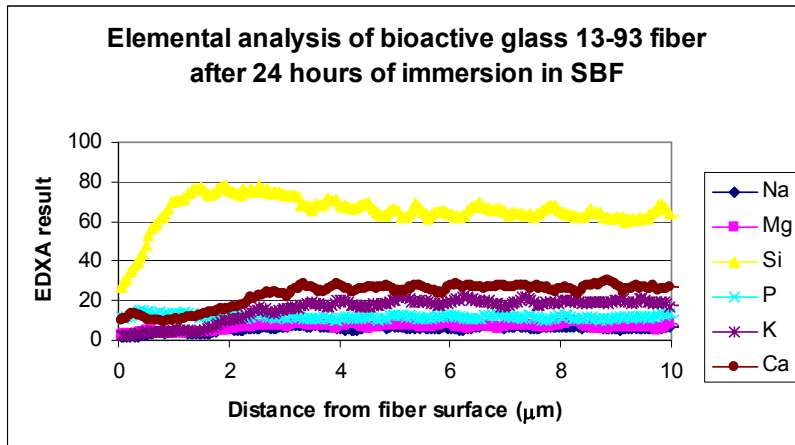


Figure 20. Compositional analysis for bioactive glass 13-93 fibre after 24 hours' immersion in simulated body fluid.

In the compositional analysis for fibres immersed for 5 weeks in SBF, there is a clear Ca- and P-rich layer on the fibre surface and a Si-rich layer beneath the CaP-rich layer, as shown in Figure 22 and Figure 23. The CaP-rich layer has a uniform thickness of approximately 2 μm over the entire fibre surface. The thickness of the Si-rich layer is variable over the fibre surface and, as shown in Figure 23, the thickness of the Si-rich layer is approximately 5 to 30 μm after 5 weeks of immersion in SBF. In Figure 23 remnants can be detected of an additional CaP-rich layer on top of the continuous CaP-rich layer. During sample preparation, it was noted that as the samples dried, the CaP-rich surface became very brittle and some of the outer layer detached from the fibre surface.

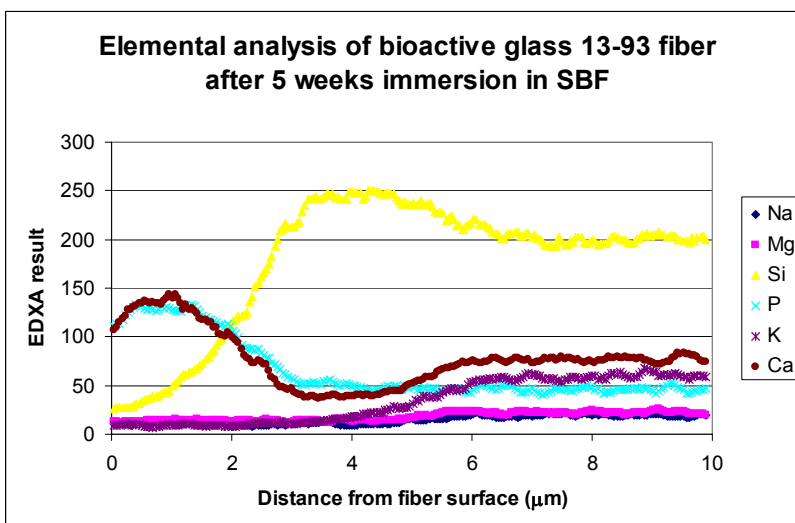


Figure 21. Compositional analysis of bioactive glass 13-93 fibres after 5 weeks immersion in simulated body fluid.

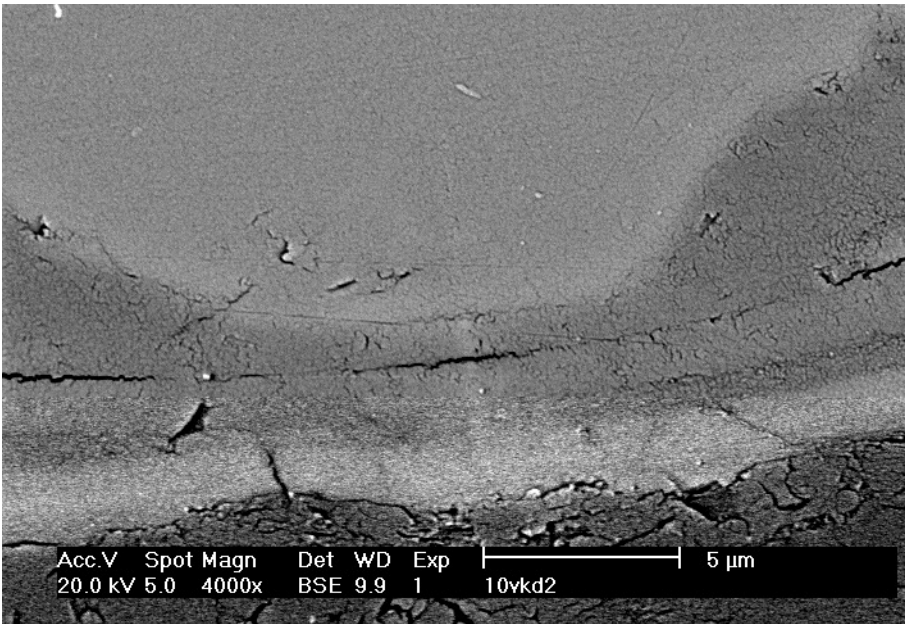


Figure 22. Scanning electron microscope image of the surface of bioactive glass 13-93 fibre after immersion in simulated body fluid for 5 weeks.

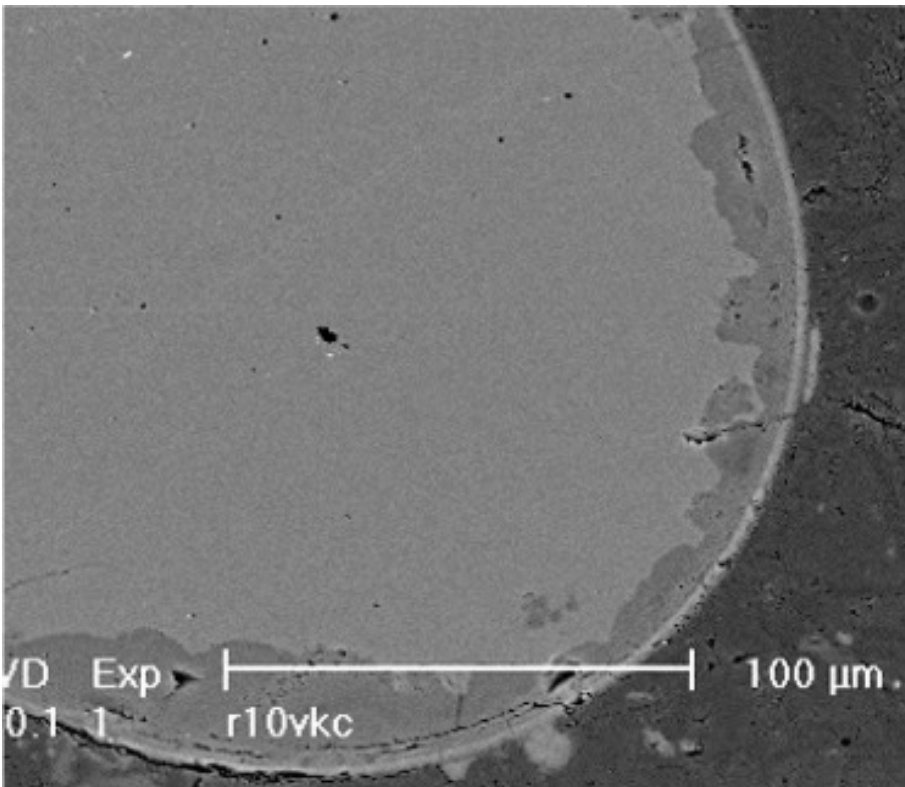


Figure 23. Scanning electron microscope image of bioactive glass 139-93 fibre after immersion in simulated body fluid for 5 weeks.

5.3 Polymer/bioactive glass fibre composites (IV, V)

The bioactive glass fibres were successfully coated with biomedical polymers using two techniques, namely, dipping and pulling through. The dipping procedure was optimal with thin fibres (fibre diameter less than 50 μm) and when only a thin layer of polymer was required (1-2 μm). The dipping of single fibres was difficult as thin fibres broke easily. Dipping the fibres as a bunch was done without difficulty. Figure 24 presents an SEM figure of a single fibre dipped with PLA 70/30 and Figure 25 presents a bunch of fibres dipped with PLA 70/30. Unless coated, thin fibres (diameter 20 – 50 μm) cannot be unwound from the roll without breakage. The coating strengthens the fibre bunch so that it can easily be unwound and further processed as a fibre bunch.

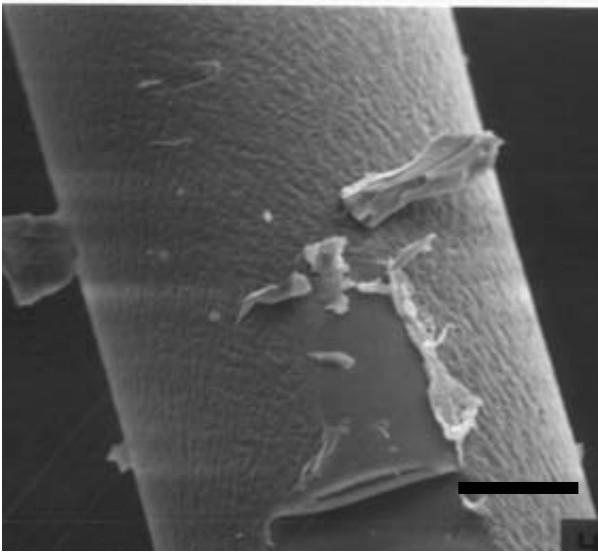


Figure 24. Scanning electron microscope image of single fibre dipped into PLA70/30 polymer-acetone solution. Cursor = 10 μm .

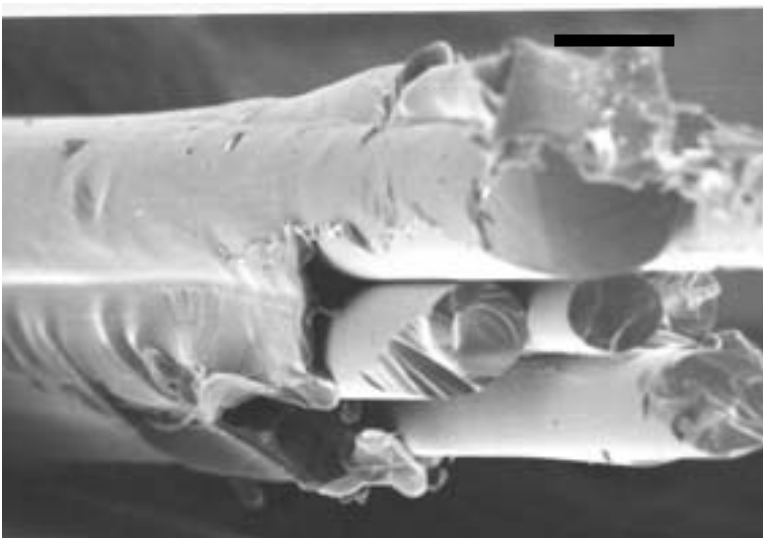


Figure 25. Scanning electron microscope image of fibre bunch coated with dipping method. Cursor = 50 μm .

Pulling through was optimal for thicker fibres (diameter 100-250 μm) and also when a thicker polymer layer was required (10-30 μm). With this technique fibres could be coated either as single fibres or as a fibre bunch. In Figure 25 fibres have been coated with PLA 70/30 as a bunch. As the fibre diameter and nozzle size was kept constant throughout the coating experiments, the viscosity of the solution had to be kept constant to obtain a homogeneous and smooth coat. Because of this, the thickness of the obtained polymer layer varied according to the polymer used. It is assumed that the thickness of the polymer layer can be varied to some degree by modifying the polymer/solvent ratio and the nozzle size.

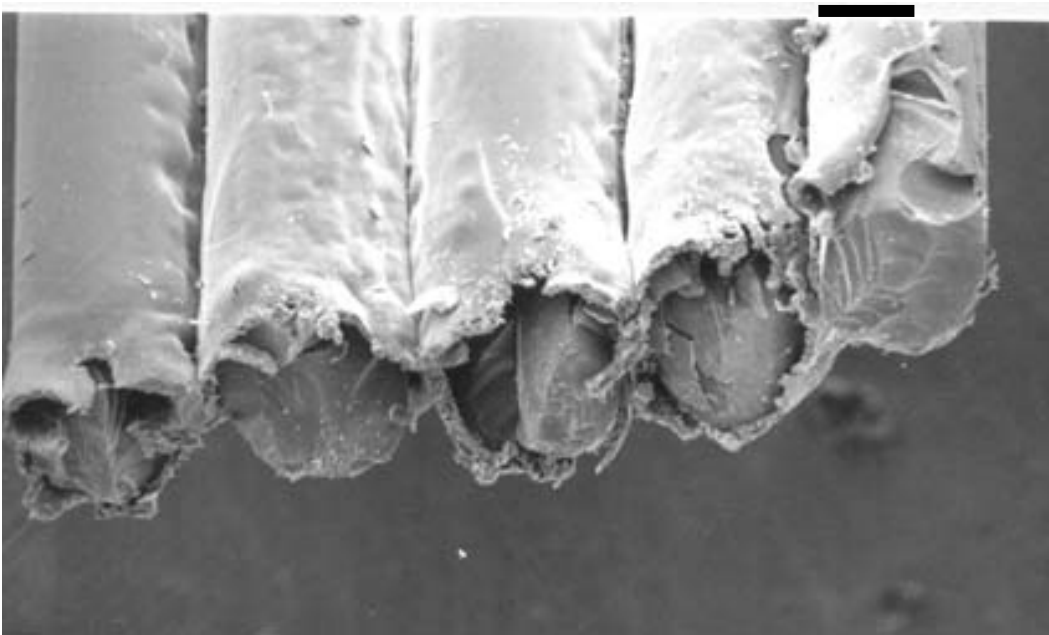


Figure 26. Scanning electron microscope image of bioactive glass 31-93 fibres coated with pulling through method. Cursor = 50 μm .

5.3.1 Mechanical properties

Measured maximum apparent strains for non-coated and coated fibres are shown in Table 13. The slight modification of the fibres to introduce scratches on their surfaces caused a huge decrease in maximum apparent strain. The apparent strain of pure fibres is 6.5 times greater than the apparent strain of modified fibres. With both poly(ϵ -caprolactone-co-L-lactide) polymer coats, the maximum apparent strain is approximately twice as great as the apparent strain of the “pure glass”. The maximum apparent strain of the fibres with other polymer coats is approximately at the same level as the “pure glass” control.

Table 13. Number of tested samples and averages and standard deviations for diameter and maximum apparent strain measurements of coated 13-93 fibres.

Fibre type	N	Average diameter of fibre μm	Stdev μm	Average coating thickness μm	Stdev μm	Average total apparent strain %	Stdev %	Average apparent strain for glass %	Stdev %
modif. glass	14	184.4	6.9					0.28	0.05
pure glass	20	189.5	10.5					1.81	0.50
P(LTMC)	20	255.8	6.5	40.3	0.9	1.56	0.03	1.35	0.04
P(CL/L) 50/50	20	276.8	2.3	31.8	0.9	3.61	0.21	3.24	0.18
P(DTEC)	20	255.9	3.3	71.4	2.4	2.82	0.07	2.21	0.04
PLLA	20	263.9	10.2	11.4	0.1	2.17	0.01	2.08	0.00
P(CL/L) 80/20	20	223.2	3.0	46.2	1.6	3.94	0.23	3.26	0.21
PLA 70/30	16	223.1	28.4	15.3	8.0	2.46	1.42	2.31	0.60
Polyactive	20	297.4	1.9	34.5	6.4	1.95	0.03	1.75	0.00

Composites

Table 14 presents the compositions of the samples (number referring to vol-% of bioactive glass fibres (GF)), number of samples (N) and results from flexural test (averages and standard deviations).

Table 14. Flexural properties of bioactive glass 13-93 fibre/poly(LD/L)LA (70/30) composites.

Composite type	N	Average strength (stdev) MPa	Max/Min strength MPa	Average Modulus (stdev) GPa	Strain at Yield (stdev) %
0 vol-% GF	5	124.8 (7.5)	129.7/113.0	2.87 (0.09)	5.3 (0.6)
10 vol-% GF	6	136.2 (17.2)	169.6/122.7	5.37 (0.84)	2.8 (0.3)
20 vol-% GF	11	177.5 (38.7)	245.9/133.6	8.41 (2.05)	1.9 (0.2)
30 vol-% GF	7	202.6 (24.3)	233.7/175.1	12.18 (1.08)	1.4 (0.1)
40 vol-% GF	6	220.4 (15.1)	239.4/205.0	14.30 (1.02)	1.2 (0.1)

The obtained flexural strength and flexural modulus values improved linearly as fibre content increased. As expected, strain at Yield decreases as the content of bioactive glass fibres is increased.

5.3.2 Structural characterization

Surface reactions *in vitro*

Calcium phosphate-like precipitation started to form on the polymeric coating after 1-3 weeks' immersion. With the poly(L-lactide-co-trimethylene-carbonate), poly(DTE Carbonate), and Poly(ϵ -caprolactone-co-L-lactide) coating the calcium phosphate-like precipitants formed an abundant layer by 2-3 weeks and after 7 weeks, consistent calcium phosphate-like precipitation encircled the entire fibre. The calcium phosphate precipitation on top of poly(ϵ -caprolactone-co-L-lactide) (80/20), and poly(DTE Carbonate) after 2 and 7 weeks' immersion in SBF can be seen in Figure 27 and Figure 28. With the poly(L-lactide-co-D,L-lactide)(70/30), poly(L-lactide) and Polyactive®

polymer coatings some calcium phosphate-like precipitates formed but the precipitation was not abundant.

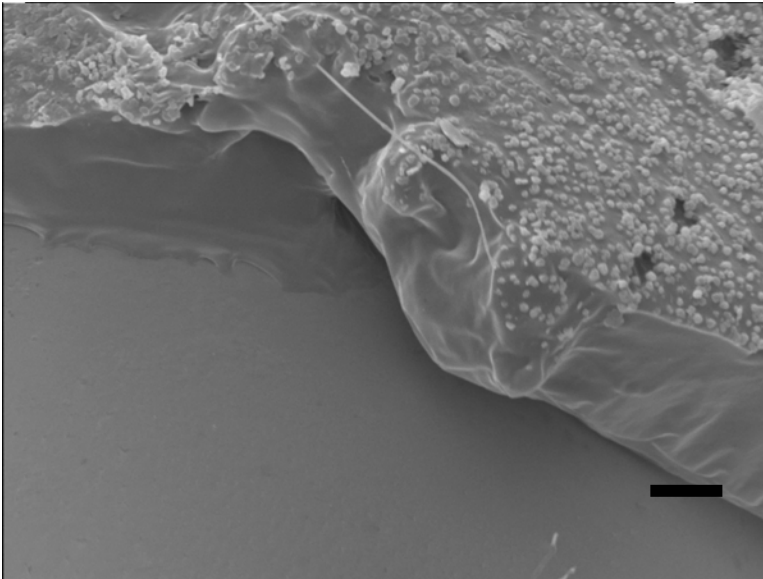


Figure 27. SEM image of poly(ϵ -caprolactone-co-L-lactide) (80/20) coating in bioactive glass surface. The calcium phosphate precipitation can be observed after 2 weeks immersion in SBF. Cursor = 10 μm .

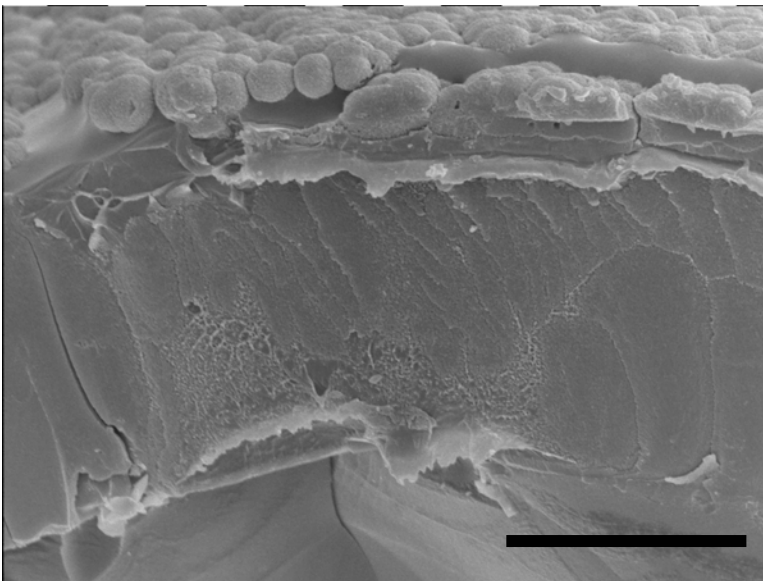


Figure 98. The calcium phosphate precipitation on top of poly(DTE Carbonate) after 7 weeks immersion in SBF. Cursor = 10 μm .

With all the different polymer coatings which were immersed in SBF occurrences of voids between the polymeric coating and fibre surface were observed in SEM analysis. This is may be due to sample preparation or poor adhesion between fibre and polymer coating. Figure 29 shows a poly(L-lactide) coated bioactive glass fibre after 3 weeks' immersion. Degradation of bioactive glass fibre

has initiated underneath the defects in the polymeric coating. There are no signs of degradation of bioactive glass in areas where the poly(L-lactide) coating remains intact after 3 weeks' immersion.

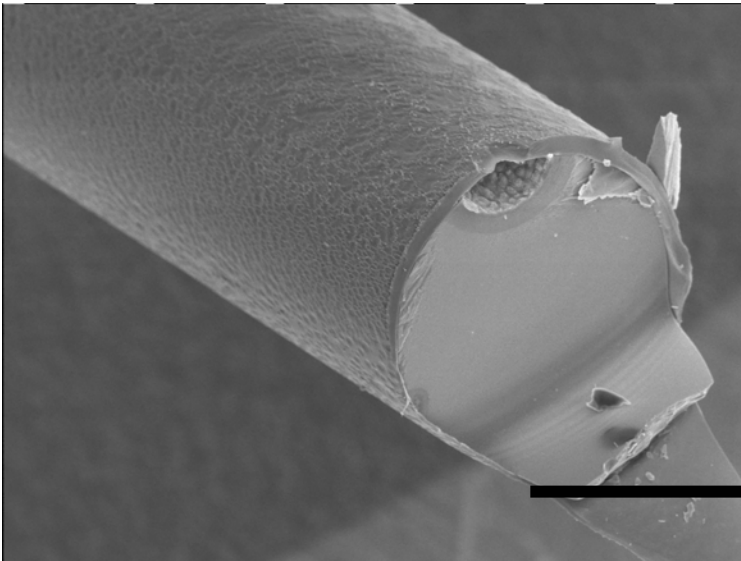


Figure 29. Scanning electron microscope image of bioactive glass 13-93 fibre coated with PLLA, after immersion in SBF for 3 weeks. Note that the glass resorption has only initiated under the defect in PLLA coating. Cursor = 100 μ m.

5.4 Sintered scaffolds (VI, VII).

5.4.1 Structural characterization

Sintering the chopped bioactive glass fibres produced a mechanically rigid three-dimensional network, with homogeneous pore distribution throughout the sample. The mean pore size values and relative porosity of scaffolds as a function of sintering temperature can be seen in Figure 30 and Figure 31. Porosity and pore size both decrease when the sintering temperature is increased.

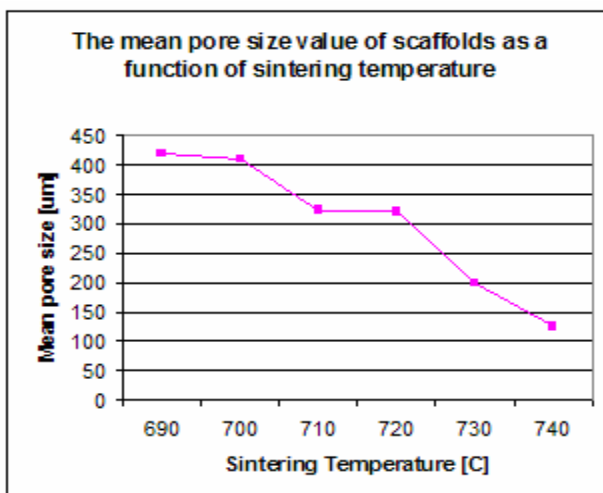


Figure 30. Mean pore size value of scaffolds as a function of sintering temperature.

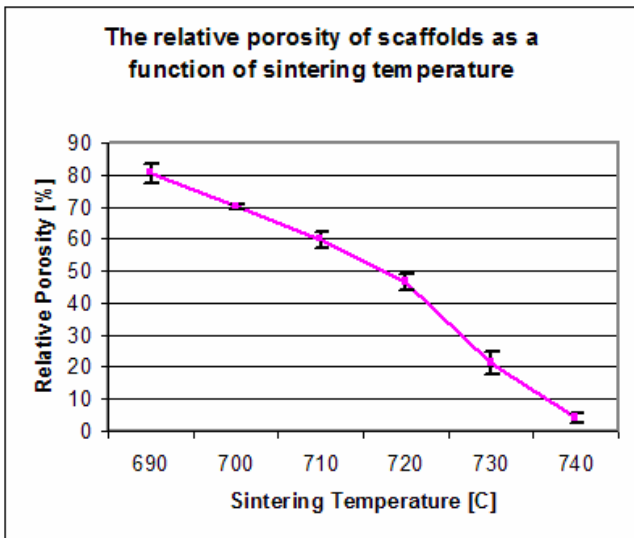


Figure 31. Relative porosity of scaffolds as a function of sintering temperature.

In Figures 32-34 scanning electron microscope (SEM) images are shown of the network, sintered at 700 °C, 720 °C and 740 °C. The SEM images make it possible to establish the interconnection of pores, as well as the homogeneous distribution of pores or voids.

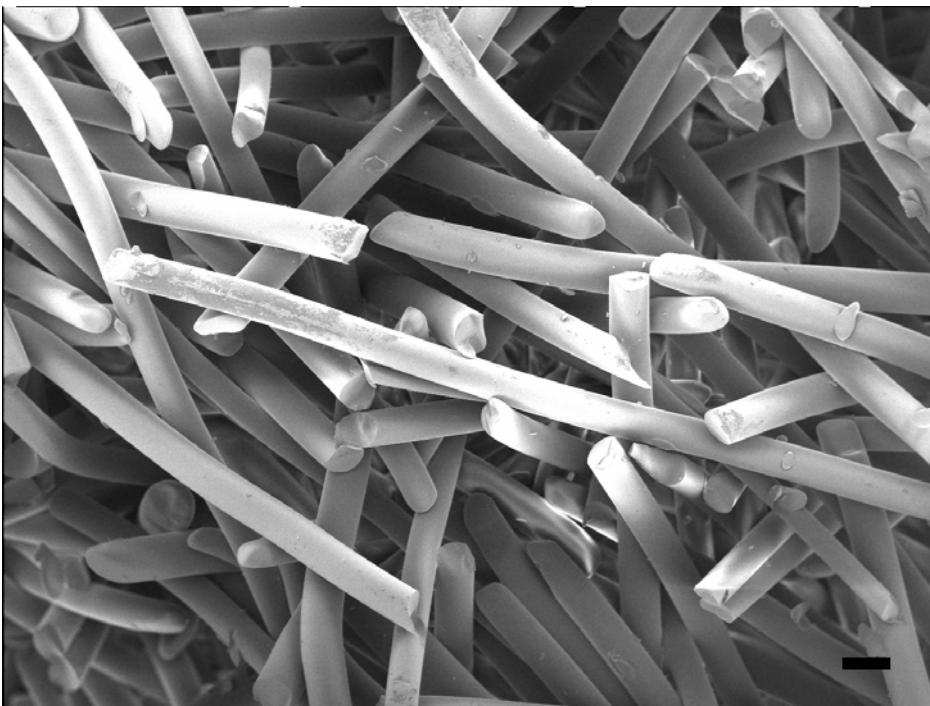


Figure 32. Bioactive glass 13-93 fibre scaffold sintered at 700 °C. Cursor = 100 μm.

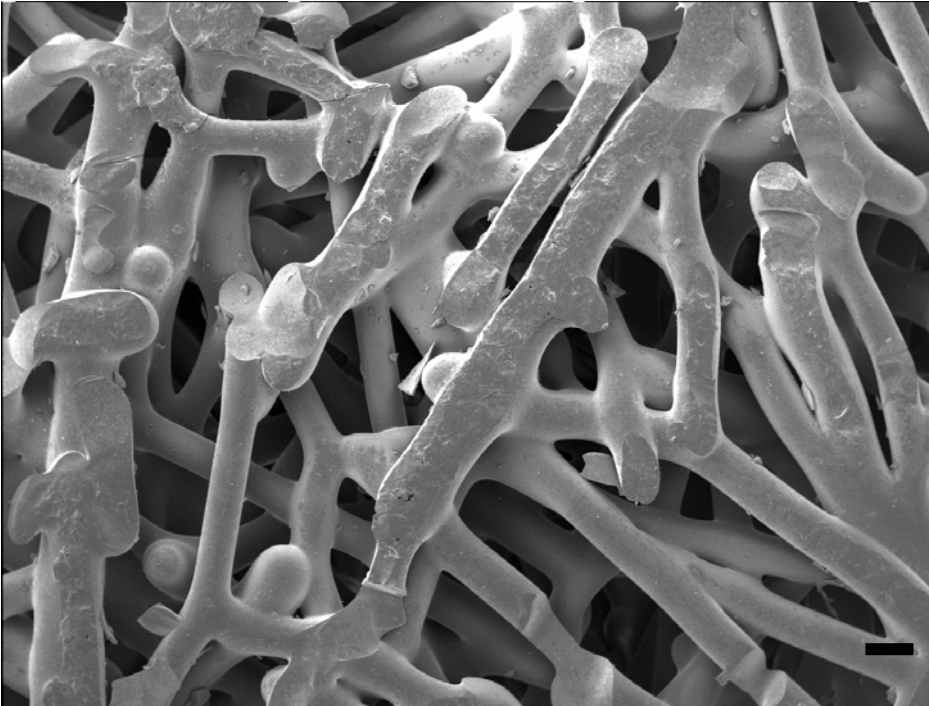


Figure 33. Bioactive glass 13-93 fibre scaffold sintered at 720 °C. Cursor = 100 μ m.

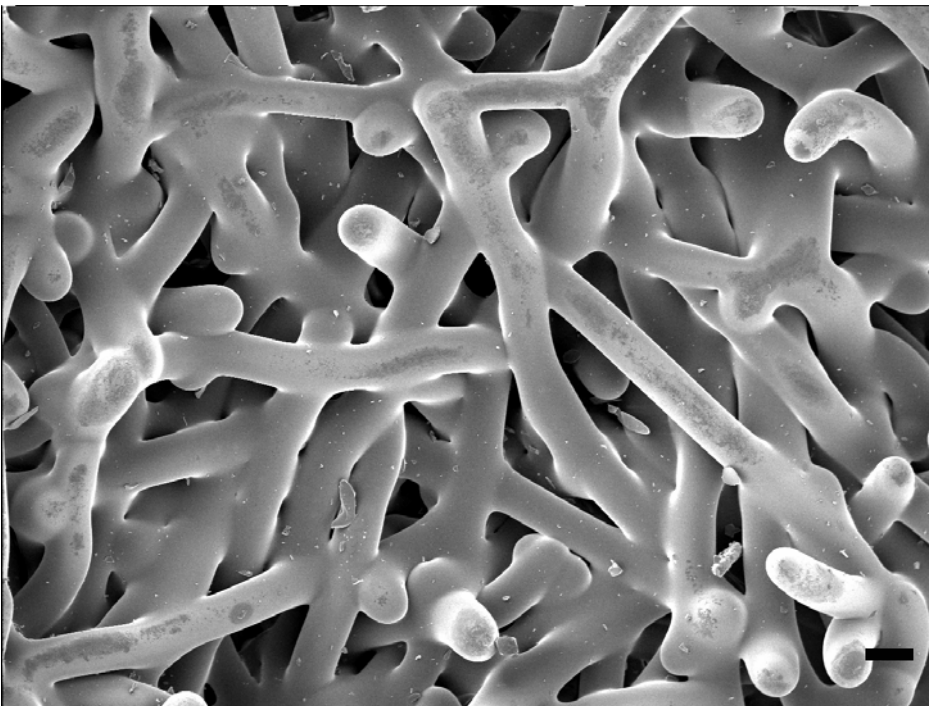


Figure 34. Bioactive glass 13-93 fibre scaffold sintered at 740 °C. Cursor = 100 μ m.

As expected, the higher the porosity, the higher the intrinsic permeability. As Figure 35 shows, porosity and intrinsic permeability are exponentially related.

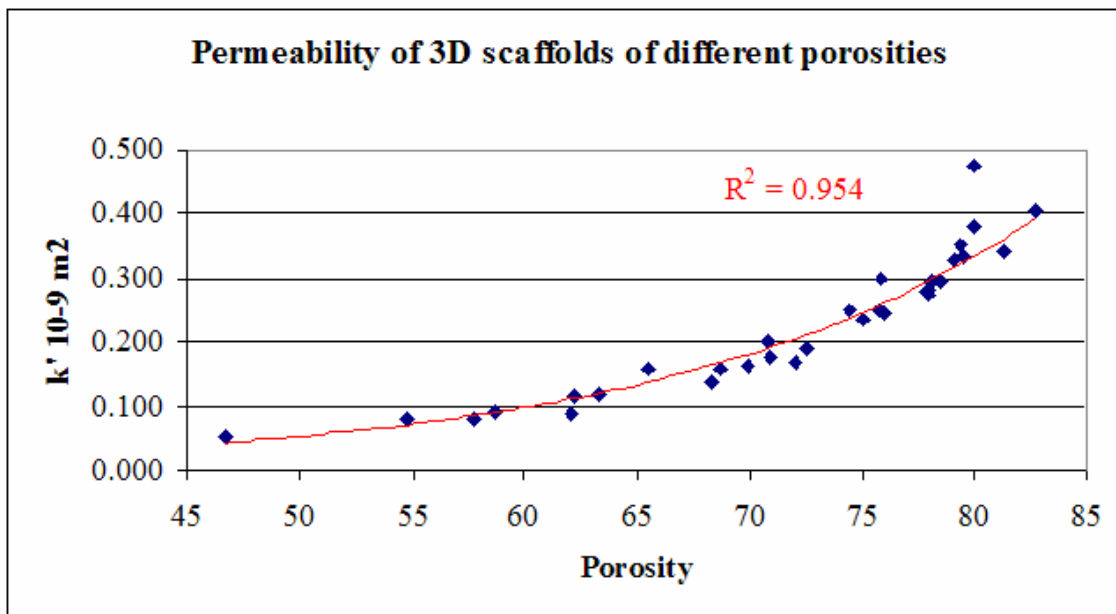


Figure 35. Correlation between porosity and intrinsic permeability.

6 Discussion

The medical field and especially the field of tissue engineering continue to set new challenges for biomaterials engineering. In recent decades resources and knowledge in the field of biomaterials have developed dramatically and biodegradable and bioactive materials have given rise to a new generation of biomaterials. Despite such impressive progress, there is still a need to further enhance the properties of these materials. One fruitful yet under-exploited area in the field of biomaterials is the use of composites. Though there has been much interest in utilizing composites, there are still only a few companies able to realise the widespread practical application of advanced composite materials for clinical use. It seems likely, therefore, that the advantageous properties of composites will play an increasingly important role in area of biomaterials engineering.

6.1 HA/PE composites

The increase in compaction temperature does decrease the strength and modulus of samples with woven fibres. This is to be expected on the basis of as based to the earlier findings. An optimum temperature of 136.5 °C is necessary to achieve a structure in which most of the polymer fibre remains crystalline and only the core melts to form a matrix in which the oriented polymer chains remain unchanged (Hine et al. 1993). As the compaction temperature increases, the amount of the melted oriented polymer chains increases. The reduction of perpendicular weft from the woven fibre layers increases the proportional amount of oriented fibres in the warp (parallel to the long axis; i.e. parallel to the testing axe), and strength and modulus properties are increased.

For single sandwich reinforced HAPEX™, the tensile modulus and strength were significantly higher than the values obtained in bending. Since the woven fibres were placed in the middle of the sample, they have only a minimal effect on the bending properties, whereas the tensile properties are more independent of the reinforcement distribution across the thickness. The comparable multiple sandwich system has a similar level of flexural and tensile properties.

The reinforcement of HAPEX™ improved the mechanical properties of the material. Replacing HAPEX™ for E.HAPEX produced a very marked improvement of the modulus but little change in strength. Nevertheless, the new system has superior flexural and tensile properties compared with control HAPEX™, while retaining and even surpassing the total hydroxyapatite content (40 vol%). This is beneficial because increasing HA content also increases the bioactivity of the composite.

6.2 Bioactive glass Fibres

Because of their low silica content, most existing bioactive glasses tend to phase-separate and devitrify when heated (Brink et al. 1997a). Such glasses are, therefore, mainly used as crushed and cast. To ensure ease of manufacture, the glass must have a large working range interval at which glass formation can take place. Another manufacturing requirement is that the glass does not devitrify during the forming process. Brink et al. found several glass compositions in Na₂O- K₂O- MgO-CaO-B₂O₃-P₂O₃-SiO₂ glass system, which have a large working range and are bioactive. On the basis of their study, the glass systems coded as 13-93 and 9-93 were selected for fibre spinning trials due to their good performance previous studies (Brink 1997a).

The formation of a hydroxycarbonate apatite layer on top of the bioactive glass is a result of the following steps: 1) leaching and formation of silanols (SiOH), 2) loss of soluble silica and formation of silanols, 3) polycondensation of silanols to form a hydrated silica gel, 4) formation of an amorphous calcium phosphate layer and (5) crystallization of a hydroxycarbonate apatite layer (Ducheyene et al. 1992; Hench and Andersson 1993). The formation of the Si- and CaP-rich layers in glass surfaces are usually analysed by techniques such as X-ray diffraction (XRD), Fourier Transform Infrared Spectroscopy (FTIR) or scanning electron microscopy (SEM)(Izquierdo-Barba, Salinas and Vallet-Regi 1999). The effect of the formation of Si- and CaP-rich layers on the mechanical properties of the glasses has not been studied earlier. When bioactive glass is drawn into fibres very uniform test specimens are achieved from which, for example, mechanical properties can be measured. In present study, the formation of reactive layers on the surface of bioactive glass 13-93 fibres was investigated, and its effect on mechanical properties and mass was analyzed.

The flexural strength of glass fibres decreased slightly after immersion in a simulated body fluid, but it later increased from the initial strength value after one week of immersion. As brittle materials, glass fibres are very sensitive to the presence of microscopic imperfections, or flaws, which behave as stress concentrators. As the Si-gel forms on the bioactive glass surface it overcomes the effect of these microscopic imperfections or flaws on the surface and thereby increases the strength of the fibres. This can also be detected from the Weibull modulus value which is 2 for non-immersed fibres, but increases up to 3.6 for immersed fibres, onto which a Si-rich layer has formed. After 1 week of immersion the flexural strength starts to decrease, which is probably due to the increased thickness of the CaP-layer. This layer forms a porous and brittle core and decreases the overall strength of the fibres. From 5 to 40 weeks further decrease in strength is rather small, which may be because the CaP-layer reaches sufficient thickness and retards further degradation and leaching of ions from the glass. The flexural modulus starts to decrease steadily after 1 week of immersion and this is probably due to the transfer of the stiff glass phase to the low modulus Si-gel layer. The high standard deviation in modulus values after two weeks' immersion is probably attributable to the inhomogeneity of the Si-gel and CaP layers.

The change in mass *in vitro* correlates strictly to the surface area of the glass samples. Since the samples with uniform surface areas but variable initial masses had a uniform change in overall mass, so the change in mass was proportional to the surface area of the samples, rather than to the total volume of the samples. The initial leaching of ions can be detected as a loss of mass. Later in the experiment the mass of the samples increased due to the continuous increase in thickness of the CaP-layer. The diffusion of the elements from the surface governs the degradation of structures manufactured from bioactive glass. The total degradation of the bioactive glass structures can be adjusted by controlling the surface/volume ratio. Thin fibres are expected to resorb and transform to calcium phosphate faster than do thicker fibres

From the compositional analysis of the reacted surfaces, the dissolution of ions was clearly evident. Analysis of glass 13-93 showed that a Si-rich layer had already formed after 24 hours' immersion and a slight increase of Ca and P ions could already be detected at this time point. After 5 weeks of immersion, the thickness of the silica layer varied from 5 to 30 μm and the inner CaP layer had a constant thickness of 2 μm . Although the CaP content of this sample was initially higher, the outer layers of CaP had disintegrated from the surface during sample preparation.

The tensile properties of 45S5 Bioglass® fibres have been studied by Clupper et al. and Diego et al. The obtained tensile strength of the studied fibres with diameters of approximately 80 μm was approximately 340 MPa (Clupper et al. 2004; Clupper et al. 2002). De Diego et al. reported tensile strengths of 93 \pm 8 and 82 \pm 14 MPa, for fibres with diameters of 165-220 μm and 250-310 μm

respectively: the Weibull modulus being between 3.0 and 3.5. (DeDiego, Coleman and Hench 1999). The studied tensile strength values for bioactive glasses 9-93 and 13-93 are superior to the values obtained with Bioglass® fibres. Fibre thickness, therefore, plays a significant role with thin fibres, possessing significantly higher strength when compared with the thicker fibres.

The Weibull modulus for the manufactured bioactive glass fibres tested in this study is rather low, approximately $m = 2$, which indicates considerable uncertainty about the stress level at which a fibre is likely to fail. Since glass fibres are highly sensitive to abrasion, and flaws drastically affect strength properties, it would be beneficial to use sizing or coupling agents for bioactive glass fibres.

As reinforcement in composites, fibre strength is the most influential factor on the strength of the composite. The strength of the glass fibre is dependent on structural defects, such as cracks, voids and impurities of the fibre, and possibly also on the stress state of the fibre (Järvelä 1983). Thinner fibres have a smaller surface area and so there is less likelihood of the existence of flaws, thus leading to higher strength values. This may also explain the variation in tensile and flexural stress values in this study. In 3-point testing, the area under maximum stress is significantly smaller than that in tensile testing. The cooling of the glass fibre in melt spinning occurs rather quickly. This causes stress distribution which affects the glass fibre, resulting in compression stress in the surface parts and tensile stress in the inner parts. This toughening phenomenon is the product of stress distribution, which is a result of density differences in the different layers of the fibre caused by cooling. For thinner fibres, cooling is more rapid than for thicker fibres, and this may also cause the difference in strength properties. In technical glass fibre manufacturing, cooling of the fibres is normally done by spraying water directly onto the fibre as it drains from the nozzle, and this further decreases the cooling time of thin fibres. Another derived benefit in manufacturing technical grade glass fibres is the use of sizing agents to cover the formed fibre surface already at the fibre spinning stage. The reported tensile strength for technical sized E-glass fibre is approximately 2 GPa or above for glass fibres with a diameter of approximately 15 μm . The reported Weibull modulus for technical E-glass fibres is approximately 5.5 (Gurvich, Dibenedetto and Pegoretti 1997; Perdini and Manhani 2002).

6.3 Glass fibre composites

Although fibre glass reinforced polymeric composites have been widely used in non-medical applications for a long time, there are so far no reports of bioactive glass fibre composites being used in medical applications. There is much interest in studying and developing methods for manufacturing composites from bioactive glass fibres and biomedical polymers. In this study experimental coating methods for bioactive glass fibres were developed and experimental bioactive glass fibre–biomedical polymer composites were manufactured by piston injection moulding. Since bioactive glass fibres are highly sensitive to abrasion, and flaws drastically affect the strength properties, it is beneficial to use coating or sizing or coupling agents for bioactive glass fibres. As this study shows, the application of a polymeric coating significantly improves the initial mechanical properties and handling of bioactive glass fibres.

By using bioactive glass fibres as a part of a polymeric composite, its properties can be enhanced as follows: 1) bioactive glass fibres reinforce the polymer and the mechanical properties of the obtained composite may reach the level of hard bone tissue and 2) bioactive glass imparts osteoconductive characteristics to the composite. The initial flexural strength and modulus of rods improved dramatically when bioactive glass fibres were implemented into structure. The increase in strength and modulus correlated closely to the volume of fibres used. It would, however, be

interesting to determine if the improvement in the strength and modulus properties is maintained when samples are immersed in simulated body fluids.

It is interesting to note, that even though biomedical polymers do not in themselves have a “bioactive nature”, a thick calcium phosphate-like layer does form on the polymer surfaces as a coating for bioactive glass. In this study the precipitates were not quantitatively analysed, though the precipitation on top of the polymeric coating is visually identical when compared to the calcium phosphate precipitations previously analysed by Kokubo (Kokubo 1992) and Kellomäki (Kellomäki et al. 2000). The formation of a calcium phosphate layer on organic materials has also previously been reported, for example, by Abe et al. (Abe, Kokubo and Yamamuro 1990). Marcolongo et al. (Marcolongo, Ducheyne and LaCourse 1997) and Niiranen et al. (Niiranen and Törmälä 1998) have also reported the “halo” effect, in which the polymeric phase of a composite containing bioactive glass and biomedical polymer also shows calcium phosphate precipitating onto its surface when immersed in simulated body fluid. In comparison with the non-coated fibre, the formation of a calcium phosphate layer in the fibre surface is retarded when bioactive glass fibre is coated with medical polymers. The hydrophobic poly(L-lactide) coating prevents water penetration into the glass thus causing the delay in the degradation and dissolution of bioactive glass. Defects in the coating allow water penetration into the glass, thereby enabling glass resorption in areas which are in contact with SBF.

Besides using bioactive glass fibres as reinforcement in composites, there is also interest in producing fabrics which are woven from them. The experiments in the present study showed that even slight abrasion of the fibre surfaces drastically reduces the maximum apparent strain. With a polymer coating, abrasion can be avoided. Unless coated, bioactive glass the fibres cannot be fabricated further as long fibres; indeed thin fibres cannot even be unwound from the coil without coating. Both coating methods produced a smooth polymeric layer on the surface of bioactive glass fibres. It seems probable that tailor-made coatings can also be produced for bioactive glass fibres to provide the optimum properties required in different manufacturing processes. However, the fibre-polymer coating adhesion is not optimal in the case of the samples manufactured in this study. The fibre-matrix interface plays a crucial role in the manufacture of high strength composites. In order to achieve high strength biomedical composites, surface adhesion between fibre and coating needs further study and probably improvement.

6.4 Bioactive glass fibre scaffolds

Despite the keen interest in developing optimal scaffold materials in recent years, further optimisation of the materials is still required. However, it does seem certain that increasing improvements in scaffold materials will be achieved by companies and research groups in the near future. Hutmacher (Hutmacher 2000) has formulated a descriptive list of the characteristics of an ideal musculoskeletal tissue engineering scaffold as follows:

- (i) three dimensional and highly porous with an interconnected pore network for cell growth and flow transport of nutrients and metabolic waste,
- (ii) biocompatible and bioresorbable with controllable degradation and resorption rate to match cell/tissue growth *in vitro* and/or *in vivo*,
- (iii) suitable surface chemistry for cell attachment, proliferation and differentiation, and
- (iv) mechanical properties to match those of the tissues at the site of implantation.

For bone tissue application, osteoconductivity would also be a desirable property (Boccaccini and Maquet 2003). Another important consideration is ease of manufacture of homogeneous batches of scaffold material at reasonable cost, since that is crucial for commercial success.

Bioactive glass is proposed as a good material choice to achieve repair of bone tissue because of its resorbability and its osteo-stimulating effect (Ducheyne and Qiu 1999). With the sintering method, in which chopped bioactive glass fibres are sintered by heat to form a porous scaffold, a scaffold with porous network is obtained. The network has highly interconnected pores as shown in Figure 32, Figure 33 and Figure 34. The porosity, pore size, scaffold architecture, mechanical properties (not measured in this study) and degradation rate of the material of the scaffold are all characteristics which can be optimised when using this method. The fibre dimensions (diameter and length of individual fibre segments), and sintering temperature are parameters which affect the scaffold architecture, porosity, pore size and mechanical properties. The degradation rate of the scaffold can be controlled, to some extent, by optimising fibre diameter and composition of the glass. These are all characteristics which play important roles in tissue engineering scaffolds (Karande, Ong and Agrawal 2004). With chopped bioactive glass fibres having a diameter of 100 μm and length of 3 mm, it was possible to manufacture porous scaffolds with porosity from 10% up to 90 % and pore size in the range of 120 – 425 μm .

A highly interconnected and accessible pore architecture is shown to be a crucial property for a tissue engineering scaffold (Malda et al. 2005; Miot et al. 2005). The permeability measurements demonstrated that porosity and intrinsic permeability are exponentially related in the manufactured porous scaffolds. It is also worth noting that the results obtained in this study are highly comparable to the results obtained on calcaneal bone by Grimm (Grimm and Williams 1997). It can be concluded, therefore, that with this technique a scaffold can be obtained which has hydrodynamic properties similar to human calcaneal bone. It is also expected that this material will be adequate for applications in bone grafting and bone tissue engineering.

7 Summary and Conclusions

With the observation that bioactive ceramics are well tolerated by living tissues and a tight bond forms between the material and bone, the manufacture of such man-made materials is not only feasible but their effects will also be beneficial. The most recent results of this decade further confirm that bioactive glasses, in particular, have a stimulating effect on various cell types and this opens up new and interesting areas of application, especially in the field of tissue engineering.

The goals of this study were to investigate the effect of composite structure on the mechanical properties of various hydroxyapatite polyethylene composites, to manufacture and characterize bioactive glass fibres formed from bioactive glasses 13-93 and 9-93 and to manufacture and characterize composites derived from the produced bioactive glass fibres.

Hydroxyapatite (HA)–polyethylene (PE) composites were manufactured with different constructions. HA in composites was used as particulates, and PE as fibres and particulates. The samples were formed by hot compaction. Very good adhesion was obtained between the various phases and the mechanical properties were markedly improved with PE fibre reinforced constructions.

The melt spinning of bioactive glasses 13-93 and 9-93 was successful and homogeneous continuous fibres were obtained. Fibres with diameters from 20 μm up to 300 μm were successfully produced. The strength of the fibres correlates closely with fibre diameter; thin fibres possessing the highest strength. Mechanical properties of the fibres are highly sensitive to abrasion of the fibre surface, and polymeric coating of fibre surface greatly improved the properties and the handling of fibres.

In simulated body fluid (SBF) a Si-rich layer and CaP precipitates form on the non-coated and coated fibre surfaces, though coating fibres with polymers delayed the formation of the CaP layers. The degradation of fibres is highly dependent on the surface area; thin fibres degrading more quickly than thick fibres. In *in vitro* conditions the strength of fibres remains at the initial level during the first weeks, after which there is drop in mechanical properties. However, in *in vitro* conditions the formed surface layers retard further degradation and the mechanical properties level off after 5 to 7 weeks time period, thus addressing the difficulty of estimating the reaction which would occur *in vivo*.

The use of high strength glass fibres as reinforcement clearly improved the mechanical properties of the composites when compared with the non-reinforced samples. Using a sintering technique, porous 3D-scaffolds were manufactured from bioactive glass fibres. By optimising both the dimensions of the fibre segments used and the sintering temperature, it is possible to optimise porosity, pore size, scaffold architecture and mechanical properties.

The medical field and tissue engineering in particular are presenting ever new challenges for biomaterials engineering. Recent decades have witnessed enormous advances in resources and knowledge of biomaterials, in particular the biodegradable and bioactive materials which have given rise to a new generation of biomaterials. Despite such remarkable development, there is still a need for further enhancement of the properties of these materials. One fruitful area of research in biomaterials is the use of composites. Despite the keen interest in utilizing composites in medical applications, numerous obstacles must still be overcome before the potential of composite technology can be fully utilized. It seems likely, therefore, that the advantageous properties which can be achieved through the use of composite engineering will assume an even greater role in the future in the field of biomaterials

Acknowledgements

This thesis is based on work carried out at the IRC in Polymer Science and Technology at University of Leeds, the Institute of Biomaterials at Tampere University of Technology, and Inion Oy during the years 1997-2006. The work has been financially supported by the Academy of Finland, the Finnish Technology and Development Centre (TEKES), Laura and Aarne Karjalainen Foundation, the City of Tampere (Kulttuurirahasto), Foundation of Technology, the Institute of Biomaterials at Tampere University of Technology, and Inion Oy.

I am especially indebted to Academy Professor, Head of the Institute of Biomaterials, Pertti Törmälä for his inspiration and help and for providing me with the opportunity to study the fascinating world of Biomaterials. I am also grateful to Professor Minna Kellomäki for her support in completing my thesis, Henna Niiranen for the great time we had exploring the early stages in bioactive glass fibre research, and to all colleagues at the Institute on Biomaterials for making it such a wonderful place to work.

I would like to express my gratitude to Hugo Ladizesky for giving me with the chance to work in IRC in Leeds. This allowed me to gain greater insight into the enthralling subject of Biomaterials.

I wish to thank Maria Brink for her guidance in the field of bioactive glasses.

I am grateful to Inion Oy for providing me with the opportunity to carry out work into bioactive glasses in recent years. Special thanks to Loredana Moimas and all friends at Inion Oy for the enjoyable time spent working with you.

Antti, Sara and Anton - thank you for your loving support.

References

- Abe, Y, T Kokubo, and T Yamamuro. 1990. "Apatite coating on ceramics, metals and polymers utilizing a biological process." *Journal of Materials Science: Materials in Medicine* 1:233-238.
- Aho, AJ, J Heikkilä, HJ Aho, Ö Andersson, and A Yli-Urpo. 1993. "Morphology of osteogenesis in bioactive glass interface." *Annales Chirurgiae et Gynaecologiae* 82:145-153.
- Aho, AJ, E Suominen, A Alanen, A Yli-Urpo, J Knuuti, and HJ Aho. 2003. "Remodeling of the tibia after grafting of a large cavity with particulate bioactive glass-hydroxylapatite--case report on treatment of fibrous dysplasia with 13 years' follow-up." *Acta Orthop Scand* 74:766-70.
- Aho, AJ, T Tirri, J Kukkonen, N Strandberg, J Rich, J Seppala, and A Yli-Urpo. 2004. "Injectable bioactive glass/biodegradable polymer composite for bone and cartilage reconstruction: concept and experimental outcome with thermoplastic composites of poly(epsilon-caprolactone-co-D,L-lactide) and bioactive glass S53P4." *J Mater Sci Mater Med* 15:1165-73.
- Aitasalo, K, J Suonpää, M Peltola, and A Yli-Urpo. 1997. "Behaviour of bioactive glass (S53P4) in human frontal sinus obliteration." in *10th International Symposium on Ceramics in Medicine*, edited by L and Rey Sedel, C. Paris, France: Elsevier Science Ltd.
- Allan, I, H Newman, and M Wilson. 2001. "Antibacterial activity of particulate Bioglass against supra- and sub gingival bacteria." *Biomaterials* 22:683-1687.
- Allan, I, H Newman, and M Wilson. 2002. "Particulate bioglass reduces the viability of bacterial biofilms formed on its surface in an in vitro model." *Clin oral impl* 13:53-58.
- Andriano, KP, and AU Daniels. 1992. "Effectiveness of silane treatment on absorbable microFibres." *J Appl Biomater* 3:191-5.
- Andriano, KP, AU Daniels, and J Heller. 1992. "Biocompatibility and mechanical properties of a totally absorbable composite material for orthopaedic fixation devices." *J Appl Biomater* 3:197-206.
- Asselin, A, S Hattar, M Oboeuf, D Greenspan, A Berdal, and JM Sautier. 2004. "The modulation of tissue-specific gene expression in rat nasal chondrocyte cultures by bioactive glasses." *Biomaterials* 25:5621-30.
- Bielby, RC, IS Christodoulou, RS Pryce, WJ Radford, LL Hench, and JM Polak. 2004. "Time- and concentration-dependent effects of dissolution products of 58S sol-gel bioactive glass on proliferation and differentiation of murine and human osteoblasts." *Tissue Eng* 10:1018-26.
- Boccaccini, AR, and V Maquet. 2003. "Bioresorbable and bioactive polymer/Bioglass® composites with tailored pore structure for tissue engineering applications." *Compos Sci Technol* 63:2417-2429.
- Bonassar, LJ, and CA Vacanti. 1998. "Tissue engineering: the first decade and beyond." *J Cell Biochem Suppl* 30:297-303.
- Bonfield, W. 1988. "Composites for bone replacement." *J Biomed Eng* 10:522-6.
- Bonfield, W. 1993. "Design of Bioactive ceramic-polymer composites." in *Advanced Series in Ceramics, An Introduction to Bioceramics*, edited by L Hench and J Wilson: World Scientific Publishing Co.
- Bonfield, W, MD Grynspas, AE Tully, J Bowman, and J Abram. 1981. "Hydroxyapatite reinforced polyethylene--a mechanically compatible implant material for bone replacement." *Biomaterials* 2:185-6.
- Bosetti, M, and M Cannas. 2005. "The effect of bioactive glasses on bone marrow stromal cells differentiation." *Biomaterials* 26:3873-9.

- Branda, F, F Arcobello-Varlese, A Costantini, and G Luciani. 2002. "Effect of the substitution of M₂O₃ (M = La, Y, In, Ga, Al) for CaO on the bioactivity of 2.5CaO x 2SiO₂ glass." *Biomaterials* 23:711-6.
- Brink, M. 1997a. "Bioactive Glasses with a large working range." Pp. 44 in *Department of Chemical Engineering*. Turku, Finland: Åbo Akademi University.
- Brink, M. 1997b. "The influence of alkali and alkaline earths on the working range for bioactive glasses." *J Biomed Mater Res* 36:109-17.
- Brink, M, P Laine, K Narva, and A Yli-Urpo. 1997a. "Implantation of bioactive and inert glass Fibres in rats- soft tissue response and short-term reactions of the glass." *Bioceramics* 10:61-64.
- Brink, M, V Pitkänen, J Tikkanen, M Paajanen, and G Graeffe. 1996. "Spherical particles of a bioactive glass- manufacturing and reactions in vitro." Pp. 127-130 in *Bioceramics, Volume 9*, edited by Tadashi Kokubo, Takashi Nakamura, and Fumiaki Miyaji: Elsevier Science Ltd.
- Brink, M, T Turunen, R-P Happonen, and A Yli-Urpo. 1997b. "Compositional dependence of bioactivity of glasses in the system Na₂O-K₂O-MgO-CaO-B₂O₃-P₂O₅-SiO₂." *J Biomed Mater Res* 37:114-121.
- Burg, KJL, S Porter, and JF Kellam. 2000. "Biomaterial developments for bone tissue engineering." *Biomaterials* 21:2347-2359.
- Cancedda, R, B Dozin, P Giannoni, and R Quarto. 2003. "Tissue engineering and cell therapy of cartilage and bone." *Matrix Biol* 22:81-91.
- Cerruti, M, D Greenspan, and K Powers. 2005a. "Effect of pH and ionic strength on the reactivity of Bioglass 45S5." *Biomaterials* 26:1665-74.
- Cerruti, MG, D Greenspan, and K Powers. 2005b. "An analytical model for the dissolution of different particle size samples of Bioglass in TRIS-buffered solution." *Biomaterials* 26:4903-11.
- Chapekar, MS. 2000. "Tissue engineering: challenges and opportunities." *J Biomed Mater Res (Appl Biomater)* 53:617-620.
- Chen, G, T Sato, T Ushida, R Hirochika, Y Shirasaki, N Ochiai, and T Tateishi. 2003. "The use of a novel PLGA Fibre/collagen composite web as a scaffold for engineering of articular cartilage tissue with adjustable thickness." *J Biomed Mater Res A* 67:1170-80.
- Chua, KN, WS Lim, P Zhang, H Lu, J Wen, S Ramakrishna, KW Leong, and HQ Mao. 2005. "Stable immobilization of rat hepatocyte spheroids on galactosylated nanoFibre scaffold." *Biomaterials* 26:2537-47.
- Clark, AE, LL Hench, and HA Paschall. 1976. "The influence of surface chemistry on implant interface histology: a theoretical basis for implant materials selection." *J Biomed Mater Res* 10:161-74.
- Clupper, DC, JE Gough, PM Embanga, I Notingher, LL Hench, and MM Hall. 2004. "Bioactive evaluation of 45S5 bioactive glass fibres and preliminary study of human osteoblast attachment." *J Mater Sci Mater Med* 15:803-8.
- Clupper, DC, MM Hall, JE Gough, and LL Hench. 2002. "52S and 45S5 Glass Fibres: Bioactive, Mechanical, and cellular evaluation." Pp. 579 in *Society for Biomaterials 28th annual meeting*.
- Day, RM. 2005. "Bioactive glass stimulates the secretion of angiogenic growth factors and angiogenesis in vitro." *Tissue Eng* 11:768-77.
- DeDiego, MA, NJ Coleman, and LL Hench. 1999. "Tensile properties of bioactive Fibres for tissue engineering applications." *J Biomed Mater Res (Appl Biomater)* 53:199-203.
- Doyle, C, ZB Luklinska, KE Tanner, and W Bonfield. 1990. *An ultra-structural study of the interface between hydroxyapatite/polymer composite and bone*. Amsterdam: Elsevier Scientific Publisher B.V.

- Ducheyne, P, P Bianco, S Radin, and E Schepers. 1992. "Bioactive Materials: Mechanisms and Bioengineering Considerations." Pp. 1-12 in *Bone Bonding*, edited by Paul Ducheyne, T Kokubo, and C. A. Van Blitterswijk.
- Ducheyne, P. 1998. "Stimulation of biological function with bioactive glass." *MRS Bulletin* 23:42-49.
- Ducheyne, P, and Q Qiu. 1999. "Bioactive ceramics: the effect of surface reactivity on bone formation and bone cell function." *Biomaterials* 20:2287-2303.
- Dunn, RL, RA Casper, and BS Kelley. 1985. "Biodegradable composites." Pp. 213 in *The 11th Annual Meeting of the Society for Biomaterials*. San Diego, California, U.S.A.
- El-Ghannam, A, P Ducheyne, and IM Shapiro. 1997. "Porous bioactive glass and hydroxyapatite ceramic affect bone cell function in vitro along different time lines." *J Biomed Mater Res* 36:167-180.
- Elshahat, A, MA Shermak, N Inoue, EYS Chao, and P Manson. 2004. "The use of Novabone and Norian in Cranioplasty: A Comparative Study." *The journal of Craniofacial surgery* 15:483-489.
- Filgueiras, MR, G La Torre, and LL Hench. 1993. "Solution effects on the surface reactions of a bioactive glass." *J Biomedical Materials Research* 27:445-453.
- Foppiano, S, SJ Marshall, GW Marshall, E Saiz, and AP Tomsia. 2004. "The influence of novel bioactive glasses on in vitro osteoblast behavior." *J Biomed Mater Res A* 71:242-9.
- Gasser, B. 2000. "About composite materials and their use in bone surgery." *Injury* 31:4.
- Gogolewski, S. 2000. "Bioresorbable polymers in trauma and bone surgery." *Injury* 31 Suppl 4:28-32.
- Gough, JE, I Notingher, and LL Hench. 2004. "Osteoblast attachment and mineralized nodule formation on rough and smooth 45S5 bioactive glass monoliths." *J Biomed Mater Res A* 68:640-50.
- Greenspan, DC, JP Zhong, and GP La Torre. 1994. "Effect of surface area to volume ratio on in vitro surface reactions of bioactive glass particulates." *Bioceramics* 7:55-60.
- Greish, YE, and PW Brown. 2000. "Characterization of bioactive glass-reinforced HAP-polymer composites." *J Biomed Mater Res* 52:687-694.
- Griffith, LG, and G Naughton. 2002. "Tissue engineering: current challenges and expanding opportunities." *Science* 295:1009-1016.
- Grimm, MJ, and JL Williams. 1997. "Measurements of permeability in human calcaneal trabecular bone." *J Biomech* 30:743-745.
- Gurvich, MR, AT Dibenedetto, and A Pegoretti. 1997. "Evaluation of the statistical parameters of a Weibull distribution." *J. Mater. Sci.* 32:3711-3716.
- Heikkilä, JT, HJ Aho, A Yli-Urpo, RP Happonen, and AJ Aho. 1995. "Bone formation in rabbit cancellous bone defects filled with bioactive glass granules." *Acta Orthop Scand* 66:463-7.
- Heikkilä, JT, AJ Aho, A Yli-Urpo, Ö Andersson, HJ Aho, and R-P. Happonen. 1993. "Bioactive glass versus hydroxyapatite in reconstruction of osteochondral defects in the rabbit." *Acta Orthop Scand* 64:678-682.
- Heikkilä, JT, KT Matila, ÖH Andersson, J. Knuuti, A Yli-Urpo, and AJ. Aho. 1995. "Behavior of bioactive glass in human bone." Pp. 35-40 in *8th International Symposium on Ceramics in Medicine*, edited by J Wilson, L Hench, and D. Greenspan. Florida, USA: Elsevier.
- Hench, LL. 1998. "Biomaterials: a forecast for the future." *Biomaterials* 19:1419-1423.
- Hench, LL, and Ö Andersson. 1993. "Bioactive glasses." Pp. 1-24 in *An Introduction to Bioceramics*, edited by L Hench and J Wilson. Florida: World Scientific.
- Hench, LL, CG Pantano, JR. Buscemi, P.J, and DC Greenspan. 1977. "Analysis of bioglass fixation of hip prostheses." *J Biomed Mater Res* 11:267-282.
- Hench, LL, and HA Paschall. 1973. "Direct chemical bond of bioactive glass-ceramic materials to bone and muscle." *J. Biomed Mater Res Symposium* 4:25-42.

- Hench, LL, and HA Paschall. 1974. "Histochemical responses at a biomaterial's interface." *J Biomed Mater Res Symposium* 5:49-64.
- Hench, LL, and JM Polak. 2002. "Third-generation biomedical materials." *Science* 295:1014-1017.
- Hench, LL, RJ Splinter, and WC Allen. 1971. "Bonding mechanisms at the interface of ceramic prosthetic materials." *J Biomed Mater Res Symposium* 2:117-141.
- Hench, LL, and J Wilson. 1984. "Surface-active biomaterials." *Science* 226:630-6.
- Hench, LL, and J Wilson. 1993. "Introduction." Pp. 1-24 in *An Introduction to Bioceramics*, edited by L Hench and J Wilson. Florida: World Scientific.
- Hiljanen-Vainio, M, T Karjalainen, and J Seppälä. 1996. "Biodegradable Lactone Copolymers I. Characterization and Mechanical Behavior of ϵ -Caprolactone and Lactide Copolymers." *J Appl Polym Sci* 59:1281-1288.
- Hine, PJ, IM Ward, RH Olley, and DC Bassett. 1993. "The hot compaction of high modulus melt-spun polyethylene Fibres." *Journal of Materials Science* 28.
- Hokugo, A, T Takamoto, and Y Tabata. 2006. "Preparation of hybrid scaffold from fibrin and biodegradable polymer Fibre." *Biomaterials* 27:61-7.
- Hull, D, and TW Clyne. 1996. *An Introduction to Composite Materials*. Cambridge: Cambridge University Press.
- Hutmacher, DW. 2000. "Scaffolds in tissue engineering bone and cartilage." *Biomaterials* 21:2529-2543.
- Ito, G, T Matsuda, N Inoue, and T Kamegai. 1987. "A histological comparison of the tissue interface of bioglass and silica glass." *J Biomed Mater Res* 21:485-97.
- Izquierdo-Barba, I, AJ Salinas, and M Vallet-Regi. 1999. "In vitro calcium phosphate layer formation on sol-gel glasses of the CaO-SiO₂ system." *J Biomed Mater Res* 47:243-50.
- Jaakkola, T, J Rich, T Tirri, T Narhi, M Jokinen, J Seppala, and A Yli-Urpo. 2004. "In vitro Ca-P precipitation on biodegradable thermoplastic composite of poly(ϵ -caprolactone-co-DL-lactide) and bioactive glass (S53P4)." *Biomaterials* 25:575-81.
- Jones, JR, S Ahir, and LL Hench. 2004. "Large-Scale Production of 3D Bioactive glass macroporous scaffolds for tissue engineering." *Journal of Sol-Gel Science and Technology* 29:179-188.
- Jones, JR, LM Ehrenfried, and LL Hench. 2006. "Optimising bioactive glass scaffolds for bone tissue engineering." *Biomaterials* 27:964-73.
- Jones, JR, and LL Hench. 2004. "Factors affecting the structure and properties of bioactive foam scaffolds for tissue engineering." *Wiley Periodicals, Inc. J Biomed Mater Res Part B: Appl Biomater* 68B:36-44.
- Jones, JR, P Sepulveda, and LL Hench. 2001. "Dose-dependent behavior of bioactive glass dissolution." *J Biomed Mater Res (Appl Biomater)* 58:720-726.
- Josset, Y, F Nasrallah, E Jallot, M Lorenzato, O Dufour-Mallet, G Balossier, and D Laurent-Maquin. 2003. "Influence of physicochemical reactions of bioactive glass on the behavior and activity of human osteoblasts in vitro." *J Biomed Mater Res A* 67:1205-18.
- Järvelä, P. 1983. "Properties of glass Fibres and their applications in porous composites." in *Department of Materials Science*. Tampere: Tampere University of Technology.
- Karande, TS, JL Ong, and CM Agrawal. 2004. "Diffusion in musculoskeletal tissue engineering scaffolds: design issues related to porosity, permeability, architecture, and nutrient mixing." *Ann Biomed Eng* 32:1728-43.
- Kellomäki, M, H Niiranen, K Puumanen, N Ashammakhi, T Waris, and P Törmälä. 2000. "Bioabsorbable scaffolds for guided bone regeneration and generation." *Biomaterials* 21:2495-2505.
- Keshaw, H, A Forbes, and RM Day. 2005. "Release of angiogenic growth factors from cells encapsulated in alginate beads with bioactive glass." *Biomaterials* 26:4171-4179.

- Khil, MS, SR Bhattarai, HY Kim, SZ Kim, and KH Lee. 2005. "Novel fabricated matrix via electrospinning for tissue engineering." *J Biomed Mater Res B Appl Biomater* 72:117-24.
- Kidoaki, S, IK Kwon, and T Matsuda. 2005. "Mesoscopic spatial designs of nano- and microFibre meshes for tissue-engineering matrix and scaffold based on newly devised multilayering and mixing electrospinning techniques." *Biomaterials* 26:37-46.
- Kim, CY, AE Clark, and LL Hench. 1989. "Early stages of calcium-phosphate layer formation in bioglasses." *Journal of Non-Cryst Solids* 133:195-202.
- Kim, H-M. 2003. "Ceramic bioactivity and related biomimetic strategy." *Current opinion in Solid State & Materials Science* 7:289-299.
- Kokubo, T. 1992. "Bioactivity of glasses and glass ceramics." Pp. 31-46 in *Bone-bonding materials*, edited by Paul Ducheyne, T Kokubo, and C. A. Van Blitterswijk. Leiderdorp, Netherlands.
- Kokubo, T, H Kushitani, S Sakka, T Kitsugi, and T Yamamuro. 1990. "Solutions able to reproduce in vivo surface-structure changes in bioactive glass-ceramic A-W." *J Biomed Mater Res* 24:721-34.
- Krebs, S, S Lin, and R King. 1993. "Characterization of HA and resorbable glass Fibres reinforced PLLA screws." in *The 19th Annual Meeting of the Society for Biomaterials*. Birmingham, AL, USA.
- Lai, W, J Garino, and P Ducheyne. 2001. "Resorption of bioactive glass." Pp. 252 in *47th Annual Meeting, Orthopaedic Research Society*. San Francisco, California, USA.
- Lee, YH, JH Lee, IG An, C Kim, DS Lee, YK Lee, and JD Nam. 2005. "Electrospun dual-porosity structure and biodegradation morphology of Montmorillonite reinforced PLLA nanocomposite scaffolds." *Biomaterials* 26:3165-72.
- Leonelli, C, G Lusvardi, G Malavasi, L Menabue, and M Tonelli. 2003. "Synthesis and characterization of cerium-doped glasses and in vitro evaluation of bioactivity." *Journal of Non-Crystalline Solids* 316:198-216.
- Lin, FH, YY Huang, MH Hon, and SC Wu. 1991. "Fabrication and biocompatibility of a porous bioglass ceramic in a Na₂O-CaO-SiO₂-P₂O₅ system." *J Biomed Eng* 13:328-34.
- Lin, TC. 1986. "Totally Absorbable Fibre Reinforced Composite For Internal Fracture Fixation Device." Pp. 166 in *The 12th Annual Meeting of the Society for Biomaterials*. Minneapolis-St.Paul, Minnesota, USA.
- Lindfors, NC, K Tallroth, and AJ Aho. 2002. "Bioactive glass as bone-graft substitute for posterior spinal fusion in rabbit." *J Biomed Mater Res (Appl Biomater)* 63:237-244.
- Livingston, T, P Ducheyne, and J Garino. 2002. "In vivo evaluation of a bioactive scaffold for bone tissue engineering." *J Biomed Mater Res* 62:1-13.
- Lossdorfer, S, Z Schwartz, CH Lohmann, DC Greenspan, DM Ranly, and BD Boyan. 2004. "Osteoblast response to bioactive glasses in vitro correlates with inorganic phosphate content." *Biomaterials* 25:2547-55.
- Low, SB, CJ King, and J Krieger. 1997. "An evaluation of bioactive ceramic in the treatment of periodontal osseous defects." *Int J Periodontics Restorative Dent* 17:358-67.
- Lu, HH, SA El-Amin, and CT Laurencin. 2001. "Polymer-bioactive glass composite scaffold for bone tissue engineering: matrix design and in vitro evaluations." *Bioengineering conference ASME* 50:693-694.
- Lu, HH, SF El-Amin, KD Scott, and CT Laurencin. 2003. "Three-dimensional, bioactive, biodegradable, polymer-bioactive glass composite scaffolds with improved mechanical properties support collagen synthesis and mineralization of human osteoblast-like cells in vitro." *J Biomed Mater Res A* 64:465-74.
- Lu, HH, A Tang, SC Oh, JP Spalazzi, and K Dionisio. 2005. "Compositional effects on the formation of a calcium phosphate layer and the response of osteoblast-like cells on polymer-bioactive glass composites." *Biomaterials* 26:6323-34.

- Lysaght, MJ, and AL Hazlehurst. 2004. "Tissue engineering: the end of the beginning." *Tissue Eng* 10:309-20.
- Ma, PX. 2004. "Scaffolds for tissue fabrication." *Materialstoday*:30-40.
- Ma, Z, M Kotaki, R Inai, and S Ramakrishna. 2005. "Potential of nanoFibre matrix as tissue-engineering scaffolds." *Tissue Eng* 11:101-9.
- Mahmood, J, H Takita, Y Ojima, M Kobayashi, T Kohgo, and Y Kubogi. 2001. "Geometric effect of matrix upon cell differentiation: BMP-induced osteogenesis using a new bioglass with a feasible structure." *J Biochem* 129:163-179.
- Malda, J, TB Woodfield, F van der Vloodt, C Wilson, DE Martens, J Tramper, CA van Blitterswijk, and J Riesle. 2005. "The effect of PEGT/PBT scaffold architecture on the composition of tissue engineered cartilage." *Biomaterials* 26:63-72.
- Maquet, V, AR Boccaccini, L Pravata, I Notingher, and R Jérôme. 2004. "Porous poly(a-hydroxyacid)/Bioglass composite scaffolds for bone tissue engineering. I: preparation and in vitro characterization." *Biomaterials* 25:4185-4194.
- Marcolongo, M, P Ducheyne, J Garino, and E Schepers. 1998. "Bioactive glass Fibre/polymeric composites bond to bone tissue." *J Biomed Res* 39:161-170.
- Marcolongo, M, P Ducheyne, and WC LaCourse. 1997. "Surface reaction layer formation in vitro on a bioactive glass Fibre/polymeric composite." *J Biomed Mater Res* 37:440-8.
- Matsuda, T, and JE Davies. 1987. "The in vitro response of osteoblasts to bioactive glass." *Biomaterials* 8:275-84.
- Maxwell, AS, AP Unwin, and IM Ward. 1996. "The effect of high pressure annealing on the molecular network in polyethylene." *Polymer* 37:3293-3301.
- Merwin, GE. 1986. "Bioglass middle ear prosthesis: preliminary report." *Ann Otol Rhinol Laryngol* 95:78-82.
- Merwin, GE, LW Rodgers, J Wilson, and RG Martin. 1986. "Facial bone augmentation using Bioglass in dogs." *Arch Otolaryngol Head Neck Surg* 112:280-4.
- Miot, S, T Woodfield, AU Daniels, R Suetterlin, I Peterschmitt, M Heberer, CA van Blitterswijk, J Riesle, and I Martin. 2005. "Effects of scaffold composition and architecture on human nasal chondrocyte redifferentiation and cartilaginous matrix deposition." *Biomaterials* 26:2479-89.
- Moritz, N, E Vedel, H Ylänen, M Jokinen, M Hupa, and A Yli-Urpo. 2004. "Characterisation of bioactive glass coatings on titanium substrates produced using a CO2 laser." *J Mater Sci Mater Med* 15:787-94.
- Moroni, L, JR de Wijn, and CA van Blitterswijk. 2005. "3D Fibre-deposited scaffolds for tissue engineering: Influence of pores geometry and architecture on dynamic mechanical properties." *Biomaterials*.
- Morye, SS, PJ Hine, RA Duckett, DJ Carr, and IM Ward. 1998. "A comparison of the properties of hot compacted gel-spun polyethylene fibre composites with conventional gel-spun polyethylene fibre composites." *Composites: Part A* 30:649-660.
- Närhi, TO, JA Jansen, T Jaakkola, A de Ruijter, J Rich, J Seppälä, and A Yli-Urpo. 2003. "Bone response to degradable thermoplastic composite in rabbits." *Biomaterials* 24:1697-704.
- Niemelä, T, H Niiranen, M Kellomäki, and P Törmälä. 2005. "Self-reinforced composites of bioabsorbable polymer and bioactive glass with different bioactive glass contents. Part I: Initial mechanical properties and bioactivity." *Acta Biomaterialia* 1:235-242.
- Niiranen, H, T Pyhalto, P Rokkanen, M Kellomäki, and P Törmälä. 2004. "In vitro and in vivo behavior of self-reinforced bioabsorbable polymer and self-reinforced bioabsorbable polymer/bioactive glass composites." *J Biomed Mater Res A* 69:699-708.
- Niiranen, H, and P Törmälä. 1998. "Bioactive glass-bioabsorbable polymer composites." Pp. 109 in *The 1st combined meeting European associations of tissue banks and musculo skeletal transplantation*. Turku, Finland.

- Ogino, M, T Futami, T Kariya, T Ichimura, and T Fujiu. 1985. "Dental implant and methos of making same." edited by Unites States Patent Office. United States.
- Ohgushi, H, M Okumura, T Yoshikawa, S Tamai, S Tabata, and Y Dohi. 1992. "Regulation of bone development and the relationship to bioactivity." Pp. 47-54 in *Bone Bonding*, edited by Paul Ducheyne, T Kokubo, and C. A. Van Blitterswijk.
- Ohura, K, T Nakamura, and T Yamamuro. 1992. "Bioactivity of CaO*SiO₂ glasses added with various ions." *J Mater Sci* 3:95-100.
- Olley, RH, DC Bassett, PJ Hine, and IM Ward. 1993. "Morphology of compacted polyethylene Fibres." *Journal of Biomedical Materials* 28:1107-1112.
- Paul, A. 1990. *Chemistry of Glasses*. Bury St. Edmunds: Chapman and Hall.
- Pazzaglia, UP, C Gabbi, B Locardi, A Di Nucci, G Zatti, and P Cherubino. 1989. "Study of the osteoconductive properties of bioactive glass Fibres." *J Biomed Mater Res* 23:1289-1297.
- Peltola, M, J Suonpää, K Altasalo, M Varpula, A Yli-Urpo, and R-P Happonen. 1998. "Obliteration of the frontal sinus cavity with bioactive glass." *Head neck* 20:315-319.
- Peltola, MJ, KM Aitasalo, JT Suonpaa, A Yli-Urpo, PJ Laippala, and AP Forsback. 2003. "Frontal sinus and skull bone defect obliteration with three synthetic bioactive materials. A comparative study." *J Biomed Mater Res B Appl Biomater* 66:364-72.
- Peltola, T, M Jokinen, S Veittola, H Rahiala, and A Yli-Urpo. 2001. "Influence of sol and stage of spinnability on in vitro bioactivity and dissolution of sol-gel-derived SiO₂ Fibres." *Biomaterials* 22:589-598.
- Perdini, LC, and LGB Manhani. 2002. "Influence of the testing gage length on the strength, Young's modulus and Weibull modulus of carbon Fibres and glass Fibres." *Mater. Res.* 5:411-420.
- Pereira, D, S Cachinho, MC Ferro, and MHV Fernandes. 2004. "Surface behaviour of high MgO-containing glasses of the Si-Ca-P-Mg system in a synthetic physiological fluid." *Journal of the European Ceramic Society* 24:3693-3701.
- Piotrowski, G, LL Hench, WC Allen, and GJ Miller. 1975. "Mechanical studies of the bone bioglass interfacial bond." *J Biomed. Mater. Res. Symposium* 6:47-61.
- Pyhältö, T, M Lapinsuo, H Pätäälä, P Rokkanen, H Niiranen, and P Törmälä. 2004. "Fixation of distal femoral osteotomies with selfreinforced poly(L/DL)lactide 70:30/ bioactive glass composite rods. An experimental study on rats." *Journal of materials science: Materials in medicine* 15:275-281.
- Radin, S, P Ducheyne, B Rothman, and A Conti. 1997. "The effect of in vitro modeling conditions on the surface reactions of bioactive glass." *J Biomed Mater Res* 37:363-75.
- Radin, S, P Dycheyne, S Falaize, and A Hammond. 2000. "In vitro transformation of bioactive glass granules into Ca-P shells." *J biomed mater res* 49:264-272.
- Radin, S, G Reilly, G Bhargave, PS Leboy, and P Ducheyne. 2005. "Osteogenic effects of bioactive glass on bone marrow stromal cells." *J Biomed Mater Res A* 73:21-9.
- Ramakrishna, S, J Mayer, E Wintermantel, and KW Leong. 2001. "Biomedical applications of polymer-composite materials: a review." *Composites Science and Technology* 61:1189-1224.
- Rich, J, T Jaakkola, T Tirri, T Närhi, A Yli-Urpo, and J Seppälä. 2002. "In vitro evaluation of poly(e-caprolactone-co-DL-lactide)/bioactive glass composites." *Biomaterials* 23:2143-2150.
- Rinehart, JD, TD Taylor, Y Tian, and RA Jr. Latour. 1999. "Real-time dissolution measurement of sized and unsized calcium phosphate glass Fibres." *J Biomed Mater Res* 48:833-40.
- Roether, JA, AR Boccaccini, LL Hench, V Maquet, S Gautier, and R Jerjme. 2002. "Development and in vitro characterisation of novel bioresorbable and bioactive composite materials based on polylactide foams and Bioglass for tissue engineering applications." *Biomaterials* 23:3871-8.

- Saikku-Backstrom, A, RM Tulamo, T Pohjonen, P Törmälä, JE Raiha, and P Rokkanen. 1999. "Material properties of absorbable self-reinforced fibrillated poly-96L/4 D-lactide (SR-PLA96) rods; a study in vitro and in vivo." *J Mater Sci Mater Med* 10:1-8.
- Scepers, E, M de Clerco, P Ducheyne, and R Kempeneers. 1991. "Bioactive glass particulate material as a filler for bone lesions." *J Oral Rehabil* 18:439-452.
- Schmitt, JM, DC Buck, SP Joh, SE Lynch, and JO Hollinger. 1997. "Comparison of porous bone mineral and biologically active glass in critical-sized defects." *J Periodontol* 68:1043-53.
- Schoppee, MM, and J Skeleton. 1974. "Bending limits of some high-modulus Fibres." *Textile Research Journal*:968-975.
- Senker, J, and S Mahdi. 2003. "Research activities and future developments of human tissue engineering in Europe and the US." Pp. 46 in *Human tissue-engineering products: Today's markets and future prospects*, edited by The network for Regenerative Biology. Brighton: SPRU Science and Technology Policy Research, University of Sussex.
- Shao, XX, DW Hutmacher, ST Ho, JC Goh, and EH Lee. 2005. "Evaluation of a hybrid scaffold/cell construct in repair of high-load-bearing osteochondral defects in rabbits." *Biomaterials*.
- Shin, H, S Jo, and AG Mikos. 2003. "Biomimetic materials for tissue engineering." *Biomaterials* 24:4353-64.
- Shin, M, H Yoshimoto, and JP Vacanti. 2004. "In vivo bone tissue engineering using mesenchymal stem cells on a novel electrospun nanofibrous scaffold." *Tissue Eng* 10:33-41.
- Stanley, HR, MB Hall, F Colaizzi, and AE Clark. 1987. "Residual alveolar ridge maintenance with a new endosseous implant material." *J Prosthet Dent* 58:607-13.
- Stock, UA, and JP Vacanti. 2001. "Tissue engineering: current state and prospects." *Annu Rev Med* 52:443-451.
- Stoor, P, V Kirstilä, E Söderling, I Kangasniemi, K Herbst, and A Yli-Urpo. 1996. "Interactions between bioactive glass and periodontal pathogens." *Microb ecol health D* 9:109-114.
- Stoor, P, E Söderling, and R Grenman. 1999. "Interactions between the bioactive glass S53P4 and the atrophic rhinitis- associated microorganism *Klebsiella azaenae*." *J biomed mater res (appl biomater)* 48:869-874.
- Stoor, P, E Söderling, and JI Salonen. 1998. "Antibacterial effects of a bioactive glass paste on oral microorganisms." *Acta Odontol Scand* 56:161-165.
- Temenoff, JS, and AG Mikos. 2000a. "Injectable biodegradable materials for orthopedic tissue engineering." *Biomaterials* 21:2405-12.
- Temenoff, JS, and AG Mikos. 2000b. "Review: tissue engineering for regeneration of articular cartilage." *Biomaterials* 21:431-440.
- Turunen, T, J Peltola, H Helenius, A Yli-Urpo, and R-P Happonen. 1997. "Bioactive glass and calcium carbonate granules as filler material around titanium and bioactive glass implants in the medullar space of the rabbit tibia." *Clin Oral Impl Res* 8:96-102.
- Turunen, T, J Peltola, T Makkonen, H Helenius, and A Yli-Urpo. 1998. "Bioactive glass granules and polytetrafluoroethylene membrane in the repair of bone defects adjacent to titanium and bioactive glass implants." *J Mat Sci Mater Med* 9:403-407.
- Turunen, T, J Peltola, A Yli-Urpo, and RP Happonen. 2004. "Bioactive glass granules as a bone adjunctive material in maxillary sinus floor augmentation." *Clin Oral Implants Res* 15:135-41.
- Törmälä, P, T Pohjonen, and P Rokkanen. 1998. "Bioabsorbable polymers: materials technology and surgical applications." *Proc Inst Mech Eng [H]* 212:101-11.
- Törmälä, P, J Vasenius, S Vainionpaa, J Laiho, T Pohjonen, and P Rokkanen. 1991. "Ultra-high-strength absorbable self-reinforced polyglycolide (SR-PGA) composite rods for internal fixation of bone fractures: in vitro and in vivo study." *J Biomed Mater Res* 25:1-22.

- Törmälä, P, P Rokkanen, J Laiho, M Tamminmäki, and M Vainionpää. 1988. "Material for Osteosynthesis devices." Pp. 6. USA: Materials Consultants Oy.
- Törmälä, P, P Rokkanen, S Vainionpää, J Laiho, V-P Heponen, and T Pohjonen. 1990. "Surgical materials and devices." Pp. 14. US.
- Valerio, P, MM Pereira, AM Goes, and MF Leite. 2004. "The effect of ionic products from bioactive glass dissolution on osteoblast proliferation and collagen production." *Biomaterials* 25:2941-8.
- Wang, M, D Porter, and W Bonfield. 1994. "Processing, characterisation, and evaluation of hydroxyapatite reinforced polyethylene composites." *British Ceramic Transactions* 93:91-93.
- Vats, A, NS Tolley, JM Polak, and JE Gough. 2003. "Scaffolds and biomaterials for tissue engineering: a review of clinical applications." *Clin Otolaryngol* 28:165-172.
- Verrier, S, JJ Blaker, V Maquet, LL Hench, and AR Boccaccini. 2004. "PDLLA/bioglass composites for soft-tissue and hard-tissue engineering: an in vitro cell biology assessment." *Biomaterials* 25:3013-3021.
- Williams, D. 1999. *The Williams Dictionary of Biomaterials*. Liverpool: Liverpool University Press.
- Williams, D. 2004. "Benefits and risk in tissue engineering." *Materialstoday*:24-29.
- Wilson, J, and GE Merwin. 1988. "Biomaterials for facial bone augmentation: comparative studies." *J Biomed Mater Res* 22:159-77.
- Wilson, J, GH Pigott, FJ Schoen, and LL Hench. 1981. "Toxicology and biocompatibility of bioglasses." *J Biomed Mater Res* 15:805-17.
- Vita Finzi Zalman, E, B Locardi, C Gabbi, and P Tranquilli Leali. 1991. "Bioactive vitreous composition for bone implants, filaments made therefrom and method." edited by World intellectual property organization.
- Vogel, M, C Voigt, C Knabe, RJ Radlanski, UM Gross, and CM Muller-Mai. 2004. "Development of multinuclear giant cells during the degradation of Bioglass particles in rabbits." *J Biomed Mater Res A* 70:370-9.
- Välimäki, VV, JJ Yrjans, EI Vuorio, and HT Aro. 2005. "Molecular biological evaluation of bioactive glass microspheres and adjunct bone morphogenetic protein 2 gene transfer in the enhancement of new bone formation." *Tissue Eng* 11:387-94.
- Xynos, ID, MVJ Hukkanen, JJ Batten, LD Buttery, LL Hench, and JM Polak. 2000. "Bioglass 45S5 stimulates osteoblast turnover and enhances bone formation in vitro. Implications and applications for bone tissue engineering." *Calcif Tissue Int* 67:321-329.
- Yamane, S, N Iwasaki, T Majima, T Funakoshi, T Masuko, K Harada, A Minami, K Monde, and S Nishimura. 2005. "Feasibility of chitosan-based hyaluronic acid hybrid biomaterial for a novel scaffold in cartilage tissue engineering." *Biomaterials* 26:611-9.
- Yao, J, S Radin, P Leboy, and P Ducheyne. 2005. "The effect of bioactive glass content on synthesis and bioactivity of composite poly (lactic-co-glycolic acid)/bioactive glass substrate for tissue engineering." *Biomaterials* 26:1935-43.
- Yoshimoto, H, YM Shin, H Terai, and JP Vacanti. 2003. "A biodegradable nanoFibre scaffold by electrospinning and its potential for bone tissue engineering." *Biomaterials* 24:2077-82.
- Zamet, JS, UR Darbar, GS Griffiths, JS Bulman, U Bragger, W Burgin, and HN Newman. 1997. "Particulate bioglass as a grafting material in the treatment of periodontal intrabony defects." *J Clin Periodontol* 24:410-8.
- Zehnder, M, E Söderling, J Salonen, and T Waltimo. 2004. "Preliminary Evaluation of Bioactive Glass S53S4 as an Endodontic Medication in Vitro." *Journal of Endodontics* 30:220-224.
- Zhang, K, Y Ma, and LF Francis. 2002. "Porous polymer/bioactive glass composites for soft-to-hard tissue interfaces." *J Biomed Mater Res* 61:551-63.

Zhang, K, Y Wang, MA Hillmyer, and LF Francis. 2004. "Processing and properties of porous poly(L-lactide)/bioactive glass composites." *Biomaterials* 25:2489-500.

Tampereen teknillinen yliopisto
PL 527
33101 Tampere

Tampere University of Technology
P.O. Box 527
FIN-33101 Tampere, Finland